Measuring and modeling the effects of hydraulic and geometrical features of pumping stations on the downstream design of bed protection

Thijs Visser
December 12, 2013

UNIVERSITY OF TWENTE

Tauw

Measuring and modeling the effects of hydraulic and geometrical features of pumping stations on the downstream design of bed protection

Thijs Visser

BSc., Civil Engineering (University of Twente, Enschede)

In partial fulfillment of the requirements for the degree of:

Master of Science in Civil Engineering and Management

University of Twente
December 12, 2013

Under supervision of the following committee:

Prof. dr. S. J. M. H. Hulscher
    University of Twente, Department of Water Engineering and Management

Dr. J.J. Warmink
    University of Twente, Department of Water Engineering and Management

Ir. R.M. van Dam
    Tauw, Business Unit Water

With special thanks to:

Abstract

Bed protection is an important aspect for the stability of hydraulic structures. It protects the bed against large currents inducing bed erosion. The discharge originating from pumping stations can be approximated as a circular turbulent jet. To design a proper bed protection downstream of pumping stations, knowledge is needed regarding the behavior of these jets. Research in the 20th century mapped the behavior of jets in a free environment thoroughly. However, no literature is available on the validity and applicability of free jet behavior in a practical context. Therefore the bed protection is designed with rules that were formulated using scale models in a laboratory setup. As the rules are used to design bed protection behind all hydraulic structures in waterways and hydraulic structures differ largely in details, the design rules are likely to be conservative.

Interviews are carried out amongst hydraulic engineers, aiming to determine the practical features and aspects which effects on the velocity field downstream of pumping stations is not clear. The results show that the current design rules provide engineers with too little information on how to take into account the effects of the angle of a valve preventing backflow and the interaction of multiple parallel discharges on the required bed protection dimensions. Also the effect of the outlet orientation with respect to the channel needs further investigation. More insight in these processes will give engineers guidance in including the effects of these features in their design. This will eventually increase an engineer's confidence in his bed protection design.

To investigate the effect of these features, first field measurements are carried out near 3 pumping stations in the Netherlands using Acoustic Doppler Current Profiler (ADCP) equipment. The measurements result in a data set containing hydraulic conditions (velocity magnitudes, current directions, discharges) and geometrical conditions (geometry of the channels, the valve angles, the bed profiles). The results show that discharges in length of a small channel tend to attach to one of the banks. When discharging in an angle with the channel, the jet crosses the channel deflecting slightly into the channel. There does not seems to be a collision with the opposing bank. At all structures circulation flow occurs along the edges of the jet, ensuring the conservation of mass.

As the valve of the angle cannot be adjusted during the field measurements, the results do not show the effects of the valve angle on the downstream near-bed velocity field. Therefore the structures are modeled using Computational Fluid Dynamics (CFD). The models are validated with the measurement results. The overall performances of the models to represent the velocity magnitudes, expressed in relative deviation, vary largely from 58% to 119%. The relative deviation of velocity magnitudes near the bed, which are more important during this study, vary from 53% to 98%. The large deviations are mainly caused by smaller velocity magnitudes. The model results shows small velocity magnitudes and circulation flow along the banks are both structurally overestimated by the models. The latter causes an underestimation of the dispersion of energy, causing velocity magnitudes further downstream of the structure to be overestimated. Also the jet attachment observed during the measurements is not simulated.

During a sensitivity analysis, the number of outlets and the valve angle of the best performing model are varied to investigate their effects on the velocity field near the bed. The results show that the maximum near bed velocity magnitude behind the pumping station is 2.6 times larger at a valve angle of 30° with respect to a valve angle of 90°. The maximum velocity near the bed at a valve angle of 30° is even larger than the depth and width averaged velocity magnitude in the pressure line near the outlet (a factor 1.1). At lower valve angles the jet seems to decelerate faster, and reach lower velocities (<0.5 m/s) sooner than at larger valve angles. The presence of an additional outlet decreases the maximum near-bed velocity magnitude slightly at larger valve angles. For smaller valve angles, the near-bed velocities downstream of the structure are slightly larger (maximal 7%).

The results of the sensitivity analysis prove hard to translate into rules for the required bed protection dimensions. The combination of larger maximum near-bed velocity magnitudes and faster deceleration of the near-bed velocity magnitude over distance, makes the formulation of a straightforward relation between the valve angle and the required bed protection length impossible. It is however proved that the improvised rule that takes the valve angle into account, oversizes the bed protection dimensions significantly. The presence of an additional outlet does affect the required bed protection length according to the results. It is found that the improvised design rule, which designs the bed protection length twice as large, is very conservative. Based on the results and their relevance in practical applications, the effect of an extra outlet can be anticipated by lengthening the bed protection with 11% with respect to the single outlet situation.

Preface

In this Master's Thesis the findings of about six months of research are presented. The goal of this study was to map the flow field behind pumping stations, in order to gain and provide insight in the effect of several geometrical and hydraulic features on this flow field. Eventually this was done by performing three case studies at the pumping stations Houtkade, Barwoutswaarder and Rapijnen, in the Netherlands. Answering the formulated research questions required expert interviews, extensive data collection at the pumping stations, building, calibrating and validating of three CFD models and performing a sensitivity analysis with these models.

Thijs Visser
Enschede, November 2013

Table of Contents

Chapter 1

Introduction

Hydraulic structures play a key role in the Dutch water management system. They are used to manage and regulate water levels and discharges in waterways varying from small ditches to large rivers. Pumping stations in particular are important in water level management, as they possess the ability to move water to water bodies with a higher water level. With this function, these structures play a significant role in protecting the Netherlands against flooding and drought.

Pumping stations discharging a large portion of their capacity often induce large currents near the bed and the banks of a receiving water. This causes large stresses at these locations. The presence of large stresses induces erosion of the bed and bank material, which could endanger the stability of the structure. In order to keep erosion away from the structure, engineers often apply bed protection and revetments near the structure. The protective material (concrete and/or granular) does not easily erode and therefore keeps the cavity/scour away from the structure. Case studies of for instance the 'Afsluitdijk' and the 'Oosterscheldekering' show the importance of the bed protection (Kortlever, 2006, RWS, 2013).

After the completion of two large discharge sluices ('Kolwerderzand' and 'Den Oever') in the Afsluitdijk in 1932, the bed protection behind these structures stretched 18 meters from the toe of the structure. Monitoring the evolution of the sandy bed, in the period between 1932 and 1962 the bed protection was lengthened from an initial 18 meters to 205-210 meters at the end. The depth of the scour hole behind the sluices was 25 meters, where originally the water depth was 5 meters (Kortlever, 2006). Would the bed protection have not been lengthened, then the sluices most likely would be undermined by the scour hole entirely.

The bed protection behind the 'Oosterscheldekering' recently reached the frontpage because engineers feared the maintenance of the bed protection was neglected for years. This fear proved just as they observed a still growing scour hole with a depth of 50 meters during the performed study. If unattended, this hole could endanger the stability of the 'Oosterscheldekering' over time. Failure would obviously endanger the water safety of the Netherlands (Biesboer, 2013).

These case studies show the importance of both the deployment of bed protection and its proper design. However bed protection is often no 'hot' topic in the design of a pumping station. This is caused by cost aspects, as the total costs of a pumping station are mainly dependent on the used pump type. Flow affecting features such as for instance the outlet dimensions and location in the water column are therefore designed such, that energy losses are as low as possible. Even though this might cause a significant increase in required bed protection material. The aim to reduce energy losses as much as possible, causes flow patterns behind different pumping stations to differ. In

order to design a robust bed protection behind all these pumping stations, a rather conservative set of design rules is needed.

This chapter first highlights available knowledge regarding the downstream behavior of discharges from pumping stations. Then the current design rules for bed protection are discussed. These sections introduce knowledge gaps with respect to the discharge behavior and weaknesses of the current design rules, which translate to the scope of the study in section 1.3. Subsequently the objective and the research questions are presented in section 1.4 and the thesis outline is discussed in section 1.5.

1.1 The behavior of a discharge

The discharge from a pumping station in an adjacent water body can be approached as a horizontal circular turbulent jet (Rajaratnam, 1976). Many research is done to explain jet behavior in a free environment (Albertson, 1950, White, 1974, Rajaratnam, 1976, Schiereck, 2001). These studies resulted in a rule set describing free jet characteristics concerning velocity profiles and physics/processes.

Albertson et al. stated in 1950 that the energy of a jet disperses due to the entrainment of water into the jet, making the jet wider. This dispersion widens the jet at a rate of 1:5. Due to the dispersion of the energy, the maximum velocity of the jet (the centerline velocity) decreases. Additionally the dispersion instigates an increase in discharge of the jet, causing a flow directed to the jet's orifice to originate ensuring the conservation of mass (Albertson, 1950, Schiereck, 2001).

As a jet leaves the orifice it develops in the 'potential core'. In this region the entrainment does not affect the centerline velocity of the jet. The entrainment at the jet's edges causes the velocity distribution inside the jet to develop from a top hat distribution to a Gaussian shape (i.e. normal distribution, bell-shaped) (Rajaratnam, 1976). When the velocity profile reaches a Gaussian shape (after approximately 6 times the orifice diameter, i.e. the mixing length), the jet continues as a 'diffused jet'. In this region the entrainment causes a decrease in the centerline velocity due to a decrease in energy here (Schiereck, 2001). A schematization of a jet is presented in **Figure 1**.
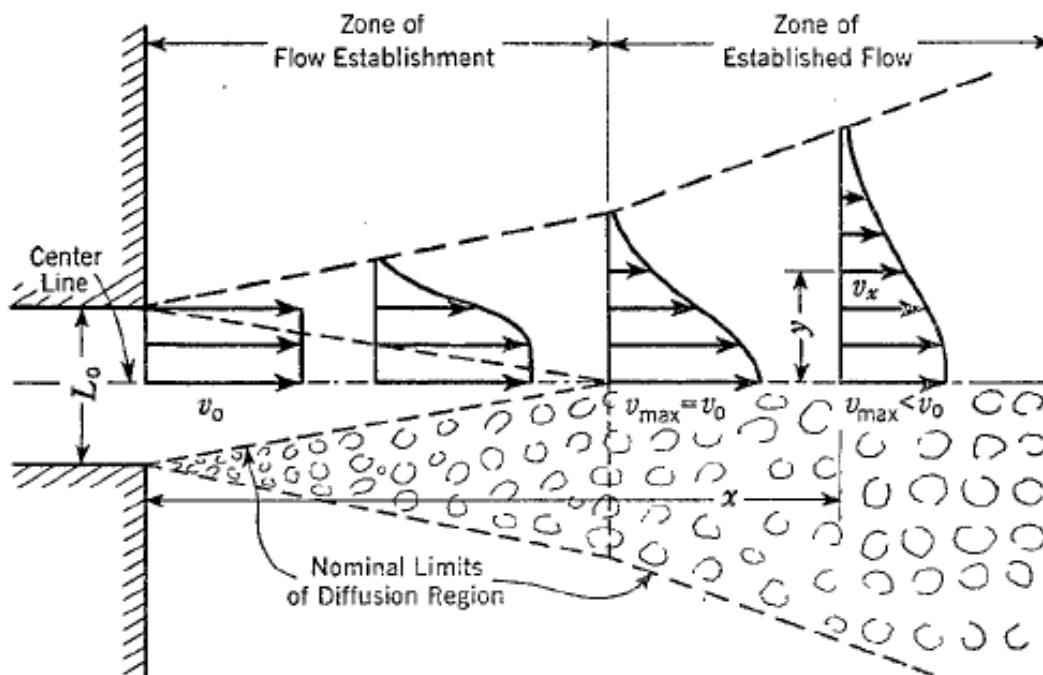
Figure 1: Schematization of a jet developing in a free environment (Albertson, 1950)

Albertson (1950), White (1974) and Schiereck (2001) developed several relations to predict the behavior of a jet in a free environment in a quantitative manner. Most importantly is the development of the centerline velocity of a diffused jet:

$$u_m = 6.3u_o * D_0/x \hspace{6cm} \textit{Eq 1}$$

This relation is however formulated for jet development in a free environment and may not be applicable in practical situations to describe the jet behavior from a pumping station. This was indicated by Johnston & Halliwell (1986), Johnston & Volker (1993) and Schiereck (2001). In these researches it was pointed out that physical boundaries have a significant effect on the jet development.

When the outflow is vertically limited by the bed and the water surface and horizontally limited by banks, the entrainment causes a backflow along the boundaries of the channel (Schiereck, 2001). Also researches of Johnston & Halliwell (1986) and Johnston & Volker (1993) show the jet tends to attach to one of the physical boundaries. The surface roughness of these walls is expected to increase turbulence, simultaneously decreasing the energy of the jet. This may lead to a faster decrease of the centerline velocity of the jet. Finally the tailwater depth (i.e. the water depth downstream of the jet orifice) can limit the vertical dispersion of the jet. This could induce a smaller reduction of the centerline velocity over distance. These effects are however all described in a qualitative manner in the literature and no answers are provided on how to include the effects of these processes in a practical context. Such as, for example, the design of bed protection.

1.2 The design rules for bed protection

With respect to the bed protection behind pumping stations, the 'Civieltechnisch Centrum Uitvoering Research en Regelgeving' (CUR) defined some design rules for structures located in waterways (CUR, 2000). These design rules are used to design the spatial bed protection dimensions behind all types of hydraulic structures (dams, sills, locks, pumping stations, sluices etc.), regardless the different physical processes playing their role at different structures. Obviously this introduces inaccuracy to the design. To acquire an accurate, or optimal design, each individual structure requires an optimization study.

The design rules are based on a relation between the expected dispersion rate, the diameter of the outlet, the depth and width averaged velocity at the outlet and the critical velocity of the bed material in the channel. The use of the depth and width averaged velocity at the outlet (calculated using the discharge of the pumping station and the cross area of the outlet) is conservative. This is chosen, as the velocity at the bed is not known, but is probably smaller than the average velocity of the jet. The dispersion rate used when calculating the required bed protection length describes the decrease of the centerline velocity over distance and is chosen safely at a rate of 1:10. The dispersion rate when calculating the required bed protection width describes the area in which velocities higher than the critical velocity may be expected. This rate is chosen 1:6 (CUR, 2000). In equations 2 and 3 the design rules for respectively the length of the bed protection (starting behind the outlet structure) and the width of the bed protection are presented. In **Figure 2** the design is schematized.

$$L = 5D_o((u_o - u_c)/u_c) \hspace{5cm} \textit{Eq 2}$$

$$B = 1/3\,L + D_o \hspace{6cm} \textit{Eq 3}$$
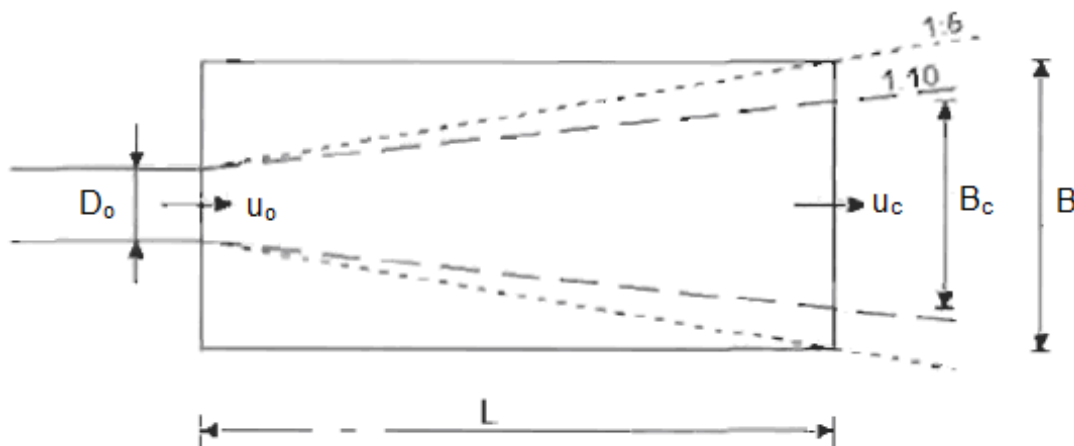
Figure 2: Dispersive characteristics of a jet from any hydraulic structure (CUR, 2000).

As literature does not provide a quantitative approach to predict jet behavior in a restricted environment, these rules were formulated otherwise. These design rules are based on the results of extensive scale experiments in laboratories carried out in the context of their formulation. The effects of the features that make jet behavior in a restricted environment differ from jet behavior in a free environment, are included in these design rules collectively. Rules on how to deal with these aspects individually are however not provided. The combination of (1) a lack of knowledge regarding the quantitative behavior of jets in a practical context and (2) the broad application area of the design rules, causes engineers to assume these rules are rather conservative in designing the required bed protection.

1.3 Study scope

Two important conclusions, which are part of the motivation for this study, can be drawn from the literature and the design rules for bed protection:

1. Jet development in a free environment is investigated thoroughly and can be predicted in a quantitative manner. The translation from this theoretical approach to a practical context, where the environment is often restricted by physical walls, has however only been made in a qualitative manner.
2. The current design rules for bed protection are general in nature. Although the effects of practical aspects are included in these design rules collectively, no rules are provided on how to deal with individual features. This is partly caused by the absence of available literature/research regarding these features' effects.

Due to this lack of knowledge, engineers don't always feel confident with their design. As the design rules do not provide them with sufficient knowledge and transparency regarding what effects are taken into account, engineers feel the bed protection might be oversized or undersized when using these rules. Both these situations are undesirable, as in both situations the total costs of a project will be higher than necessary. When optimization is of the essence, engineers should perform an additional case study in order to find the minimum required dimensions of the bed protection. This additional study will take time to perform and therefore increases design costs. This means the design process of bed protection is often a tradeoff between construction costs and design costs. **Figure 3** presents the aim of an optimization study for the bed protection design.
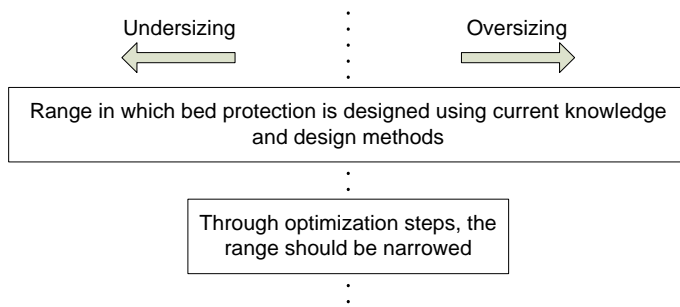
Figure 3: Optimizing bed protection design rules.

In order to reduce the construction costs (i.e. reduce over- and undersizing) and keep design costs low, first more insight is needed in the occurring flow processes around pumping stations. It is therefore important to map the main flow affecting features near structures and to analyze the actual effect they have on the velocity field. More insight in these processes will provide the engineers with more knowledge and increased confidence in their design of bed protection. The need for an optimization step in bed protection design can therefore be translated into a need for more knowledge regarding the effects of practical aspects on the development of jets.

1.4 Objective and research questions

The **objective** of this study is defined as:

'(1) To identify the physical features of outlets that influence the velocity field which need further investigation by carrying out an expert study and (2) to map their effects, using Computational Fluid Dynamics and field data, in order to optimize the design of bed protection.'

This study aims to clarify the individual effects of several features on the velocity field, which are unclear to engineers. Therefore the selection of these features is based on an expert study where engineers of bed protection can indicate the features whose effects they like to see clarified. Tauw's expertise lays mainly in the design, renovation and testing of pumping stations. Therefore this optimization study focuses on the required bed protection behind these particular structures. Three case studies are carried out in which models of existing pumping stations (validated with field data) are used to investigate the effects of flow affecting features on the velocity field development behind a structure. These models are built in the Computational Fluid Dynamics module of the software package COMSOL (Version 4.3b). This study can be characterized as an optimization study. It serves as a step in this process by providing insight in the actual flow field behind a pumping station. A total of 3 **research questions** are formulated to reach the research objective.

1. *To what extend do the contents of the current design rules for bed protection match with the engineers' need?*
2. *What is the effect of the subjects of the appointed knowledge gaps on the velocity field downstream of pumping stations?*
3. *How can these effects be translated into rules for the design of bed protection?*

1.5 Thesis outline and research approach

In order to reach the formulated objective, first an expert study is carried out amongst hydraulic engineers with experience in the design of pumping stations and bed protection. During this expert study the relevant features whose effects need further investigation are identified. This expert study is described in chapter 2 of this Thesis.

Subsequently three pumping stations were selected as case studies. At these structures field measurements are carried out using Acoustic Doppler Current Profiler (ADCP) equipment, to provide insight in the velocity field downstream of these structures and to use for validation of the models' results. The selection of the case studies and the measurement setup and results are presented in chapter 3.

In chapter 4 the CFD models are presented and validated. The CFD models are used to give a 3D insight in the velocity field downstream of the structures. When validated, one of the models is used to perform a sensitivity analysis on the relevant model parameters for this study. This way the velocity field under normal conditions is analyzed as well as the effect of specific features on the velocity field. The sensitivity analysis is presented in chapter 5. Here the practical relevance of the results for the design of bed protection is also discussed and the velocity field behavior is translated back to the requirements for the bed protection.

In chapter 6 the results of the study are discussed and placed in the proper context, while finally in chapter 7 conclusions and recommendations are given. The research model is presented in **Figure 4**.
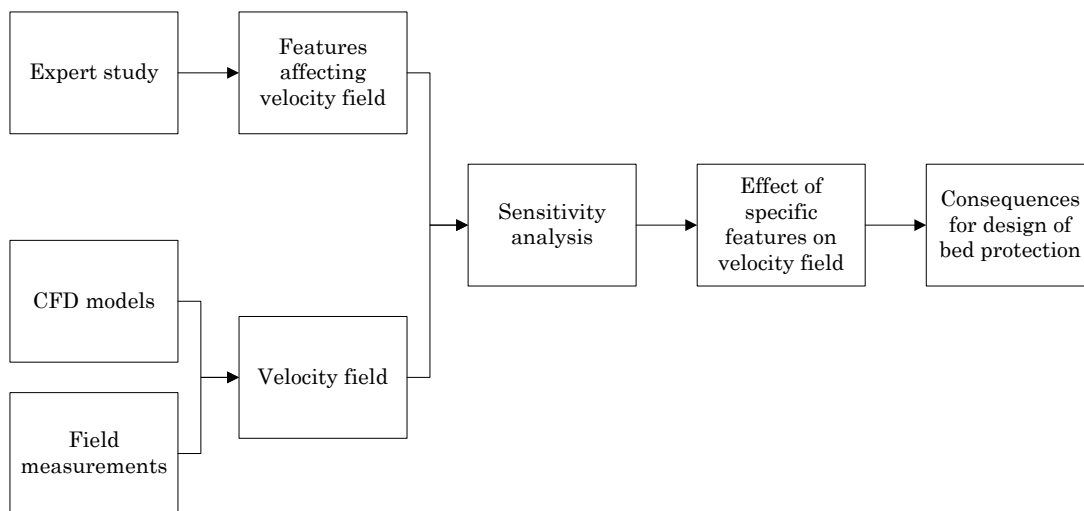
Figure 4: The research model

Chapter 2

Expert's view

In the context of the first research question, concerning the provided knowledge of the design rules and the needs of the engineers, interviews were carried out. Three goals were formulated prior to these interviews:

1. Identify which aspects and/or processes should best be investigated, in order to improve the accuracy of bed protection behind pumping stations;
2. Acquire criteria on which the selection of the case studies can be based;
3. Get insight in the processes, considerations and decisions of defining the bed protection design rules as formulated in CUR 197 (2000) to place the rules in a proper context and analyze the sources of weaknesses in current design rules.

In this chapter the results of these interviews are presented and the features that need further investigation are identified.

2.1 Interview method

In this section the selection procedure of the experts, the profiles of the experts, the interview questions and the interpretation are discussed.

2.1.1 The experts

The respondents were selected based on their area of expertise (hydraulic engineering, pumping stations and/or the design of bed-/bank protection). Aimed was to compose a team of respondents with different levels of working experience (i.e. senior experts, medior experts and junior experts), as senior experts often carry a lot of knowledge and experience, while junior experts often have a fresh look at the existing design rules and the features that are not included in them. Eventually six experts were interviewed:

1. **Ing. C. J. M. Rommens:**
   - ➢ Senior project advisor at Tauw;
   - ➢ 40 year of working experience;
   - ➢ Expert on the subjects of hydraulic engineering, sewage treatment, hydraulics of pumping stations and designing and renovating hydraulic structures.
2. **Ir. G. Pragt:**
   - ➢ Project manager at Tauw;
   - ➢ 29 years of working experience;
   - ➢ Expert on the subjects of hydraulic engineering, designing and renovating hydraulic structures, sustainable energy, process industry and project management.

3. **Ir. R. M. van Dam:**
   - ➢ Project advisor at Tauw;
   - ➢ 6.5 years of working experience;
   - ➢ Expert on the subjects of bed-, bank- and coastal protection, dike reinforcement, pumping stations and water safety assessment.
4. **MSc. H. T. J. Overman:**
   - ➢ Project employee at Tauw;
   - ➢ 4 years of working experience;
   - ➢ Expert on the subjects of hydraulic works and hydraulic structures, including bed- and bank protection, piping and reliability of closing of structures.
5. **Ing. N. van der Plicht:**
   - ➢ Project advisor at Tauw;
   - ➢ 6 years of working experience;
   - ➢ Expert on the subjects of hydraulic engineering, design and assessment of primary dikes and structures, design of bed- and bank protection and guidelines for waterways.
6. **Ir. M. van der Wal:**
   - ➢ Senior project advisor/researcher at Deltares;
   - ➢ 37 years of working experience;
   - ➢ Expert on the subjects of river engineering, hydraulic structures, bank protections, environmentally friendly banks, physical modeling and ship induced water motion;
   - ➢ Was involved in writing and publishing the CUR 197 handbook.

Respondents 1 and 2 are experienced hydraulic engineers at Tauw. These experts possess a lot of knowledge regarding the dimensions of pumping stations often designed by Tauw and were therefore interviewed to acquire criteria on which the case studies can be selected. Respondents 3, 4 and 5 are engineers at Tauw who are often involved in designing bed- and bank protection behind hydraulic structures. They were interviewed to identify the aspects which need further investigation when designing bed protection. Respondent 6 is an experienced engineer at Deltares with a high level of expertise in hydraulic engineering who was involved in formulating design rules. Therefore this expert was interviewed to gain insight in the process of defining these design rules.

2.1.2 Interviews and interpretation

In face-to-face interviews of approximately 45 minutes, experts were asked about the design of pumping stations, the design of bed protection and the design rules provided by the CUR 197 (2000). These interviews were situated one on one, so respondents could focus on aspects they thought important, without being influenced by other experts. The given answers of the different experts are therefore considered independent. The actual questions of the interviews are presented in appendix C. This paragraph focuses on the type of questions.

To determine criteria to select the case studies, respondents 1 and 2 were asked about common dimensions of pumping stations where Tauw is often involved in the design- or renovation process. The questions concerned the discharge, velocities in the pressure line (and therefore the outlet dimensions), the angle of a valve preventing backflow, the presence of multiple outlets, the dimensions of the outlet structure and the orientation of outlets with respect to the channel. Eventually the results of the two interviews were compared on similarities and differences and dimensional criteria were defined for the case study selection.

To identify aspects in the design process of bed protection where a knowledge gap exists, respondents 3, 4 and 5 were interviewed about the design of bed protection. Questions were asked about the accuracy of the design rules, the used dispersion pattern, the use of models during the design process, critical bed velocities and the effects of physical restrictions of channels on the discharge. Most importantly they were asked whether they need to deal with features/aspects for which no answer is provided by the design rules in CUR 197 (2000) and if they use alternate (improvised) rules to do this. The results of these interviews were analyzed by counting the number of experts that mentioned a certain aspect or feature. The aspects that were mentioned most, were selected to investigate in the remainder of this study.

To get a complete view on the formulation of the bed protection design rules to place them in a proper context, respondent 6 was interviewed about the application area of the rules, the ability of the rules to design an accurate bed protection and the process of formulating the design rules. The results of this interview were used to identify the cause(s) of the conservative nature of the design rules and to present possibilities to optimize the design rules.

2.2 Interview results

Respondent 1 mentioned Tauw is involved in designing and renovating all pumping station sizes, but since there are far more small to medium sized pumping stations, these structures are dealt with the most. The design of the pumping station dimensions is based on the discharge capacity and the pump type. The dimensions of the pressure line are often designed such that the depth and width averaged velocity here is approximately 2 m/s. Towards the outlet, the cross area of the line increases to decrease the averaged velocity to approximately 1 m/s. The valve, preventing backflow into the pressure line, is designed at an angle of 50°/60° at maximum discharge. Would this angle be larger, it would be damaged when closing as the pumping station is turned off. Pumping stations are most often situated perpendicular to the channel. A summary of the dimensions is provided in **Table 1**.

Respondent 2 stated Tauw is most often involved in designing and renovating small to middle large pumping stations. Small pumping stations often discharge through one outlet, while middle large pumping station discharge through two or three outlets. Large pumping stations discharge through three or four outlets. The dimensions of the pressure line are designed such that the averaged velocity is around 2 m/s. The outlet is often situated near the bed of the receiving channel where velocities are approximately 1 m/s. Upon entering the channel, the discharge is first leaded through an outlet structure of approximately 2-3 meters. The valve is always designed to have an angle of 90° at maximum discharge. Pumping stations often discharge perpendicular to the channel. For some small structures, this can also happen in length of the channel. A summary of the dimensions is provided in **Table 1**.

Table 1: Results of interviews with respondents 1 and 2. The presented dimensions represent common pumping station dimensions and characteristics that Tauw works on.

Respondent	Discharge [m³/m]	Velocity in pressure line [m/s]	Number of outlets	Angle of the valve [°]	Orientation of outflow
1	40-300	2	-	50-60	T-junction
2	60-400	2	1-3	90	T-junction or in length

Respondent 3 indicated the handbook for designing bed protection fails to speak of some aspects, leaving engineers with less confidence in their design. The effects of respectively the valve angle, the interaction between multiple outlets, the bed roughness, the vertical dispersion and the discharge orientation are not clearly mentioned in CUR 197 (2000). Additionally it is not clear how to act when the channel dimensions (width, length) limit the decrease of the velocity of the discharge. Currently, alternate rules are used to keep in mind the angle of the valve, the interaction between outlets and the scour when velocity cannot be decreased below acceptable margins (i.e. critical bed velocity). The accuracy of these rules is however not known.

Respondent 4 acknowledged the final design of bed protection is based on CUR publications 197 and 201. Computer models are never used in the design process. Insight in vertical velocity profiles can help to understand the processes downstream of the structure. Especially effects of the angle of the valve, the interaction between multiple outlets and the discharge orientation on the velocity field need to be mapped more clearly, as the CUR does not mention these situations. Improvised rules are used to take into account the interaction between outlets. The outlet diameter in Eq 2 and Eq 3 is considered as the sum of the two outlet diameters. Critical velocities of the bed material in Dutch channels lay often between 0.2 and 0.5 m/s. The length of the bed protection is considered an important factor for the bed protection dimensions, as this is also used as input for the bed protection width.

Respondent 5 confirmed the use of the CUR publications 197 and 201 in the final design of the bed protection. The Rockmanual (CIRIA, 2007) can also be used for less conservative design rules for the sorting. The spatial dimensions are however not mentioned in this publication. The largest conservatism of the current design rules is however not nested in the chosen sorting, but in the spatial dimensions. Computer models are never used in the design process. The current design rules provide insufficient knowledge and guidelines on how to deal with effects of the angle of a valve, the interaction between outlets and the discharge orientation on the velocity field. The latter aspect concerns orientations perpendicular, in length and in an angle with the channel direction. Improvised rules are used for the first two. To take into account the valve angle, the velocity is recalculated using the decreased flow area and the discharge. For multiple discharges, the outlet diameter in Eq 2 and Eq 3 is considered as the sum of the two outlet diameters. Critical velocities of the bed material in Dutch channels lay often between 0.2 and 0.5 m/s. In **Figure 5** the results of the interviews with respondents 3, 4 and 5 are presented.
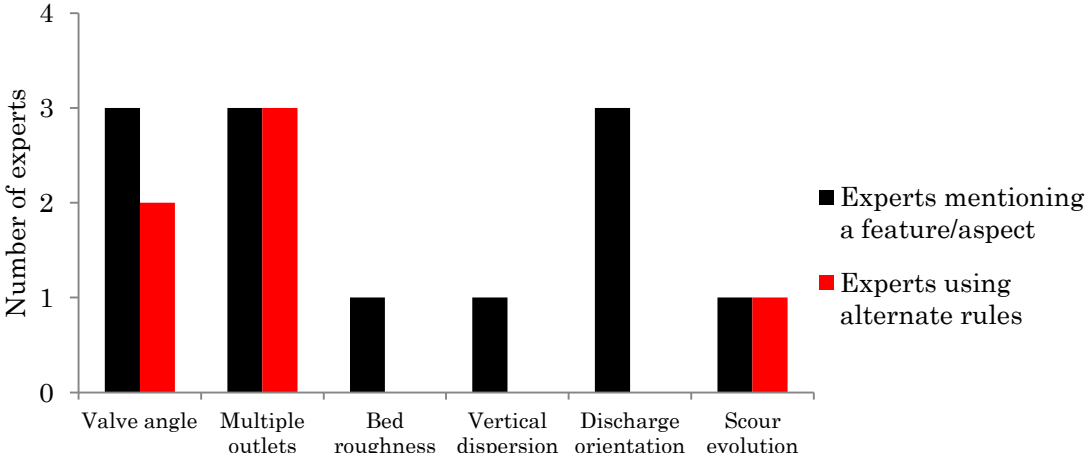
Figure 5: Results of interviews 3, 4 and 5. Important features whose downstream effects are unclear.

Respondent 6 was interviewed about the formulation of the design rules in CUR 197 (2000). The presented relations are determined based on results from scaled experimental setups of structures in laboratories. These design rules are used for hydraulic structures in waterways, for which bed protection can be oversized for the purpose of simplicity. Effects of site specific features like multiple parallel outlets or partly closed valves are taken into account by this slight oversizing. In the Rockmanual (CIRIA, 2007) more accurate design rules are given. However, due to the use of quite specific information, like turbulence intensities, often mistakes are made while using this method. Looking at dispersion, the characteristics of an outflow are very dependent on the geometry. The geometry also determines the role of vertical dispersion, which is not included in the CUR. According to the respondent structures vary largely in detail. Therefore it is not realistic that relations are found determining the required bed protection for all pumping stations accurately. Important steps could include better turbulence modeling, modeling of 3D flow/velocity patterns or improving deployment methods of a chosen sorting.

2.3 Interview discussion

In this section, first the most important information from the interviews is summarized in paragraph 2.3.1. Subsequently in 2.3.2 the features whose effect on the velocity field will be investigated in this study and the criteria for case study selection are determined.

2.3.1 Interview conclusions

The criteria for the selection of case studies mainly relate to the discharge and the orientation of the outlet. Respondents 1 and 2 mentioned that the structures that are relevant have a discharge of respectively 40-300 m³/minute and 60-400 m³/minute. Therefore pumping stations with a discharge of 60-300 m³/minute are considered relevant. When this criterion cannot be met, the discharge should at least lay within the margins 40-400 m³/minute. Respondents 1 and 2 both stated pumping stations often discharge perpendicular to the channel. Additionally, respondents 2 and 5 mentioned the possibility of pumping stations discharging in length of a channel. As respondents 3, 4 and 5 identified the outlet orientation as a feature which effects on the velocity field are not clear and respondent 5 also mentioned the discharge in an angle with the channel, pumping stations are sought that discharge perpendicular to the channel, in length with the channel and (when possible) in an angle with the channel.

The aspects whose effects on the velocity field downstream of pumping stations should be investigated are according to respondents 3, 4 and 5 the angle of the valve, the interaction between multiple outlets and the discharge orientation with respect to the channel. As only respondent 3 mentioned the bed roughness, the vertical dispersion and the scour development, these features are not further assessed in this study. Improvised rules are currently used to take into account the interaction between multiple outlets (respondents 3, 4 and 5) and the valve angle (respondents 3 and 5) when designing bed protection. Modeling of 3D flow/velocity patterns is a way to investigate the effect of these features on the velocity field downstream of structures (according to respondents 4 and 6). With the results, the actual effects of these features and the accuracy of and need for the improvised rules can be evaluated. According to respondent 6, these results should not be used to create bed protection design rules with an application area of all pumping stations, as this is not realistic. The study better aims to present the relation between velocity field characteristics and the selected features.

2.3.2 Concluding remarks

The expert study's results show there is a lack of information regarding the effects of several hydraulic and geometrical aspects on the downstream velocity field behind pumping stations. Two aspects are chosen for further investigation during this study, as all experts mentioned the lack of knowledge regarding the suspected effects of these aspects:

1. The angle of the valve preventing backflow into the structure;
2. The presence of multiple outlets.

To take some of the uncertainty away from the engineers, the individual effects of these aspects on the velocity field are mapped during this study. This is done based on case studies of existing pumping stations, consisting of field measurements and a model study analyzing the effect of these two aspects on the downstream design of bed protection. These cases are selected such, that they meet the criteria derived from the results of this expert study. These criteria are:

1. Preferably, structures are chosen with a discharge between 60-300 m³/minute (when not possible, at least within 40-400 m³/minute);
2. The cases should cover all three possible outlet orientations (perpendicular to the channel, in line with the channel and in an angle with the channel);
3. Preferably, one of the pumping stations has 2 outlets.

With the second criterion, the velocity field is mapped behind pumping stations with different outlet orientations with respect to the channel. The results can be used to map the flow field characteristics at different discharge orientations, albeit to a smaller extent than the two main subjects. In the next chapter these criteria are used to select the cases for this study and the field measurements carried out at these locations are discussed.

Chapter 3

Measurements

Three pumping stations were chosen to act as case studies to evaluate the effect of the outlet orientation, the presence of multiple outlets and the valve angle. During this study, field measurements were carried out at two of these locations, while at the other one measurements were already available. Important for the measurements was the cooperation and the collaboration of AquaVision, a commercial organization specialized in   field measurements at hydraulic structures and waterways, and waterboard 'Hoogheemraadschap de Stichtse Rijnlanden' (HDSR). This waterboard owns, regulates and maintains the pumping stations that were used as case studies. AquaVision had an advisory role in selecting the relevant and interesting pumping stations and additionally carried out the measurements. HDSR was also present during the measurements as they regulated the pumping stations. They also provided the technical information regarding the pumping station's design. Additionally, part of the measurement costs were paid by HDSR. With their help two pumping stations could be measured.

3.1 Measurement method

This section first discusses the selection procedure of the case studies. Then the measurement setup is described.

3.1.1 Selection of pumping stations

To choose pumping stations to act as case studies, first a selection of available structures was made. The selection was based on the relevance of the structure for the study (based on criteria derived from interviews), the possibility to carry out measurements at the location (financial and practical/temporal) and the availability of technical data of the structure (dimensions and characteristics). As a result of the mentioned cooperation, the structures were chosen in the policy area of HDSR. With the criteria regarding the discharge, the outlet orientation, the number of outlets and the presence of a valve, six pumping stations were selected as possible case studies.

1. **Houtkade**, north of Kamerik, is a pumping station with two outlets and a fish pass, which is irrelevant for this study, with a total capacity of 200 m³/min (2 x 100). It's situated in the 'Grecht', a channel north of Woerden. It discharges water perpendicular to the flow direction of the 'Grecht' (T-junction). The construction of 'Houtkade' was completed in 2012. After the completion, the bed protection was found to be insufficient. As part of a case study, measurements were done at the outlet in the context of a capacity check, a cross-flow evaluation for navigation and an evaluation of flow velocities at the bed. At these measurements the small angle of

the valve caught the attention of the engineers. This case is one of the motivations to perform this study;

2. **De Geer** is a pumping station located in Wijk bij Duurstede, consisting of a single outlet with a discharge of 86 m³/min. It discharges into the 'Kromme Rijn' with an angle to the flow direction;

3. **Rapijnen** is a pumping station located in Linschoten, south of Woerden. It discharges a maximum capacity of 100 m³/min through a single outlet in a small channel called 'Voorvliet'. The discharge enters the 'Voorvliet' with an angle of approximately 45 degrees after running through a small ditch of 10 meters long;

4. **Galecop**, located in Utrecht, discharges 170 m³/min perpendicular into the 'Amsterdam-Rijnkanaal'. This is done with two outlets. The Amsterdam-Rijnkanaal is relatively wide (100m-120m) and deep (6m) compared to the waterways where the other selected pumping stations are discharging. Also, the flow velocity is relatively large and there is a lot of navigation;

5. **Bijleveld**, located near Harmelen (between Woerden and Utrecht), discharges 140 m³/min through two outlets. The pumping stations discharges in a T-junction. Directly behind the outlet the discharge is deflected by a grille. This grille is probably placed to protect the banks at the other side of the channel;

6. **Barwoutswaarder** is a pumping station with a single outlet, located west of Woerden. Its discharge flows through a waterway of approximately 500 meters long to the Oude Rijn. The discharge flows in the longitudinal direction of the adjacent waterway, which is approximately 7-8 meters wide. The capacity of this structure is 75 m³/min.

The characteristics of these pumping stations are schematized in **Table 2**. The locations of these pumping stations are shown in **Figure 6**.

Table 2: Specifications of available pumping stations. Concerning the field data, x means measurement results were already available, xx means measurements could be carried out as part of the collaboration with HDSR.

	Single Outlet	Multiple Outlets	In length of channel	T-Junction	In angle with the channel	Capacity [m³/min]	Field data
Houtkade		x		x		200	x
De Geer	x				x	86	x
Rapijnen	x				x	100	xx
Bijleveld		x		x		140	xx
Galecop		x		x		170	xx
Barwouts-waarder	x		x			75	xx

Figure 6: Locations of the selected pumping stations.

Eventually three pumping stations were selected to act as case studies:

1. Houtkade;
2. Barwoutswaarder;
3. Rapijnen.

This selection covered all discharge orientations and contained pumping stations with one outlet and one pumping station with two outlets. Additionally all structures contained a valve. Bijleveld and Galecop were considered harder to measure, as the discharge at Bijleveld was affected by a grille and Galecop discharged into a large river, causing effects of navigation and current to influence the measurements. De Geer was considered less relevant than Rapijnen, as Rapijnen had a higher discharge. A research budget made it possible to measure at two locations. As Houtkade measurements were carried out previous to the study, Barwoutswaarder and Rapijnen were measured now.

3.1.2 Measurement setup

The measurements were carried out with ADCP equipment (see appendix D for more information). This equipment can be used at fixed locations in a water body (fixed vessel) or by navigating along a route (moving vessel). The chosen setup depended on the goal of the measurements. These measurements were carried out to:

1. Obtain velocity magnitudes and directions at different depths downstream of the discharging pumping stations;
2. Obtain hydraulic conditions like the discharge and the water depth downstream of the pumping stations;
3. Obtain geometrical boundary conditions regarding the channel dimensions, the bed profile of the channel and the angle of the valve.

The measurements at the Houtkade, Barwoutswaarder and Rapijnen were performed using both methods. Moving vessel measurements were used to assess the discharge of the pumping stations, as this aspect demands the flow to be analyzed over the entire width of the channel (Muste et al., 2013). The vessel was slowly navigated across the channel six times. Fixed vessel measurements were used to gain insight in the velocity field downstream of the structures, as the measurements were carried out in turbulent water (Muste et al., 2013). At each location, the equipment measured 1 minute continuous. At Rapijnen and Barwoutswaarder also a moving vessel measurement was done to evaluate the development of the centerline velocity. Additionally GPS measurements were done to determine the geometry of the channel and the water depth and bottom track measurements were carried out to determine the depth profile of the channel. The valve angles were estimated on sight.

The measurements were carried out at three different pump levels (i.e. three discharges). Before the pumps were turned on, the initial current in the channel was measured. The measurements at Houtkade were carried out previous to this study and the measurement setup was therefore not optimized for this study's goals. The results give less data regarding geometrical conditions and the velocity field is presented with less detail. The setup of the measurements at Houtkade, Barwoutswaarder and Rapijnen are presented in respectively **Figure 7**, **Figure 8** and **Figure 9**.
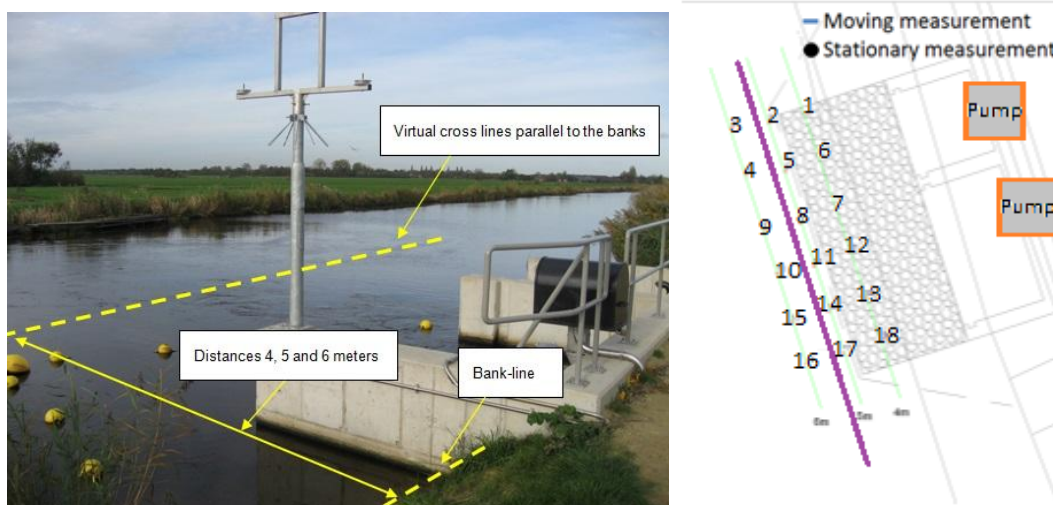
Figure 7: Measurement setup at Houtkade.
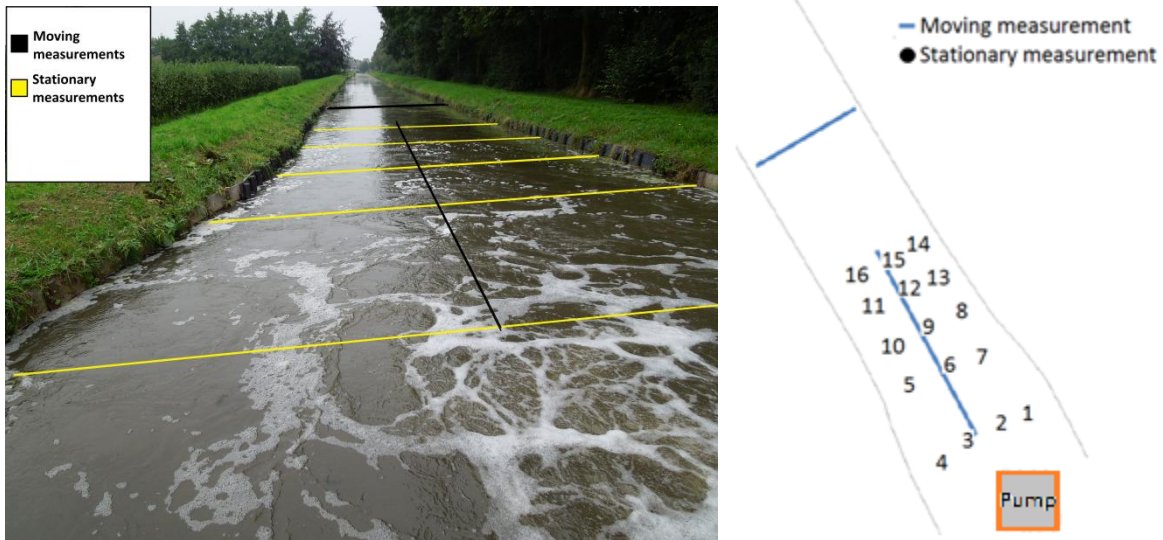
Figure 8: Measurement setup at Barwoutswaarder.
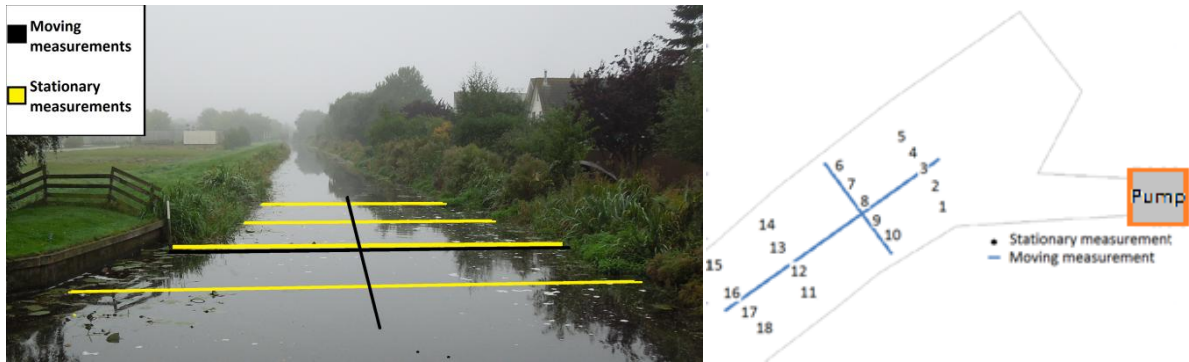
Figure 9: Measurement setup at Rapijnen.

The quality of the measurements is closely related to the settings of the equipment. These settings relate to the bin size (resolution of the results), the number of pings per ensemble (number of acoustic signals before rough data is averaged), the ensemble interval (the time between two collections of pings) and the measurement time (determining the total amount of ensembles in a measurement). The equipment settings during the measurements are presented in **Table 3**.

Table 3: Measurement settings at different locations. At Houtkade no results of the bed profiler are available. The bed profiler measurements are moving vessel measurements and therefore there is not measurement time available.

	Houtkade	Barwoutswaarder		Rapijnen	
Profiler	Current	Current	Bed	Current	Bed
Max depth [m]	5	3	3	3	3
Ensemble interval [s]	3	0.2	0.2	0.2	0.2
Pings per ensemble	1	1	1	1	1
Cell height [m]	0.1	0.1	0.15	0.1	0.15
Measurement time [s]	60	60	-	60	-

17

3.2 Measurement results

The measurement results are divided into geometrical and hydraulic boundary conditions (3.2.1) and jet characteristics (3.2.2).

3.2.1 Geometrical and hydraulic boundary conditions

The discharges corresponding to the pumping levels are presented in **Table 4**. Also the estimated positions of the valves are mentioned. Water levels were measured for all pumping stations. These are presented in **Table 5**.

Table 4: Discharge and valve angle results for all measurements.

Round	Houtkade		Barwoutswaarder		Rapijnen	
	Q [m³/m]	Valve angle [°]	Q [m³/m]	Valve angle [°]	Q [m³/m]	Valve angle [°]
1	230	-	73	90	98.3	60
2	210	-	46.6	90	80.3	50
3	196	-	35.7	90	35.7	40

Table 5: Water levels during measurements.

Round	Houtkade		Barwoutswaarder		Rapijnen	
	Start [mNAP]	End [mNAP]	Start [mNAP]	End [mNAP]	Start [mNAP]	End [mNAP]
T_0						
1	-0.4	-0.39	-0.44	-0.44	-0.33	-0.33
2	-0.39	-0.37	-0.44	-0.44	-0.33	-0.33
3	-0.36	-0.36	-0.44	-0.44	-0.33	-0.33

The bed profile was measured at Barwoutswaarder and at Rapijnen. The results for the total channel are presented in **Figure 10**.
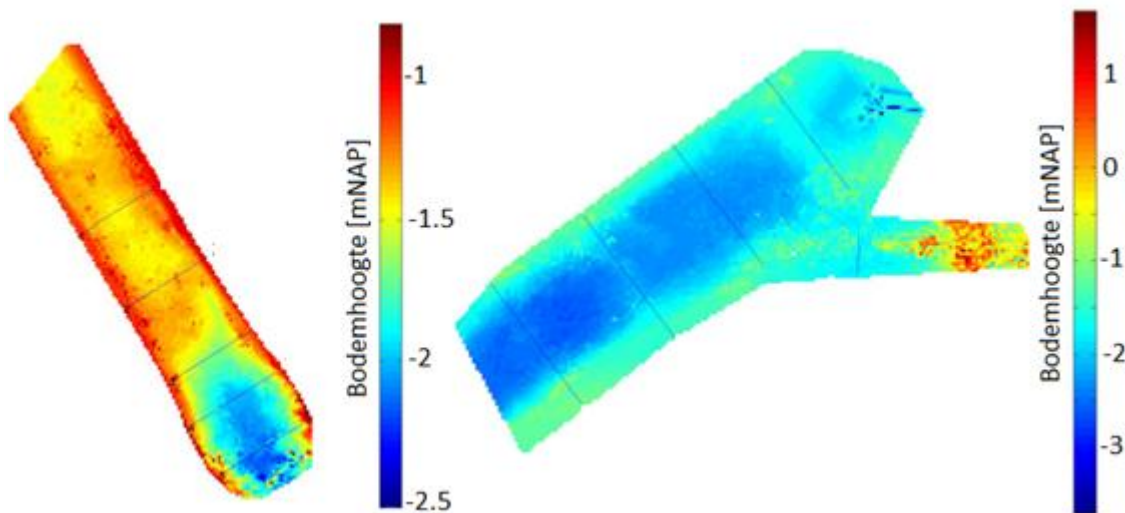
Figure 10: Measured bed profiles. Left: Barwoutswaarder. Right: Rapijnen.

3.2.2 Flow characteristics

The flow measurements result in velocity magnitudes and current directions at the measurement locations for each 10 cm of water depth. This way data sets for these parameters were created with 288 (Houtkade), 122 (Barwoutswaarder) and 212 data points (Rapijnen) per pump level. These data sets are produced into tables which are

presented in Appendix E. Only the data of the measurements during the design discharges are used in this report (i.e. Houtkade = 196 m³/min, Barwoutswaarder: 73 m³/min and Rapijnen 98.3 m³/min). The data shows some flow characteristics which can be related to jet behavior, hydraulic conditions and/or measurement setup. The results regarding flow behavior are presented regarding:

1. Vertical profiles of the velocity magnitude and current direction at several locations;
2. The velocity magnitude distribution over cross sections of the channels;
3. Current directions in the channel.

The **vertical profiles** of the velocity magnitudes and the current directions are presented in Appendix E. Current directions are presented with the unit [°], resembling the angle with respect to north. **Figure 11** presents this information for all three structures at one measurement location (Locations Houtkade: 8, Barwoutswaarder: 6 and Rapijnen: 8).
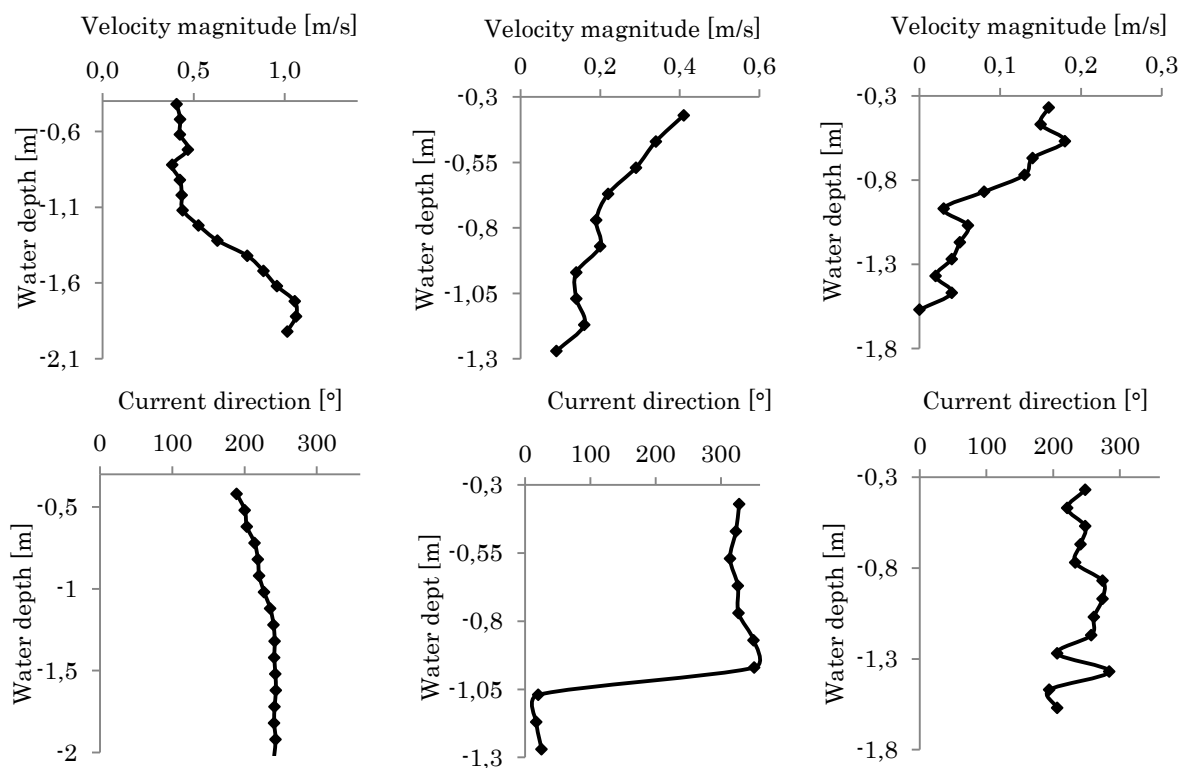
Figure 11: **Above**: Vertical profiles of measured velocity magnitudes at respectively Houtkade, Barwoutswaarder and Rapijnen. **Below**: Vertical profiles of the current direction at Houtkade, Barwoutswaarder and Rapijnen.

The figures (along with those in appendix E) show the velocity magnitudes at Barwoutswaarder and Rapijnen show erratic behavior. At Houtkade the vertical velocity profile develops quite smooth. At Houtkade larger velocities magnitudes are measured near the bed, while the higher velocities at Barwoutswaarder and Rapijnen are measured in the upper regions of the water column.

The vertical development of the current direction at Houtkade and Barwoutswaarder is quite smooth. Note that the 'jump' at Barwoutswaarder resembles a direction change from 351° to 20°. This is only a change of 29°, which cannot easily be spotted on first sight in the figure. At Rapijnen the vertical development shows an erratic profile like with the velocity magnitude.

The **velocity magnitudes** and the **current directions** at the measurement locations in the channels are displayed in **Figure 12**, **Figure 13** and **Figure 14**.

At Houtkade (**Figure 12**), the water column can be divided into three regions. In the lower region, near the bed, the highest velocities are found. They concentrate directly behind the outlets (locations 4-12). Here current directions are uniformly directed away from the structure. Only at locations 1 and 2 the current directions show water entrainment into the jet and at locations 13, 14, 17 and 18 the current directions show horizontal dispersion of the jets. In the middle of the water column the velocity magnitudes decrease and the current directions deviate from the current directions in the lower parts. Here the water is likely (vertically) entrained into the jet. However as vertical directions cannot be displayed, this is mere speculation. Closer to the water surface the current directions deviate even more, while velocity magnitudes start to increase again. As the water from the middle regions of the water column is entrained in the jets, a pressure gradient originates here. Due to this pressure gradient, water from the quieter upper parts of the water column flows perpendicular to the jet direction ensuring the conservation of mass.

Moving away from the structure the jet develops vertically and horizontally; it disperses. The maximum velocity decreases and the jet's horizontal development is mainly in the southern direction (the right side of the figure). The maximum velocity decreases from 1.33 m/s right behind the structure to 0.96 m/s 2 meters further downstream.
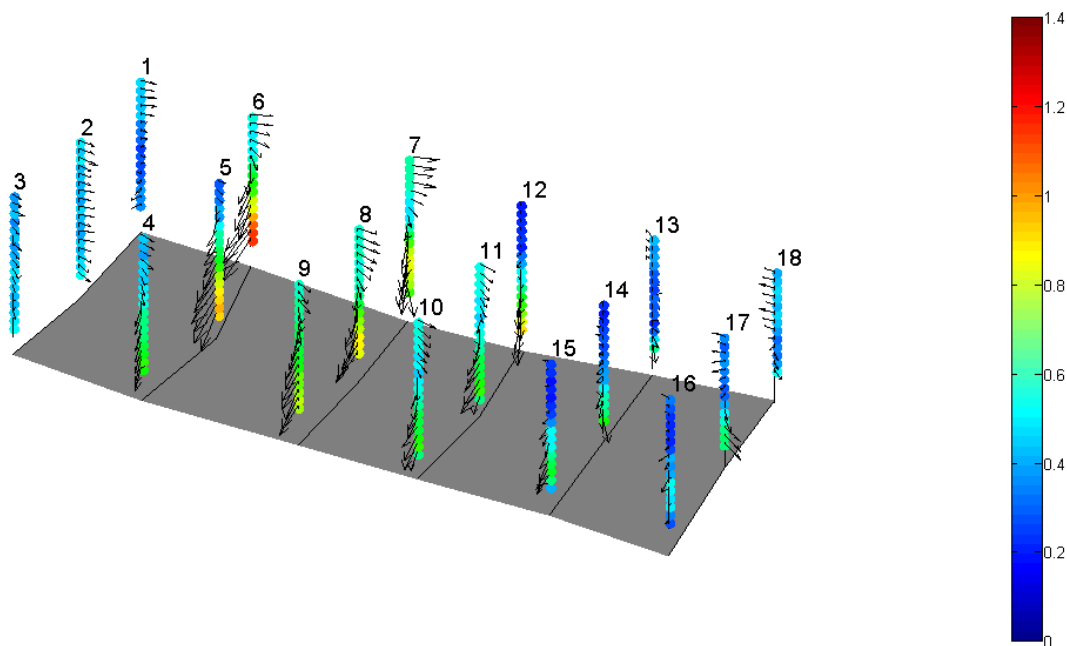
Figure 12: Measured velocity magnitudes and current directions at Houtkade.

At Barwoutswaarder (**Figure 13**) the highest velocities are found behind the outlet near the surface (location 3). As the discharge develops into the channel it seems to attach to the left bank. At the right bank backflow occurs. This is observed at locations 1, 7 and 8. At the left bank, location 4 shows some backflow. The largest backflow is observed at location 2, which is relatively close to the outlet. The jet disperses horizontally and vertically into the channel while the highest velocities stay in the upper region of the channel. Further downstream, at locations 14, 15 and 16 the jet seems to develop into an uniform flow. The maximum velocity decreases from 0.57 m/s to 0.35 m/s.
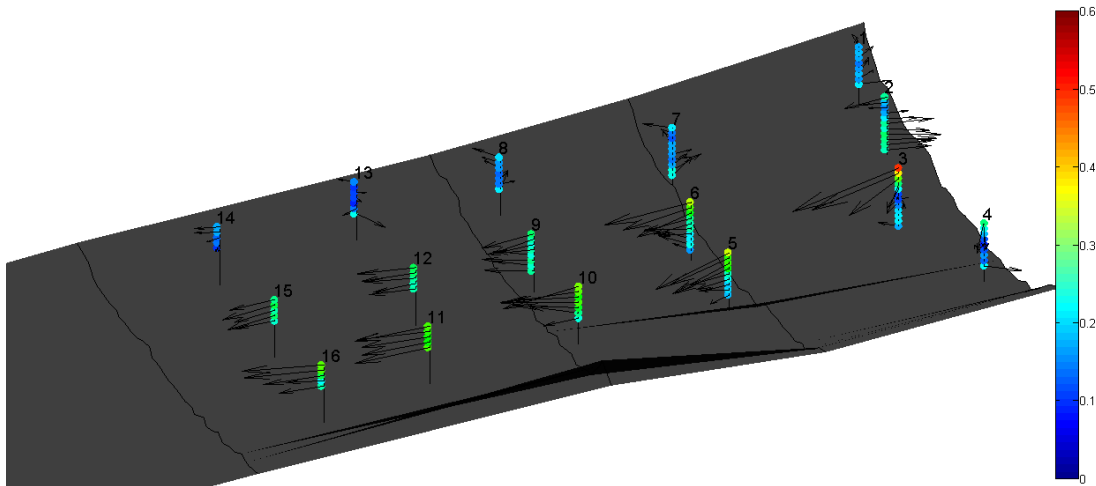
Figure 13: Measured velocity magnitudes and current directions at Barwoutswaarder

At Rapijnen the high velocities are also found in the upper regions of the water column. Upon entering the channel the jet starts crossing the channel, simultaneously dispersing vertically and horizontally, until it reaches the opposite bank. In the meantime the maximum velocity of the jet develops from around 0.65 m/s to 0.28 m/s. The measurements show backflow at locations 3-7 and at a smaller scale at locations 11 and 18.
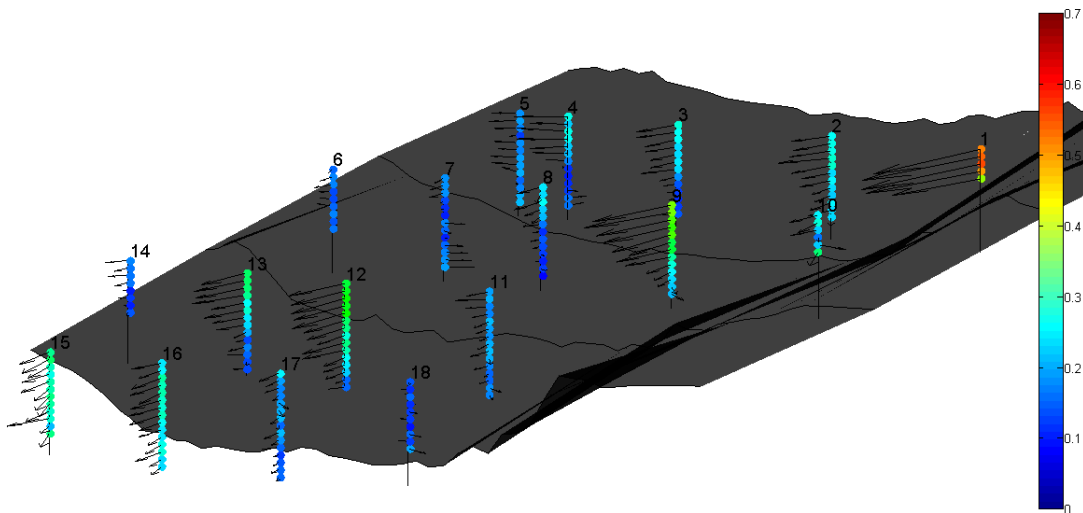
Figure 14: Measured velocity magnitudes and current directions at Rapijnen.

3.3 Summary of measurements results

Based on the measurement results, some concluding remarks are made regarding the reliability of the measurements and the observed physical processes of jets:

1. The measured discharges are all very close to the design discharges of the pumping stations (Houtkade: 196 m³/min measured vs. 200 m³/min design, Barwoutswaarder: 73 m³/min vs. 75 m³/min and Rapijnen: 98.3 m³/min vs. 100 m³/min);
2. The measurements of the bed profiles are not disturbed by plants. Only the measurements in the side channel at Rapijnen show some discontinuities;
3. The GPS measurements used to determine the channels' geometries have an accuracy of 3 cm in the horizontal direction. This is negligible as the width of the channels is minimal 7 meters. Therefore channel geometries are considered reliable;

4. As **Figure 11**   shows, the measured velocity magnitudes show erratic vertical profiles at Barwoutswaarder and Rapijnen. This could be caused by a combination of large turbulence and too short measurement times (or too small frequencies). The measurements are however not corrected, as the profiles show realistic behavior. At Rapijnen the vertical development of the current direction also shows erratic behavior;

5. The higher velocities at Houtkade are located in the lower parts of the water column. At Barwoutswaarder and Rapijnen the higher velocities are located in the upper parts of the water column;

6. The increase of velocity magnitudes at the surface (Houtkade) found while analyzing the vertical profiles, is probably caused by pressure gradients at these locations. Looking at the current directions, these currents are orientated in the opposite direction or perpendicular to the discharge direction. Therefore it is likely these currents ensure the conservation of mass as is discussed in chapter 1;

7. The backflow along the banks towards the outlet as a result of the entrainment, which was mentioned in literature, is also observed in the field. At Barwoutswaarder and Rapijnen the backflow is clearly visible along at least one the banks of the channel. At Houtkade the entrainment of water is clearly visible north of the structure;

8. The potential core of the jet discussed in the literature is not clearly observable in the measurement results;

9. The attachment of the jets to a bank can be observed at Barwoutswaarder;

10. Discharging in line with the channel direction causes the jet to attach to one of the banks of the channel. At the other bank backflow occurs.

Chapter 4

CFD modeling and validation

The measurements give good insight in the jet behavior with respect to velocity magnitudes and directions, but do not provide 3D insight at all locations in the channel. To acquire this, without risking scaling effects and with the ability to change amongst others the valve angle and the amount of outlets, the Computational Fluid Dynamics (CFD) module of the software package COMSOL was used. In this chapter the model is defined and validated.

4.1 Method

This section starts with a framework on CFD modeling. Subsequently a model definition is given, describing initial conditions, boundary conditions, the physical model and the mesh of the model. Finally the validation method is presented.

4.1.1 Model framework

The way the model approaches a problem is covered by choosing a turbulence model, in some cases combined with a turbulence closure model. There are several turbulence models available in COMSOL, differing largely in computational effort and accuracy. In this case the most appropriate was a Reynolds Averaged Navier Stokes (RANS) model with a k-ε closure model. The RANS model was chosen based on the relatively little amount of required computational effort. The k-ε closure model was chosen, because it is the most used closure model in hydraulic engineering due to its computational efficiency and the overall good quality of the results (Tu et al., 2013).

The models were solved with a time-dependent solver, as they were all very turbulent, which made the problem hard to solve with a stationary solver. A non-stationary approach gives the results the freedom to differ in time when no exact equilibrium situation can be found. By finding the moment that the results do not vary more than within a pre-defined range, the results can be assumed to approximate a stationary solution.

Lastly the choice for the turbulence model and the closure model include some assumptions. Important assumptions of the model concern:

1. The flow at boundary layers:

To describe the flow near walls, the model makes use of so called wall functions. These wall functions are analytical expressions that approximate a velocity profile based on a

roughness parameter of the wall. At default the wall is assumed hydraulically smooth. However, as the roughness parameter was originally developed to describe the roughness in pipes rather than the surface roughness of bed protection material with a large Nikuradse roughness, there is no general value for this parameter in such conditions. Additionally, the effect of this roughness parameter decreases significantly at Reynolds numbers significantly larger than in pipe flow (Wilcox, 2002). The theoretical background of the roughness parameter is discussed in appendix F.

2. The physical approximation of the water surface:
The water surface is defined as a wall with 'slip function'. This describes a situation in which no penetration occurs, but also no boundary layer develops. Practically this means the water level does not change and the velocity is not decreased by any boundary layer. However, observations show the water level does fluctuate when a pumping stations is turned on.

4.1.2 Model setup
The pumping stations were modeled by defining in COMSOL:

1. The geometry;
2. The initial- and boundary conditions;
3. The mesh;
4. The solver settings.

The **geometries** of the pumping stations were determined using the technical drawings regarding their design. Environmental characteristics like the bed profile, the water level, the width of the channel and the angle of the valve (90° is fully opened, 0° is fully closed) were determined during the field measurements on location. The complex bed profiles could not be rebuild easily, so they were approximated with less detail. Visualizations of the models are presented in **Figure 15**. Additionally in **Table 6**, some important parameter values are listed.
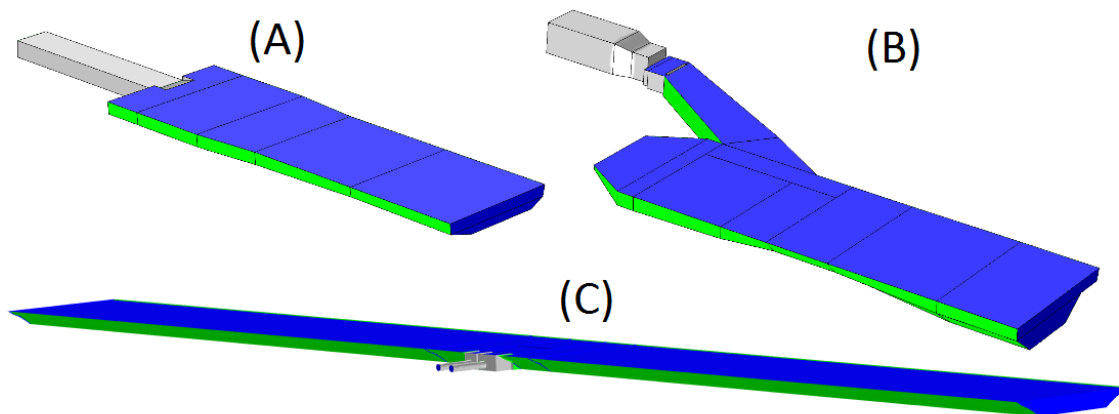
Figure 15: Geometries of the CFD models for (A) Barwoutswaarder, (B) Rapijnen and (C) Houtkade

Table 6: Input parameters for CFD models

Parameter	Houtkade	Barwoutswaarder	Rapijnen
Water level [m]	-0.4	-0.44	-0.33
Discharge [m³/s]	1.64	1.22	1.63
Valve angle [°]	70	90	60

The **initial- and boundary conditions** of the models relate to the characteristics of the medium (water) and the inlets/outlets of the models. Incompressible flow was assumed and the default settings of the medium (temperature, density etc.) were not changed. The inlet velocity was defined as the discharge from **Table 6** divided by the cross area of the pressure lines where the water entered the model (i.e. the inlet). The outlets of the models, located 30-50 meters downstream, were defined as boundaries with an initial pressure condition describing the entire boundary was not subjected to any pressure differences in the initial situation.

The **meshes** of the models were built with high resolutions near the outlet (i.e. first 15-20 meters), because of the expected large turbulence in this region. Further downstream of the structure (i.e. 15-20 meters), the resolutions were chosen lower, as less turbulence was expected here. For Houtkade, spatially the largest model, a mesh was build consisting of tetrahedral elements in the pumping station and in the channel close to the structure. In the context of temporal and computational efficiency, further downstream of the structure, the channel was meshed using triangular elements which were swept along the channel, becoming larger while nearing the outlet. Additional to these so-called domain elements, the mesh was completed with boundary layer elements, to enable more accurate simulations here. Due to more detailed bed profiles at Barwoutswaarder and Rapijnen, the meshes here could not be swept. These meshes consist only of tetrahedral elements and boundary layer elements. The effect of the mesh size was minimized by refining the mesh resolution, while solving the models.

To **solve** the models, first a simplified solution was generated by acquiring a stationary solution with an increased viscosity (1000 times the default). In doing so, the turbulence of the model was decreased, as the Reynolds number is inversely proportional to the dynamic viscosity, and the stationary solver was able to compute a solution. These results were used as an initial solution for the time dependent solver. Subsequently, the time dependent solver was used to simulate 1000 seconds, providing results each 50 seconds. Due to the size of the computed period, the final results were expected to be unaffected by the uncertainty in the initial values. The results of the time dependent solver were analyzed on the variety between the solutions of subsequent time steps. When the results were considered in equilibrium, they were used for further investigation. When this was not the case, the solver was run for a larger amount of time, until an equilibrium situation was found.

4.1.3 Validation method

The models' performance was evaluated by comparing the model results with the measurement results (chapter 3) for all three structures. To determine the ability of the models to reproduce the measured velocity field, several aspects of the velocity field are assessed:

1. The velocity magnitudes over the entire water column at all measured locations;
2. The velocity magnitudes near the bed (i.e. in the lower 0.2 m of the water column);
3. Current directions (x, y) in the entire channel and near the bed;

The velocity magnitudes and current directions are quantitatively compared using the root mean square error (RMSE):

$$RMSE = \sqrt{\frac{\sum_i^n (u_i - \hat{u}_i)^2}{n}} \qquad\qquad \textit{Eq 4}$$

This measure for the estimated error is computed for (1) all data points and for (2) near bed data points. For further analysis of the velocity magnitudes, the averaged absolute relative deviation is assessed:

$$MD = \frac{1}{n}\sum_i^n |RD_i| \qquad\qquad\qquad\qquad \textbf{\textit{Eq 5}}$$

This measure for the relative difference between measured velocities and computed velocities was also evaluated for (1) all data points and for (2) near bed data points.

4.2 Results

First the results of the validation are presented. Subsequently, the results of the models are presented describing the main characteristics of the modeled velocity fields.

4.2.1 Model performance

The comparison of the **velocity magnitudes** at all data points is presented in **Figure 16** and for the near bed data points the comparison is shown in **Figure 17**.
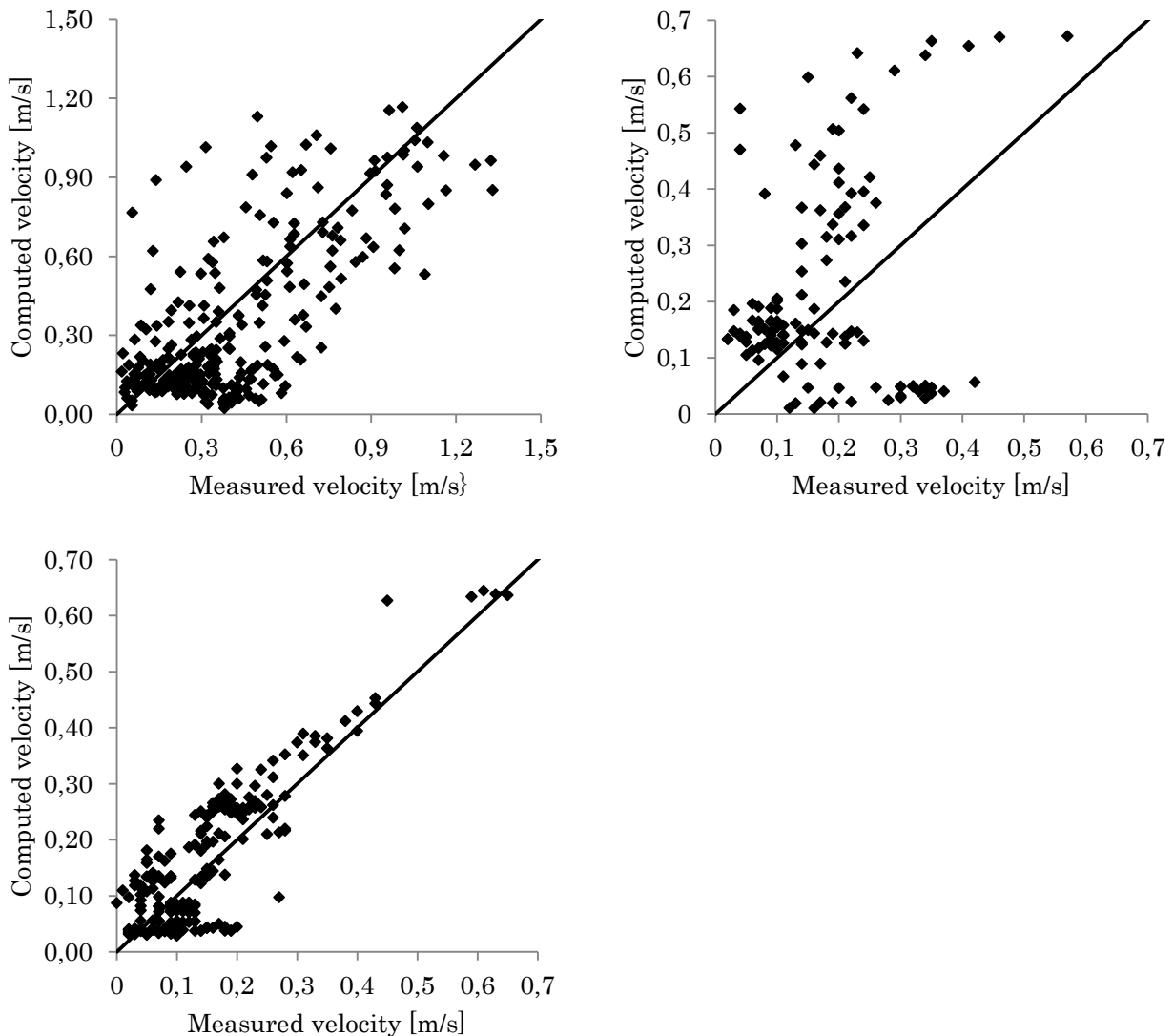
Figure 16: Scatter plot of computed velocity magnitudes as function of measured velocity magnitudes at all data points. **Above**: Houtkade & Barwoutswaarder. **Below**: Rapijnen.
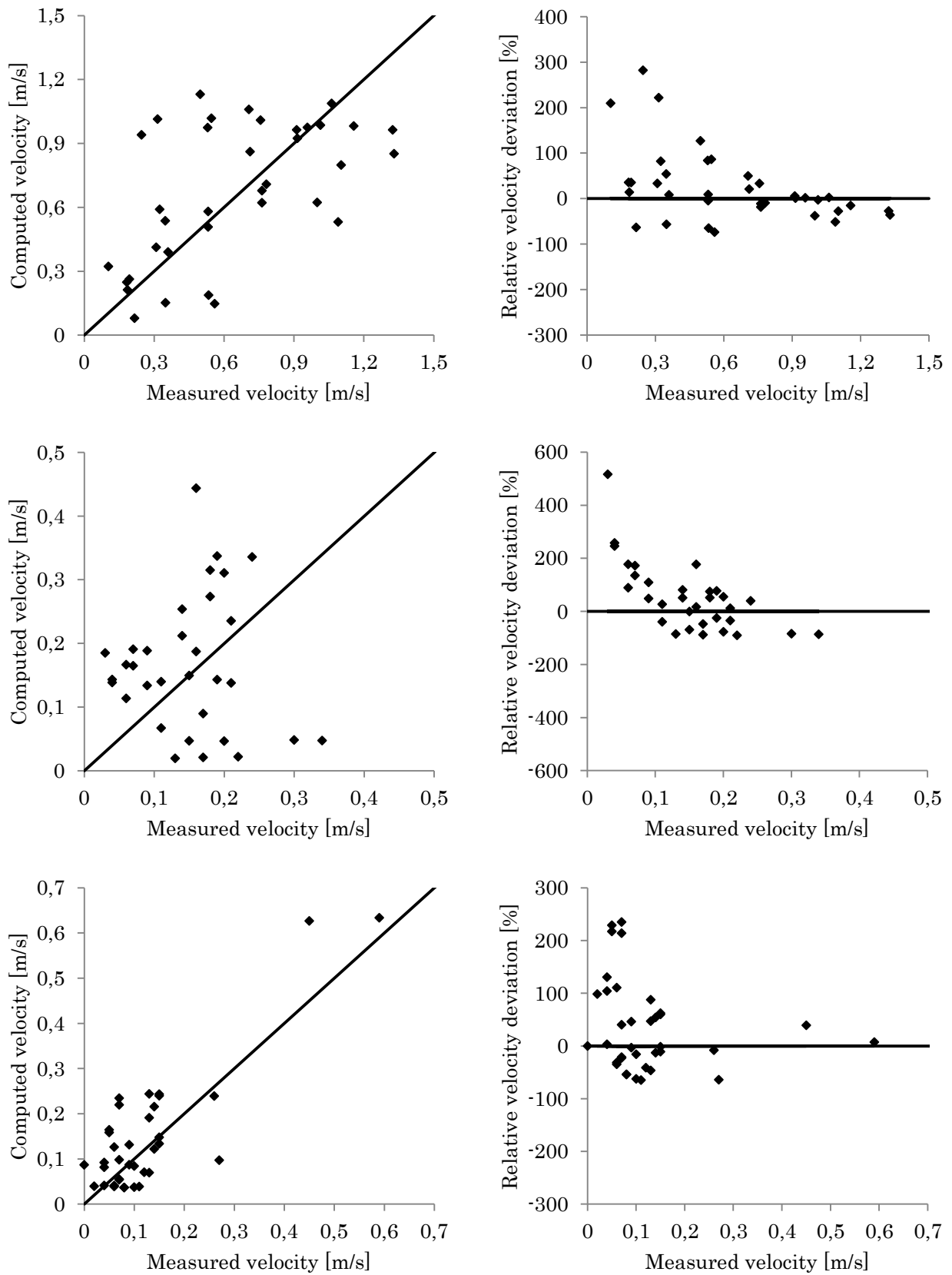
Figure 17: **Left**: Scatter plots with computed velocity magnitudes near the bed as function of measured velocity magnitudes. **Right**: Relative deviations of the modeled velocity magnitudes near the bed as function of the measured velocities. Reading from top down, the figures represent respectively Houtkade, Barwoutswaarder and Rapijnen.

Figure 16 shows for **Houtkade** the scatters are distributed around line x = y, which represents a perfect model. The velocity magnitudes are not generally overestimated or underestimated by the model. There are however some significant outliers observable. For **Barwoutswaarder** the scatters are diverging from the line x = y. The model seems to overestimate the velocity magnitude significantly at several data points. Especially at larger magnitudes, the scatters do not approach the x = y line. For **Rapijnen** the figure shows relatively good comparison. The scatters are concentrated near the x = y line, especially for larger velocity magnitudes.

Figure 17 shows for Houtkade the scatters representing the near bed velocity magnitude are distributed around line x = y. Outliers are mainly found at lower velocity magnitudes (±0.3 m/s). At Barwoutswaarder the velocity magnitudes are deviating significantly from the observed velocities. Relative deviations are often found near 100% or even higher. For Rapijnen the scatters show a good concentration near the line x = y. The relative deviation plot shows mainly for velocities around 0.1m/s some larger deviations (100% or higher).

Table 7 shows the results of the validation with respect to the mean errors and the relative deviations of the velocity magnitudes at all data points and near the bed. For all models the relative deviations are significant. This is partly caused by the over- and underestimations of the small velocities (for Houtkade <0.3, for Barwoutswaarder and Rapijnen <0.1). Looking at the mean error of the near bed velocities (respectively 0.31m/s, 0.13m/s and 0.08 m/s), these errors would at the smaller velocity magnitudes (i.e. 0.3 m/s for Houtkade and 0.1 m/s for the other models) cause a MD of around 100%. Would these low velocity magnitudes be filtered from the data sets, the MD near the bed for the models would respectively be 41.9%, 60.4% and 40.3%.

Table 7: The mean errors and the relative deviations of the modeled velocity magnitudes.

	RSME [m/s]	RSME near bed [m/s]	MD [%]	MD near bed [%]
Houtkade	0.23	0.31	67.3	52.7
Barwoutswaarder	0.19	0.13	119.0	98.3
Rapijnen	0.07	0.08	58.4	66.7

The validation results of the **current directions**, describing the dispersion pattern and the jet behavior downstream of the structures, are presented in **Figure 18** and **Table 8**.

In **Figure 18** it is shown that the scatters at Houtkade are concentrated near the line x = y. This is the case for the entire model, including the near bed directions. Note also, that scatters located in the top left corner of the plots do actually resemble good results as 360° is equal to 0°. At Barwoutswaarder the current directions are modeled with less precision. The range of the computed directions lays between 250° and 60°, while the measured directions vary over the entire range 0°-360°. At the bed the current directions are computed poorly at several locations. At Rapijnen the modeled directions are all in the range 190°-270°. The measured directions show a larger range of mainly 120°-350°. The model however computes correct directions for most data points as the concentration of scatters around the line x = y shows. At the bed the comparison looks similar.

In **Table 8** the mean errors at all data points and at the bed are presented for the models. These show the current directions at Houtkade are better simulated near the bed than in other parts of the water column. For Barwoutswaarder and Rapijnen this is not the case. The mean error at Houtkade is smaller than in the other models. Certainly near the bed the mean error of 34.6° is far lower than respectively 85.6° and 73.9°.
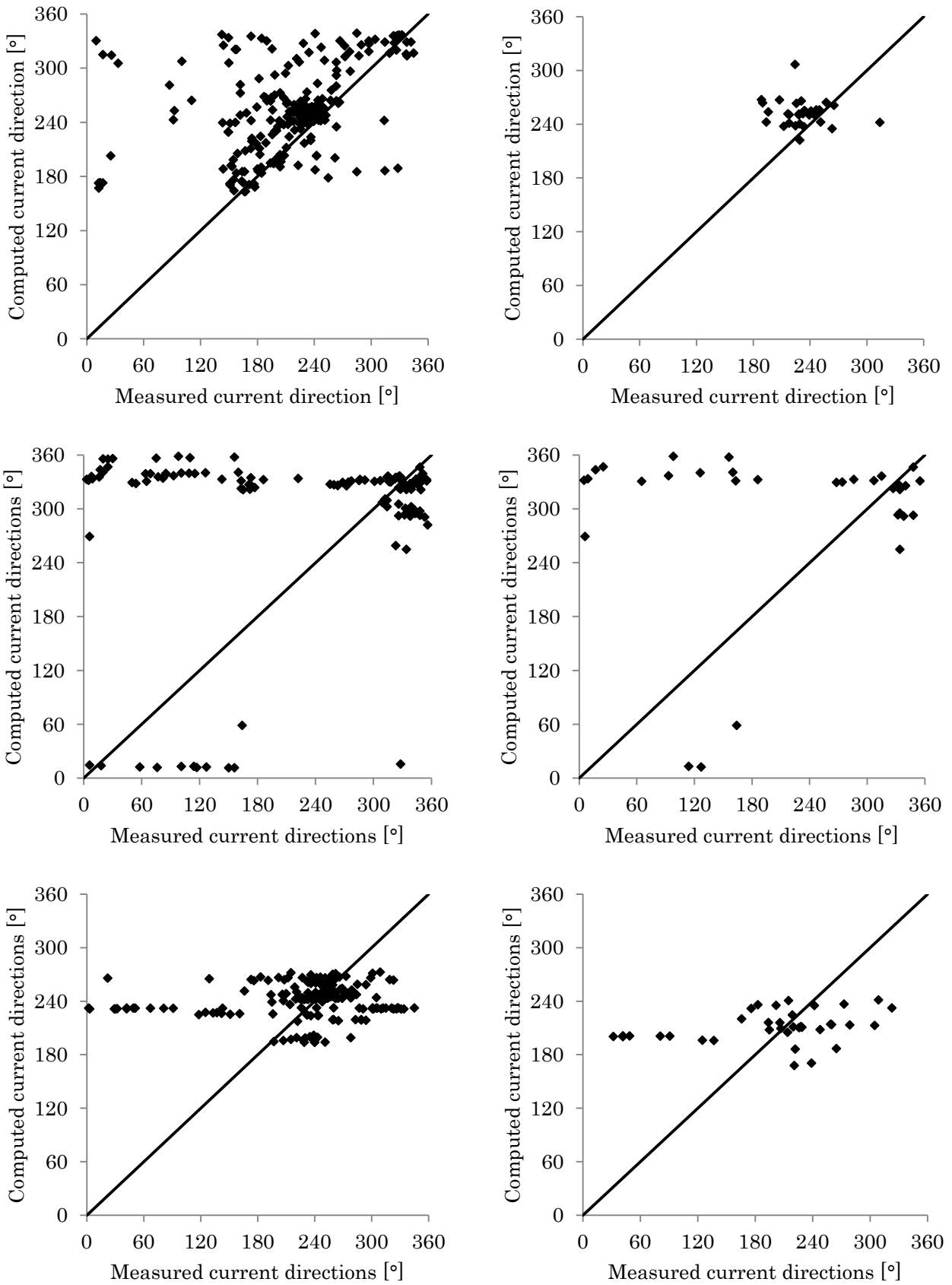
Figure 18: Scatter plots with computed current directions as function of measured current directions. **Left**: at all data points. **Right**: Near the bed. Reading from top down, the figures represent respectively Houtkade, Barwoutswaarder and Rapijnen.

Table 8: Mean errors of the computed current directions for all data points and near the bed.

	RSME [°]	RSME near bed [°]
Houtkade	56.8	34.6
Barwoutswaarder	81.9	85.6
Rapijnen	56.6	73.9

4.2.2 Velocity field behind pumping stations

The results of the models are used to analyze the same aspects as were analyzed with the measurement results, but with the models a total 3D image can be created:

1. Vertical profiles of the velocity magnitude and current direction at several locations;
2. The velocity magnitude distribution over cross sections of the channels;
3. Current directions in the channel.

In **Figure 19** the **vertical profiles** of the velocity magnitudes and current directions are presented for the same locations as in **Figure 11** on page 19. Here the measurement results are included in the figure to enable easy comparison.
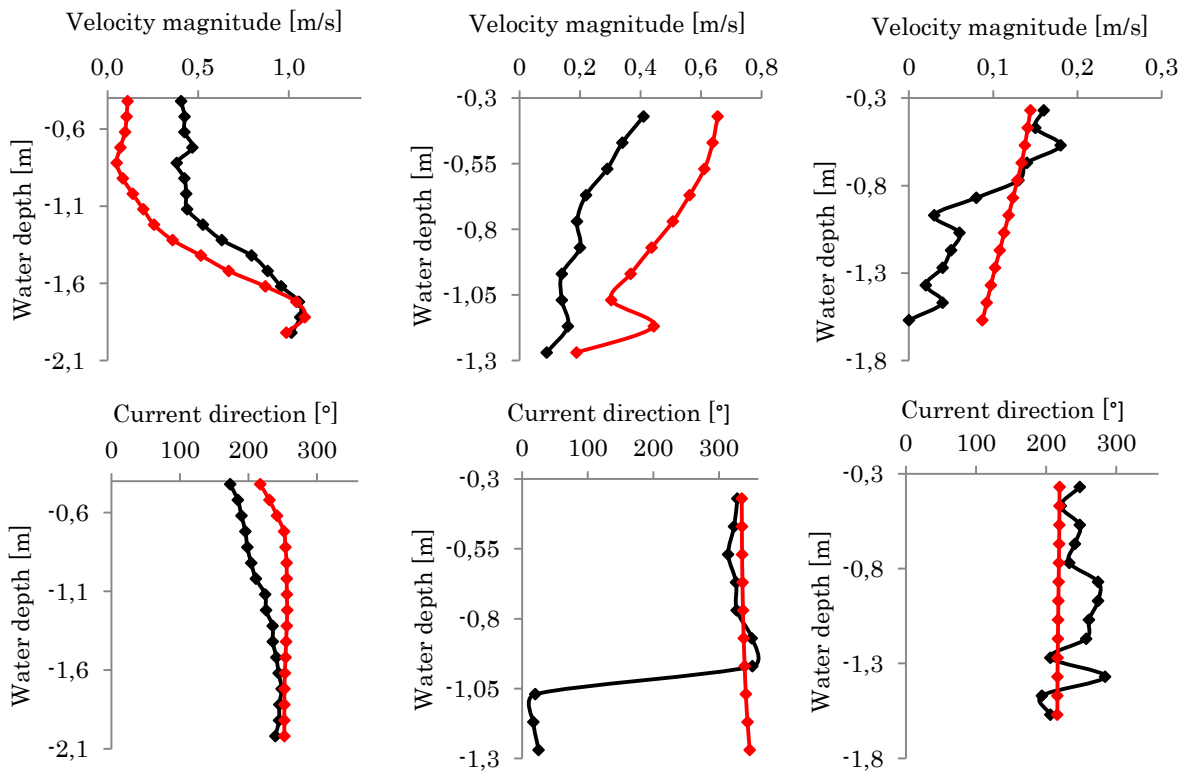
Figure 19: **Above**: Vertical profiles of computed (red) and measured (black) velocity magnitudes at respectively Houtkade, Barwoutswaarder and Rapijnen. **Below**: Vertical profiles of the computed (red) and measured (black) current direction at Houtkade, Barwoutswaarder and Rapijnen.

The figures show that the models describe the vertical profiles of the velocity magnitude and the current direction smoother than the reality according to the measurements. This resembles the fact that the model needs to be considered an approximation of the reality and seemingly large errors and relative deviations found during the validation can be explained with logic.

The computed **velocity magnitude**s as well as the computed **current directions** at the measurement locations are presented in **Figure 20**, **Figure 21** and **Figure 22**.

The computed velocity field at Houtkade (**Figure 20**) shows some similarities and some differences with the measured velocity field. The higher velocities are found in the lower region of the water column. The jets disperse in both the vertical and the horizontal direction. The horizontal dispersion of the jet happens primarily behind the wider outlet structure. After the jets are deflected by the opposite bank, the higher velocities are computed in the upper parts of the water column. Velocity magnitudes are still quite large here (up to 0.4 m/s). On the other side of the channel (where the pumping station is located) the velocities are higher further downstream of the structure (0.2 m/s to 0.1 m/s). The current directions in the upper regions of the water column differ from the (uniform) current directions in the lower regions. Main differences in flow directions with the measurements are found in upper regions of the water column between the two jets.
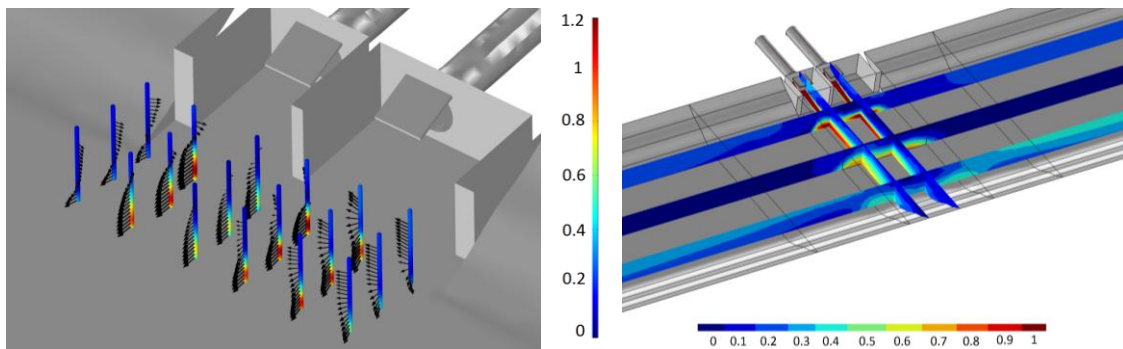
Figure 20: Computed velocity magnitudes and current directions at Houtkade. **Left**: The data represented at the measurement locations. **Right**: Further analysis of the jet behavior.

At Barwoutswaarder (**Figure 21**) The larger velocities are measured in the centre of the channel in the upper parts of the water column. This means the jet does not attach to the bank. At the banks the velocity magnitudes do increase, but this is the cause of backflow/circulation flow. The jet disperses both horizontally and vertically, so near bed velocities do increase further downstream. Eventually the jet develops an uniform flow through the entire channel. Maximum velocity magnitudes decrease from 0.5 m/s to 0.3 m/s in approximately 15 meters. The backflow which was observed in the lower regions of the water column is not computed by the model.
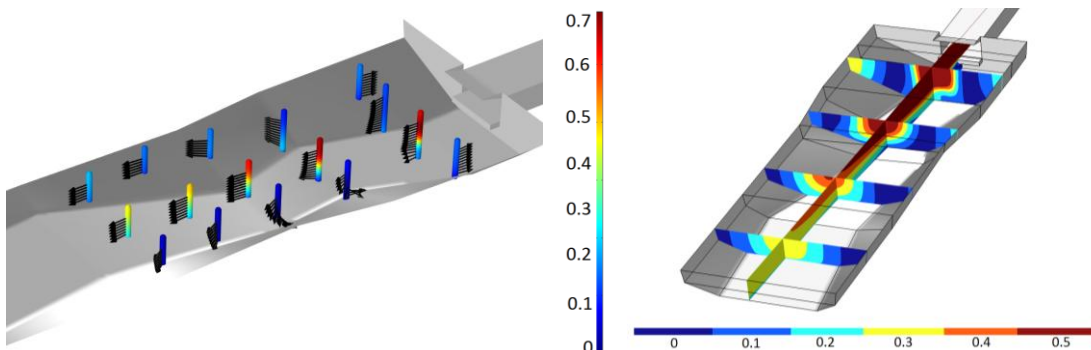
Figure 21: Computed velocity magnitudes and current directions at Barwoutswaarder. **Left**: The data represented at the measurement locations. **Right**: Further analysis of the jet behavior.

At Rapijnen (**Figure 22**) the higher velocities are computed in the upper parts of the water column. With respect to the measurements, the model results show a narrow dispersion pattern of the jet. Especially in the upper parts of the water column the

dispersive behavior is underestimated. The circulation flow/backflow along the banks is overestimated by the model. Upon entering the side channel, the discharge collides with the left bank. This causes the largest velocities to concentrate near this bank. When entering the main channel, the jet first attaches to the left bank before crossing the channel to the opposite bank. The point where the jet reaches the opposite bank is therefore further downstream than the geometry of the channel would suggest. Due to both horizontal and vertical dispersion maximum velocity magnitudes decrease from 0.5 m/s to 0.3 m/s in approximately 15 meters.
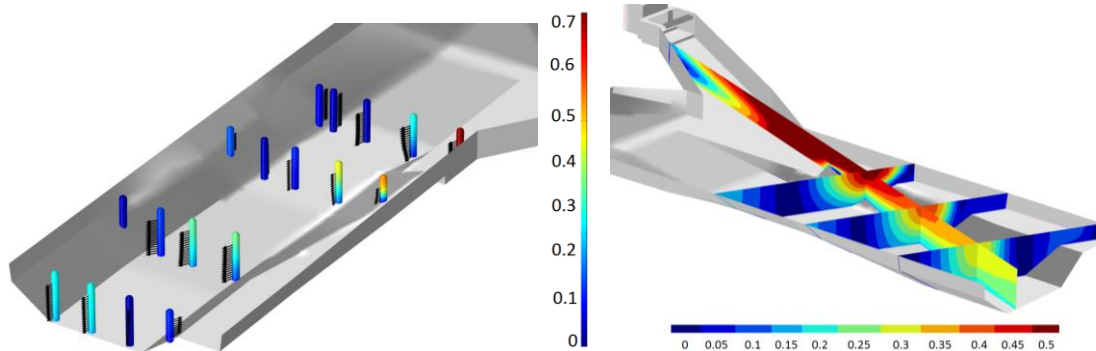
Figure 22: Computed velocity magnitudes and current directions at Rapijnen. **Left**: The data represented at the measurement locations. **Right**: Further analysis of the jet behavior.

4.3 Summary and discussion of model and validation results

In this section the results of this chapter are summarized and discussed using the topics:

1. The performance of the models to reproduce the field measurements;
2. The computed velocity field behind the structures and its differences with respect to the measurement results.

The **performance** of the models is assessed based on the RSME, the MD and the scatter plots of both the velocity magnitudes and the current directions. The important findings in this chapter regarding the model performance are now discussed:

1. The performance of the models with respect to the velocity magnitudes at all data points is variable. The results show no significant over- or underestimation caused by the approximation of the model. At Houtkade and Rapijnen the simulated velocity magnitudes are distributed around the line x = y, while at Barwoutswaarder this is not the case. Rapijnen (relative deviation of 58.4%) performs better than Houtkade (67.3%) and Barwoutswaarder (119%). The largest deviations at Rapijnen are observed at lower velocity magnitudes. At Houtkade the large deviations are found over the entire range of velocity magnitudes. Barwoutswaarder shows rather poor comparison to the field measurements;
2. The velocity magnitudes near the bed are best modeled at Houtkade (52.7%). For Barwoutswaarder and Rapijnen the relative deviations are respectively 98.3% and 66.7%. **Figure 17** shows the largest deviations are found at lower velocity magnitudes. Higher velocities are modeled more accurate. Also this figure shows the near bed velocity magnitudes are overestimated for lower velocities, while higher velocities are more often slightly underestimated. As lower near-bed velocities are often found further downstream of the structure, the models are very likely to

overestimate the distance behind a structure at which certain velocity magnitudes occur;

3. With respect to the current directions, the scatter plots in **Figure 18** show the range of current directions is larger in the measurements than in the models. The models show a maximum range of 180°, while the measurements often show a range of the full 360 degrees. This means the models generate smoother flow patterns than that were measured in the field. The models of Houtkade and Rapijnen compute the current directions at all data points together with a similar accuracy (mean error of 56.8° vs. 56.6°). At Barwoutswaarder the current directions are computed with less accuracy (mean error of 81.9°);

4. Near the bed, the range of the simulated current directions at Houtkade is similar to the measured range. At Barwoutswaarder and Rapijnen the ranges still differ significantly as was the case for the entire model. The mean error in the current directions is therefore for Houtkade (34.6°) far smaller than for Rapijnen (73.9°) and Barwoutswaarder (85.6°);

5. Overall the model of Houtkade is considered the most accurate in this study, as the current directions and the velocity magnitudes at the bed are computed with more accuracy than with the other models. The largest restriction of the model, based on the validation results, is the overestimation of the smaller velocities located further downstream of the structure.

The **computed velocity field** behind the structures is compared to the measured velocity field and theoretical knowledge on jet behavior. Here further weaknesses and strengths of the models are identified and the velocity field behind the structures is analyzed.

1. The general characteristics of the models differ from the measurements on some important points:
   ➤ The computed velocity and current direction profiles over depth at Barwoutswaarder and Rapijnen show smoother behavior than the measurements suggest. At Houtkade the measurements show a less erratic profile and the simulation therefore differs less from the measurements. This can also be seen in **Figure 19**;
   ➤ The models all overestimate the backflow along the banks. This affects the dispersion of the jets and the velocity magnitudes in the jets and the banks;
   ➤ The suggested jet attachment to the bank (Barwoutswaarder) derived from the measurements, is not observed in the results of the model.

2. The observed results of the models show some discrepancies to expected jet behavior based on the theoretical framework sketched in Chapter 1:
   ➤ Upon leaving the outlet, the jet develops from the potential core to a diffused jet (mixing length of approximately 6 times the outlet diameter). In the potential core the maximum velocity (i.e. centerline velocity) is not affected by water entrainment. However, the model results show the centerline velocity starts decreasing immediately upon entering the channel;
   ➤ The dispersion of the free jet is estimated at a rate of 1:6. The design rules for bed protection use dispersion angles of 1:10 and 1:6 to determine respectively the required length of the bed protection (i.e. the decrease rate of the centerline velocity) and the required width of the bed protection. The models show the need for this rather conservative approach. The dispersion angles found in the models differ for each individual model.

3. At Houtkade the modeled velocity field downstream of the structure develops with the following characteristics:
   - The largest velocity magnitudes are concentrated near the bed. In the upper parts of the water column the velocities are higher than in the centre parts, as backflow ensures the conservation of mass here;
   - The dispersion of the jets is relatively wide compared to the results of the other models, because the jets are not restricted in developing wider. The jets disperse wider behind the wider outlet structure. This causes larger maximum velocity magnitudes behind the small outlet structure;
   - The overestimation of backflow along the bank causes the jet to stay close to the bank further downstream of the structure. This could cause an overestimation of the velocity magnitudes in this region as dispersion is limited and therefore the energy stays concentrated;
   - Before colliding with the opposite bank, a large portions of the jets deflects into the channel. The remainder of the jet travels towards the bank at a slower pace. This behavior is probably caused by the large turbulence in this region. This causes the averaged velocities to be smaller than the actual occurring velocities. This is an additional weakness of the model of Houtkade.
4. At Barwoutswaarder the velocity field downstream of the structure develops with the following characteristics:
   - The largest velocity magnitudes are concentrated near the water surface. The lateral cross sections contain 3 regions where velocity magnitudes are large: At the banks of the channel and in the centre of the channel;
   - The increased velocity magnitudes at the banks are caused by backflow. This backflow seems to be overestimated and forms a restriction for the dispersion pattern of the jet. Therefore the velocity magnitudes initially stay large and the dispersion rate is smaller than at Houtkade. After the region with backflow is passed, the jet disperses significantly more;
   - Upon entering the channel, the jet travels to the centre of the channel. This is different from the measurement results. These show the jet attaches to the bank and backflow only occurs at the other bank;
   - Further downstream of the structure, the jet starts to develop a uniform flow through the channel.
5. At Rapijnen the velocity field downstream of the structure develops with the following characteristics:
   - The largest velocity magnitudes are concentrated near the water surface. Also here the lateral cross sections contain 3 regions where velocity magnitudes are large: At the banks of the channel and in the centre of the jet, which crosses the channel at an angle;
   - Increased velocity magnitudes at the banks are caused by backflow. Also here the overestimation of the backflow, certainly at the water surface, causes a restriction for the dispersion of the jet;
   - Due to the overestimation of the backflow further downstream of the structure, the jet stays narrow and does not develop an uniform flow, while this is the case according to the measurements.

As the models are used to predict velocity field behavior downstream of structures, it is important to keep in mind the mentioned weaknesses of the model.

Chapter 5

Sensitivity analysis

The model study provided a more detailed insight in the 3D, compared to field measurements and additionally identified the best performing model. However, conclusions cannot yet be drawn concerning the effects of the valve angle and the presence of multiple outlets on the velocity field. Therefore a sensitivity analysis was carried out on one of the models to assess the effects of these features in a quantitative manner. As the validation showed that the model of Houtkade is the best performing for this study, this model was used for the sensitivity analysis.

5.1 Analysis method

The effect of the valve angle was investigated by computing the flow field behind one of the outlets at different valve angles (30°, 45°, 60°, 75° and 90°). The effects of multiple outlets on the velocity field were investigated by computing the velocity field behind Houtkade where both outlets are discharging. This was done for all valve angles. These results were than compared with the results of the single outlets. The setup of this investigation is presented in **Table 9**.

The geometry of the model was adjusted in order to perform the sensitivity analysis for the effect of multiple outlets. The outlet structures of the pumping station were made identical to exclude the effect of different structure dimensions.

Table 9: Setup for sensitivity analysis with the model of Houtkade

Run number	Discharge outlet 1 [m³/s]	Discharge outlet 2 [m³/s]	Valve angle [°]
Run 1	0	1.64	90
Run 2	0	1.64	75
Run 3	0	1.64	60
Run 4	0	1.64	45
Run 5	0	1.64	30
Run 6	1.64	1.64	90
Run 7	1.64	1.64	75
Run 8	1.64	1.64	60
Run 9	1.64	1.64	45
Run 10	1.64	1.64	30

The effects of the valve angle and the interaction of multiple discharges on the velocity field behind pumping stations were quantitatively expressed using velocity field characteristics:

1. The maximum near bed velocity magnitude at the bed and its distance downstream of the outlet;
2. The development of the near bed velocity behind the outlet, before the jets are deflected by the opposite bank;

These characteristics were made dimensionless by relating them to the model's initial conditions. The velocity magnitudes were expressed relative to the width and depth averaged velocity in the outlet u_o and the distance downstream of the structure was expressed relative to the outlet diameter D_o (as these are important parameters for the jet development in Eq 1, 2 and 3).

The maximum near bed velocity magnitude and its location were compared for all computations mutually. The development of the near bed velocity behind the outlet was for each computation compared to the expected development according to Eq 1 and Eq 2. Additionally the near bed velocity development for all computations were compared mutually. The near-velocities were only assessed before the jets were deflected by the bank, because the turbulence and the deflection of the jets are very likely to affect the velocity field.

5.2 Parameter sensitivity results

In **Figure 23** the development of a jet when affected by the **valve angle** is presented. It is observed that the maximum velocity magnitude near the bed increases when the angle of the valve decreases (i.e. when the valve closes). Also the location where the maximum near bed velocity occurs, shifts towards the outlet. The near-bed velocities however seem to decrease at a higher rate.

To enable easier comparison between the different situations, **Figure 24** and **Figure 25** show respectively the maximum velocity magnitude and its location and the velocity development near the bed for all situations. The behavior of the velocity field when affected by the angle of the valve observed in **Figure 23** is acknowledged here. The maximum velocity magnitude near the bed is larger when the valve angle is smaller. Also it is located closer to the outlet. Between 90° and 30° the maximum velocities differ a factor 2.6. The maximum velocity at the bed when the valve is 30°, exceeds the depth and width averaged outlet velocity by a factor 1.1. The location of the maximum velocity for smaller angles is much closer to the structure than for larger valve angles. Especially the large 'step' between the location at 60° and the location at 75° is striking.

The development of the near-bed velocity magnitudes (**Figure 25**) shows the velocity decreases faster when the valve angle is smaller. The model results show initially low near-bed velocities, as the jet has not reached the bed here. When the jet reaches the bed, the velocities increase rapidly for the smaller valve angles (30°, 45° and 60°). At larger valve angles (75° and 90°) the increase of near-bed velocity occurs more slowly. The decrease of the velocity magnitude after reaching its maximum is also faster for the smaller valve angles (especially for 30° and 45°). Eventually the velocity magnitudes of 30° drops under the velocity magnitudes of 45°, 60°, 75° and even 90°. The velocity magnitudes of the 45° situation drop under the velocity magnitudes of 60°, 75° and 90°. This indicates that the velocity magnitudes near the bed decrease faster when the valve angle is smaller.

Angle: 30

Angle: 45

Angle: 60

Angle: 75

Angle: 90

0 0.1 0.2 0.3 0.4 0.5 0.6 0.7 0.8 0.9 1
velocity magnitude [m/s]
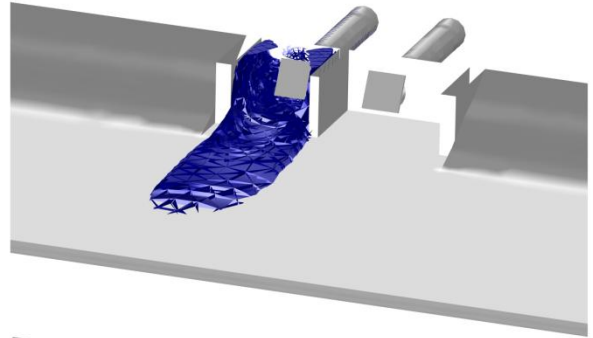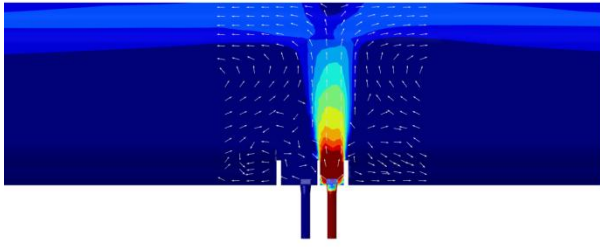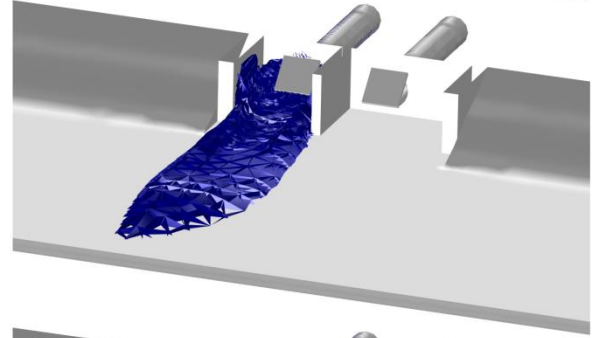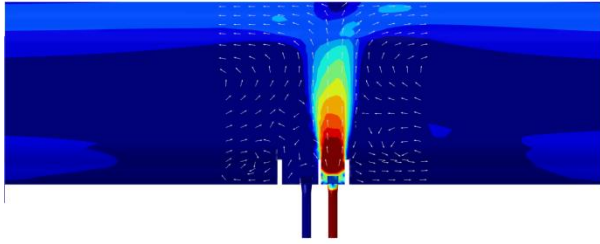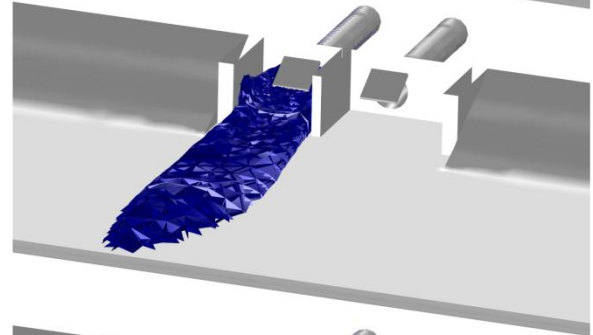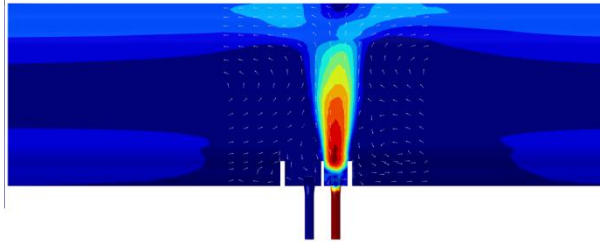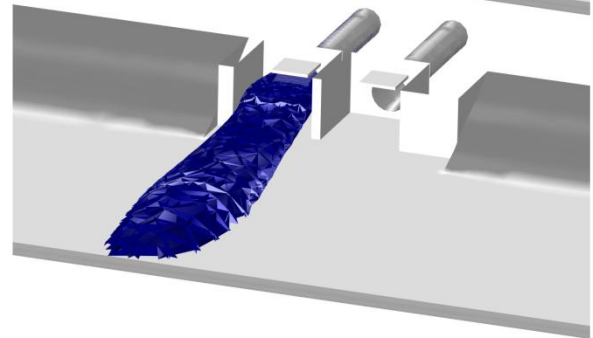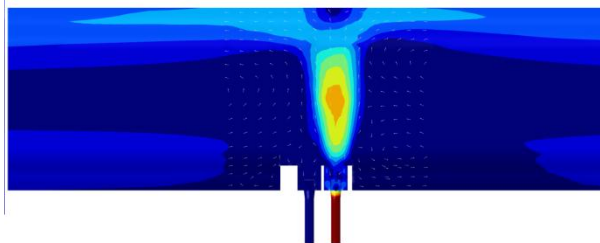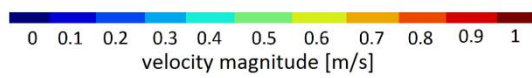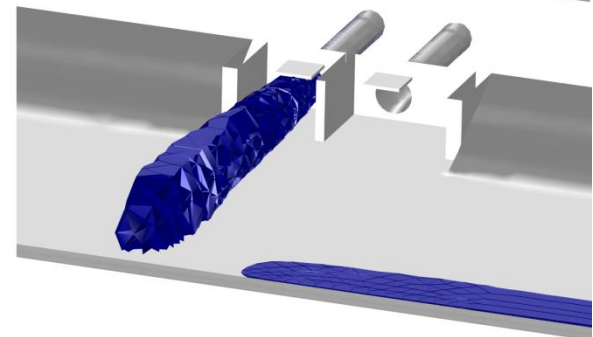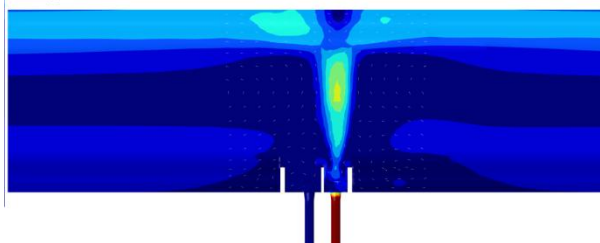
Figure 23: **Left**: The near-bed velocity field. **Right**: The 3D orientation of the jet (where velocities exceed 0.5 m/s).
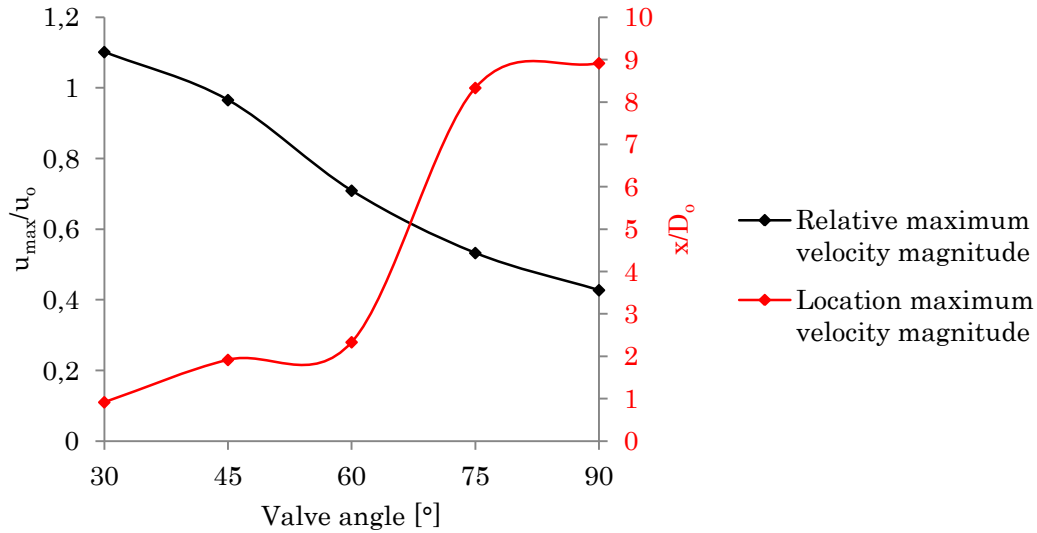
Figure 24: The relative maximum velocity magnitude (black) and the location of this maximum velocity magnitude (red). The maximum velocity magnitude is expressed relative to the expected outlet velocity u_o (i.e. discharge/flow area). The location where this occurs is expressed relative to the outlet diameter D_o.
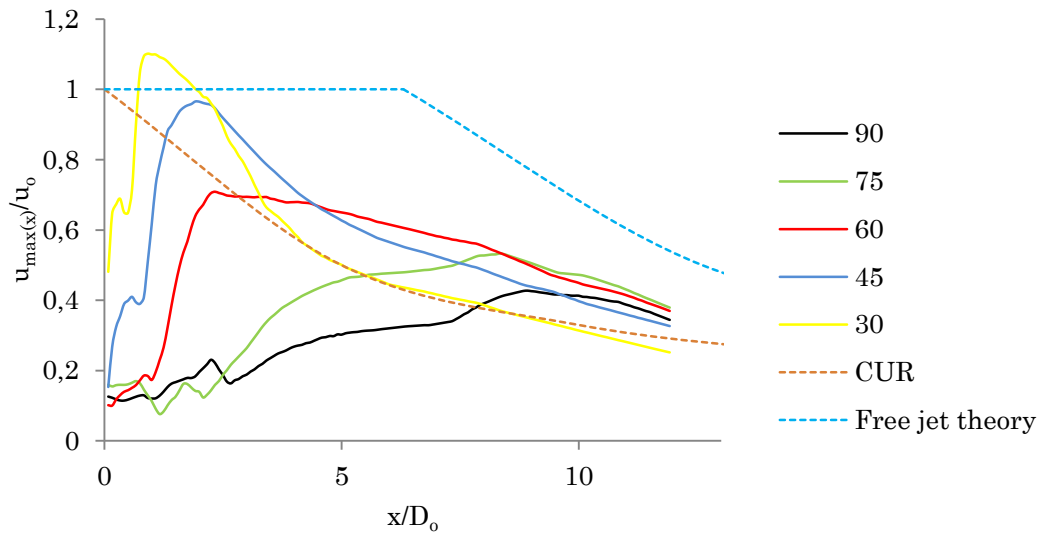
Figure 25: The development of the near bed velocity when moving downstream of the structure for all valve angle situations. The maximum velocity magnitude at a distance x ($u_{max(x)}$) is expressed relative to the expected outlet velocity u_o, while the distance is expressed relative to the outlet diameter D_o. The figure additionally contains the expected velocity development based on free jet theory and the current design rules for bed protection.

When comparing the velocity magnitude development of the different situations in **Figure 25** with the expected velocity development based on the CUR rules, some of the velocity development characteristics can be extracted from the figures. The expected velocity development of the CUR shows the deceleration of the jet near the bed decreases with distance (as the slope of the curve decreases). This is also observed clearly in the situations where the valve is 30° and 45°. At 60° this is however not observed. The other jets have not yet developed far enough to observe this behavior. The dimensionless velocity profile of the CUR rules starts at a value 1, as the design rules actually describe the development of the depth averaged velocity magnitude. The model results show the dimensionless near-bed velocity magnitude. This starts lower, as it takes some time for the jet to reach the bed. The initially erratic profile in the first region after the outlet is

caused by the turbulence in the outlet structure. According to the figure, the CUR design rules underestimate some of the modeled jet development when traveling further downstream. Note however that the slope of the curves suggests that the modeled magnitudes would eventually decrease under the expected magnitudes by the CUR further downstream. This can however only be speculated.

Comparison to the free jet theory also shows the decreasing deceleration of the jet when traveling further downstream. All modeled velocity magnitudes (with an exception of the maximum velocity magnitude at 30°) are lower than the magnitudes expected by the free jet development. Also the curve of the CUR rules lies lower than the free jet theory curve. This suggests that the jet velocities decrease significantly due to restrictions in practical applications.

The 3D schematizations of the jets presented in **Figure 23** show some explanations for the observed behavior. The maximum velocity magnitudes near the bed are larger when the valve angle is smaller, because the jet is deflected towards the bed. At smaller angles, this deflection becomes steeper (i.e. higher velocities occur). As the valve directs the jet towards the bed, it also shifts the location of the maximum velocity magnitude closer to the outlet. The velocity magnitudes at the bed decrease faster, as the closing of the valve increases the turbulence in the outlet structure and at the bed, inducing more dissipation of the energy.

In **Figure 26** the development of the velocity field near the bed is presented when **both outlets are discharging**. The figures show similar maximum velocity magnitudes as with a single discharge (**Figure 23**). The location of the maximum velocity also seems to be very similar. The decrease rate of the near bed velocity magnitudes are comparable before the jets are deflected by the opposing bank. After deflection the decrease rate seems lower and higher velocities occur with respect to the single outlet situation. Overall the width of the region where higher velocities are found is obviously larger. This seems to be mainly caused by the fact that two outlets are discharging. No increase or decrease in horizontal dispersion rate is noticed.

In **Figure 27** the maximum near bed velocity magnitude and its location are compared for a single outlet and a double outlet. The results show, with an exception of the maximum velocity location at 60°, very similar magnitudes. The maximum near bed velocity magnitude at the single outlet is slightly higher for the larger valve angles. The locations of the maximum near bed velocity at smaller angles are for the single discharge slightly closer to the structure.

In **Figure 28** the velocity development of the situations with a single outlet are compared to the situations with a double outlet. With a valve angle of 90°, larger velocity magnitudes are observed downstream of a single outlet. This is also the case with a valve angle of 75°. With a valve angle of 60°, the velocity magnitudes are slightly higher for the double outlet situation. With smaller valve angles (45° and 30°), differences between the velocity magnitudes are small (approximately 7%). The velocity magnitudes downstream of the double outlet are higher. The deceleration rate of the centerline velocity (i.e. the slope of the curve) is also very similar.

Figure 26 shows the velocity magnitudes after deflection (directed into the channel) are larger at the double outlet than at the single outlet. Because (1) the geometry of the channel changes here, (2) the validation shows an overestimation of the backflow/circulation flow (causing a restricted dispersion pattern in this region) and (3) the overestimation of smaller velocity magnitudes, the behavior in this region is not further analyzed.

Angle: 30

Angle: 45

Angle: 60

Angle: 75

Angle: 90

0   0.1   0.2   0.3   0.4   0.5   0.6   0.7   0.8   0.9   1
velocity magnitude [m/s]
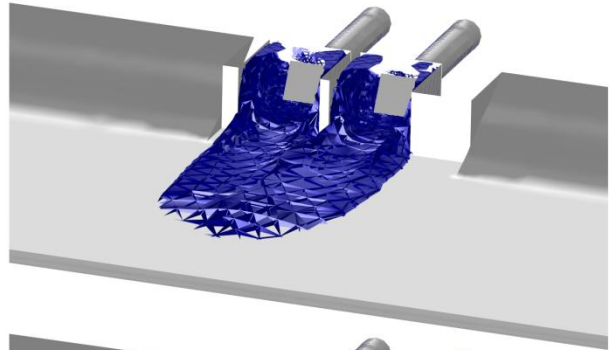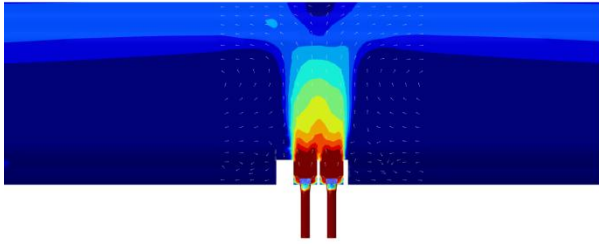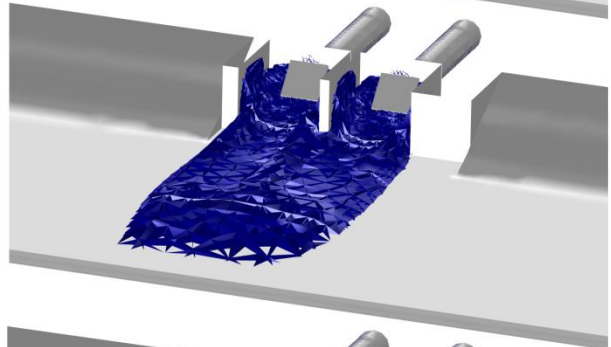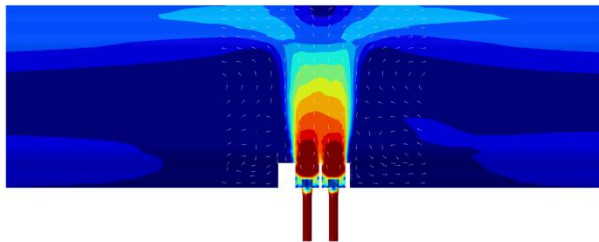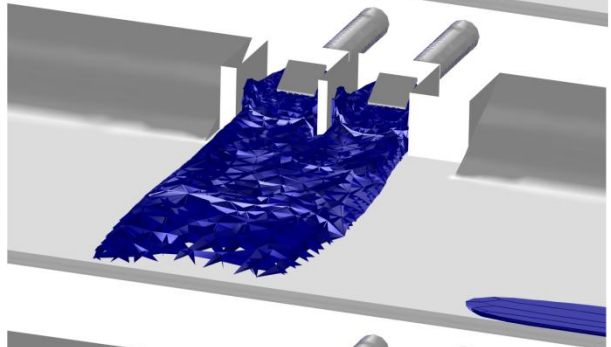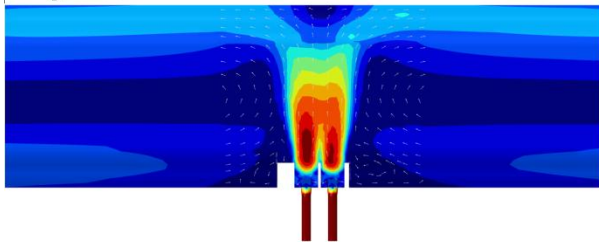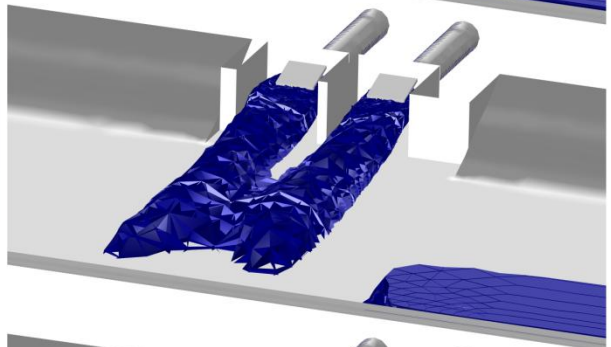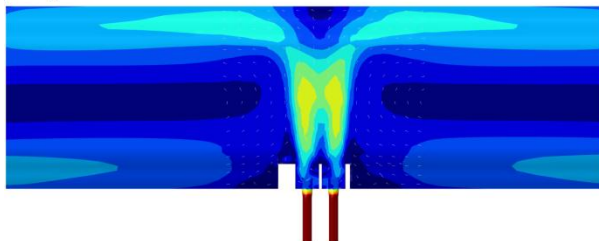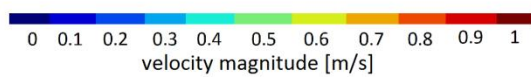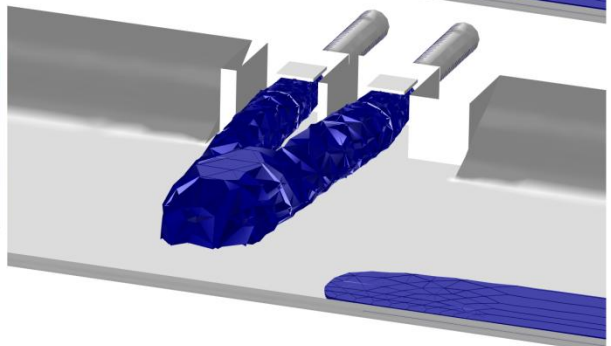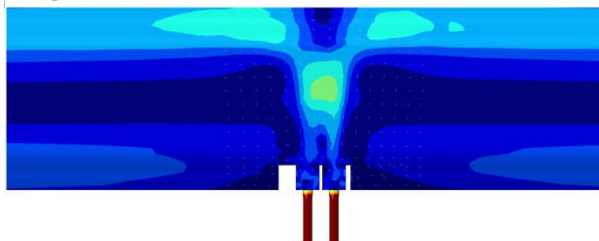
Figure 26: **Left**: The near bed velocity field. **Right**: The 3D orientation of the jet (where velocities exceed 0.5 m/s).
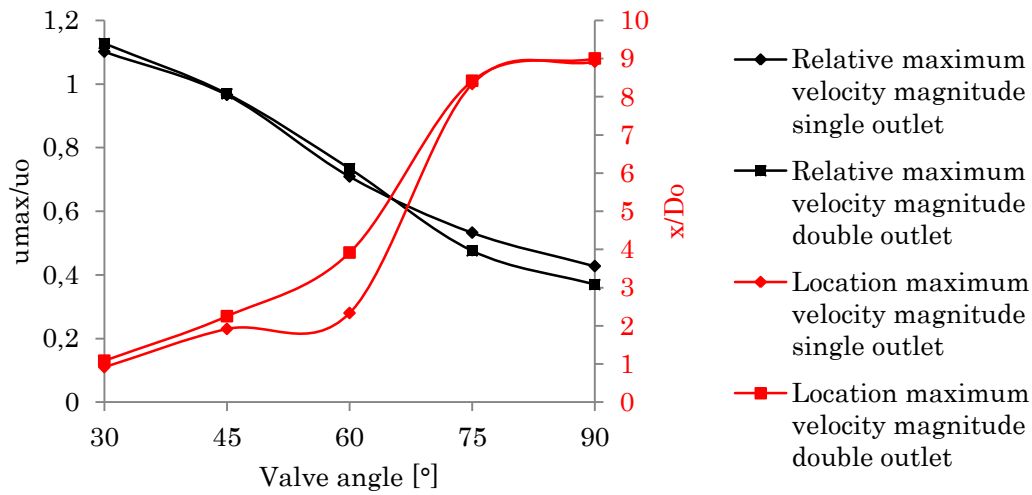
Figure 27: The relative maximum velocity magnitude (black) and the location of this maximum velocity magnitude (red) for a single outlet and for a double outlet. The maximum velocity magnitude is expressed relative to the expected outlet velocity u_o (i.e. discharge/flow area). The location where this occurs is expressed relative to the outlet diameter D_o.
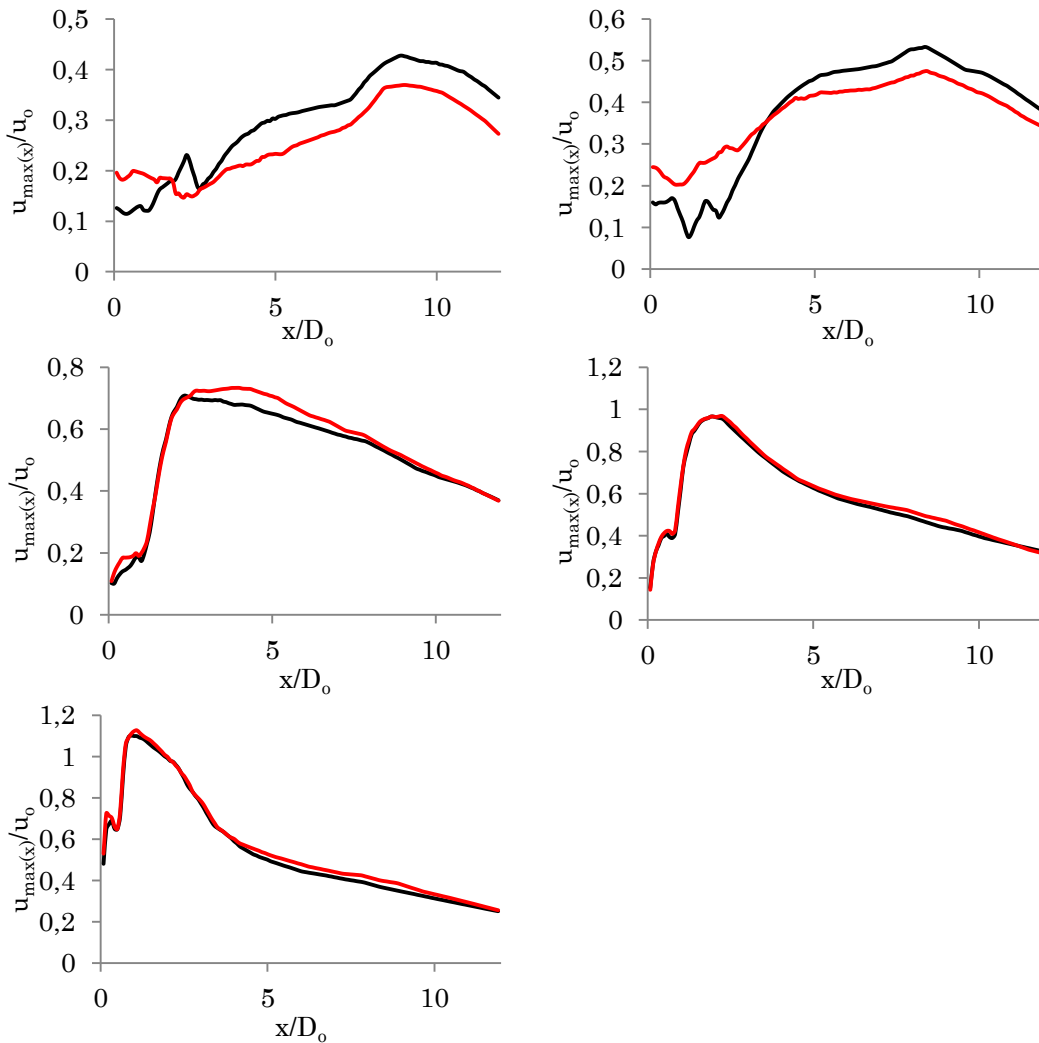
Figure 28: The comparison of the near bed velocity development when moving downstream of the structure for a single outlet (black) and a double outlet (red) for all valve angles. The figures represent respectively 90°, 75°, 60°, 45° and 30°. The maximum velocity magnitude at a distance x ($u_{max(x)}$) is expressed relative to the expected outlet velocity u_o, while the distance is expressed relative to the outlet diameter D_o.

41

5.3 Sensitivity analysis discussion

In this section the results of the sensitivity analysis are summarized by analyzing the effect of the valve angle and multiple outlets on the velocity field downstream of Houtkade. Additionally, in 5.3.2 the consequences of these results for the required bed protection is analyzed.

5.3.1 The effects of the valve angle and the interaction of multiple outlets

The **valve angle** affects the maximum near bed velocity magnitude downstream of the structure, the location of this maximum velocity and the deceleration rate of the jet. This is caused by the deflection of the jet towards the bed and the increased turbulence inside the outlet structure.

The maximum near bed velocity magnitude increases when the valve angle is smaller. At an angle of 90°, the maximum velocity is significantly smaller than the depth and width averaged velocity at the outlet (in this case approximately a factor 0.43). When the angle decreases (i.e. the valve closes) the maximum velocity magnitude increases to respectively 0.53, 0.71, 0.97 and even 1.1 times the outlet velocity. This means the maximum velocity magnitude near the bed can exceed the depth and width averaged outlet velocity. Note that the maximum near-bed velocity magnitude at an angle of 30° is 2.6 times larger than at an angle of 90°. At the double outlet situation, the maximum near-bed velocity magnitude shows similar behavior when affected by the valve angle.

The location of the maximum near bed velocity magnitude shifts towards the structure when the angle is smaller. At an angle of 90°, the jet is not deflected by the valve and the maximum velocity near the bed is eventually found a distance of $9D_o$. The increase of the velocity at the bed is mainly caused by the vertical dispersion of the jet. When the angle decreases, the jet is deflected towards the bed. This causes the centerline velocity to be directed towards the bed. At 75° this causes the location to be slightly closer to the outlet (i.e. $8.5D_o$). At smaller angles the location is significantly closer to the structure. At 60°, 45° and 30° the maximum velocity magnitude lays respectively $2.3D_o$, $1.9D_o$ and $0.9D_o$ downstream of the structure. At the double outlet situation, the location shows similar values except for the 60° angle. The transition between 45°, 60° and 75° is more smooth here.

The near bed velocity development downstream of the structure depends largely on the valve angle. At large angles (90° and 75°) the velocity magnitude slowly approaches its maximum. At angles of 60°, 75° and 90° the maximum velocity magnitude (which is higher) is reached considerably faster. Besides reaching the maximum velocity sooner, the jets from the smaller angles also decrease towards smaller velocities faster. This means the effect of the valve angle on the distance downstream of the structure at which a certain velocity magnitude is no longer exceeded, depends on the magnitude of this value. At smaller valve angles the higher velocities reach further downstream than at larger angles, while on the other hand smaller velocities are reached faster due to the larger deceleration. This means the effect of the valve angle on the required bed protection length depends on the critical velocity.

The **interaction of multiple discharges** affects the maximum near bed velocity slightly. At larger valve angles (i.e. 90° and 75°) the maximum near bed velocity magnitudes downstream of the structure are smaller (a factor 0.86 and 0.89). The locations of the maximum near-bed velocity are only affected on a small scale.

The development of the near-bed velocity when traveling downstream is affected by the double outlet. For larger valve angles the addition of an outlet causes smaller near-bed velocity magnitudes. At 60° the velocity magnitudes are slightly larger for the

double outlet situation. For smaller velocities (i.e. $u_{x(max)}/u_o<0.45$) the differences between the two situations are negligible. At small valve angles the addition of an outlet causes a slight increase of the velocity magnitude. This increase is however very small (maximal 7%).

The presence of multiple outlets seems to translate mainly in a significant increase in jet width with respect to a single outlet situation, which is simply caused by the addition of an outlet. The suggested higher bed velocities after the jets deflect due to the opposing bank, are likely caused by the larger total discharge which disperses at a similar rate as at a single outlet situation. This is caused by the limited possibility to disperse as a result of the overestimated circulation flow. Additionally the slope of the bank (i.e. smaller depth) causes the velocities to increase further. This is therefore not considered an effect of the double outlet.

5.3.2 Consequences for required bed protection dimensions

The effect of the **valve angle** on the required bed protection length cannot easily be formulated as it depends on the critical velocity of the bed material. This means the required bed protection length behind an outlet with a certain valve angle, cannot be related to a portion of the required bed protection length behind an outlet where the valve angle is different. Partly this is caused by fact that the maximum near-bed velocity is higher for smaller valve angles, while the dimensionless velocity profile eventually drops under the dimensionless development of the near-bed velocity behind larger valve angles.

These characteristic effects of the dimensionless velocity profiles when affected by the valve angle were already visualized in **Figure 25**. In **Figure 29** the required lengths for bed protection per valve angle are presented in terms of D_o for several critical bed velocities. Comparing the required bed protection length when the critical velocity is $0.4u_o$, shows the required bed protection length is largest for the 75° situation. For 30° the required length is however smaller than for 90°. However for larger values of the u_c/u_o-ratio, no bed protection is needed behind structures with larger valve angles. From the figure more examples can be pointed out which prove that the effect of the valve angle on the required bed protection length cannot be described with a straightforward relation between required bed protection lengths for 90° and other angles.
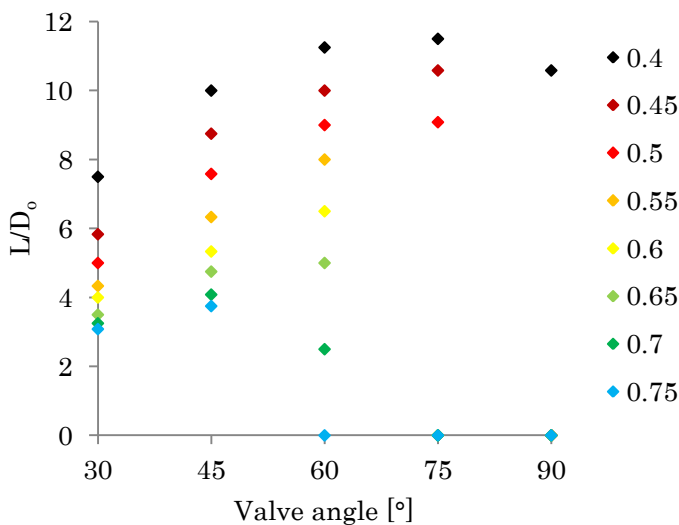
Figure 29: The required dimensionless bed protection length per angle for different dimensionless critical velocities (i.e. u_c/u_o-ratios).

The figure shows that the likeliness that a bed protection is necessary, is larger behind structures with small valve angles. Therefore it could be stated that additional rules are necessary to take into account the effect of a valve. However, the current improvised rule that takes into account the effect of the valve increases the bed protection length, regardless the effect of the critical velocity magnitude of the bed material. This will cause significant oversizing of the bed protection at smaller valve angles when smaller critical velocity magnitudes are used. In **Figure 30** the effect of using the improvised rules to take into account the valve of the angle is presented. The results show the current design rules for bed protection, which are suspected to oversize the bed protection, actually undersize the bed protection length for the 'normal' situation (single outlet and 90°). The figure shows that the modeled dimensionless velocity field approaches the CUR-line for smaller dimensionless critical velocities. Certainly for smaller valve angles, the improvised rules overestimate the velocity magnitudes significantly. For example: at lower critical velocity magnitudes (i.e. an u_c/u_o-ratio of 0.4), the bed protection length behind the 30° outlet is designed 3.5 times longer than necessary.
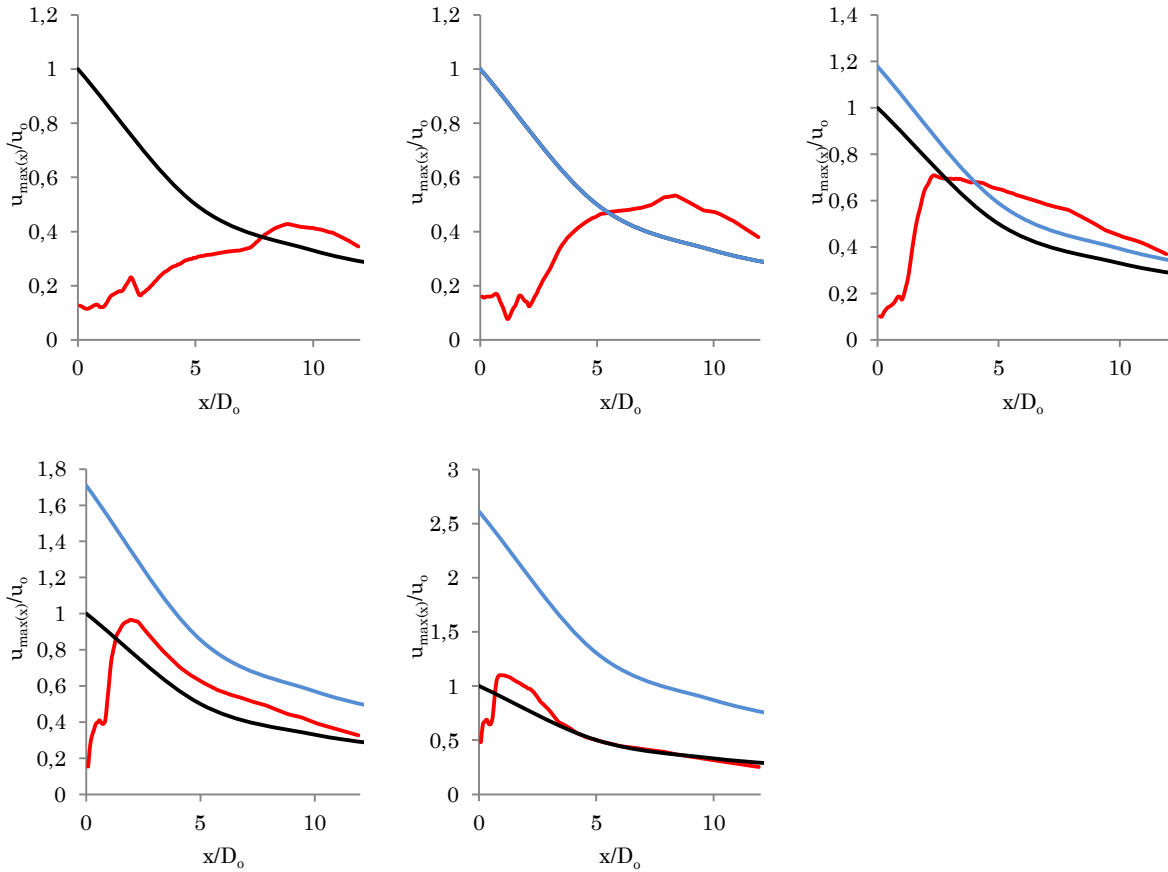
Figure 30: Dimensionless velocity profiles for the current design rules (black), the improvised design rules (blue) and the model results (red). The figures represent respectively the dimensionless velocity profiles at an angle of 90°, 75°, 60°, 45° and 30°. To extract the required bed protection length, $u_{max(x)}$ can be translated to u_c and x can be translated to L. Note that the model results show relevant information regarding the required bed protection length only at the right side of the crest.

Besides showing the required length of the bed protection, the sensitivity analysis results show the effects of the valve angle on the required sorting. The maximum near-bed velocity magnitude is larger for smaller valve angles. This effect mainly translates into demands regarding the material used for bed protection. The results show the

maximum near-bed velocity magnitude can exceed the width and depth averaged outlet velocity. Therefore, when the bed protection is designed behind pumping stations where the valve angle is expected to be small (i.e. <60°), the used bed protection material should at least be able to remain in place when subjected to the outlet velocity. For larger valve angles, the present near bed velocities are likely to be much smaller than the outlet velocity.

The relative effect of the **interaction of multiple outlets** on the required bed protection length is presented in **Figure 31**. Here the dimensionless bed protection length behind a double outlet is compared to the dimensionless bed protection length behind a single outlet with the same valve angle.
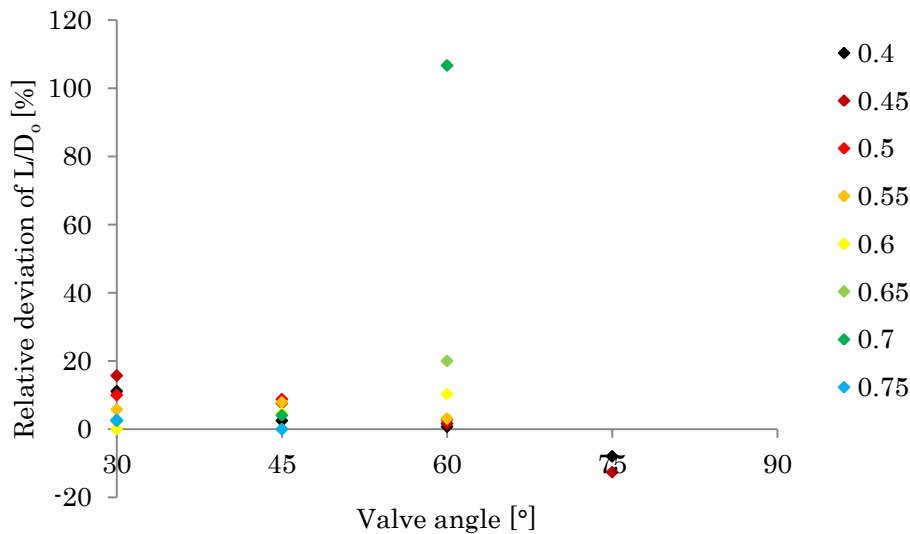
Figure 31: The relative deviation of the dimensionless bed protection length for the double outlet situations, with respect to the single outlet situations. A positive deviation represents a larger required bed protection length for the double outlet. The different series represent different dimensionless critical velocities (i.e. u_c/u_o-ratios)

The figure shows that for some valve angles the required bed protection length is larger for the double outlet situation, while for other valve angles the bed protection length is larger for the single outlet situation. Although for one situation the relative deviation is 100%, the differences for small critical velocities (i.e. $u_c/u_o<0.5$) are relatively small (maximum of +11%). However the effect of the double outlet should still be taken into account. The currently used improvised rule however causes the bed protection length behind a double outlet to be designed twice as large behind a single outlet. In **Figure 32** the effect of this rule is presented.

The results presented in **Figure 31** show that, to design a robust bed protection, the length of the bed protection behind a double outlet probably needs to be lengthened an additional 11% with respect to the situation with one outlet (although still conservative). The 100% relative deviation of the required bed protection length is found at an u_c/u_o-ratio of 0.7. This is however a very high ratio, which is according to the respondents not found often in practical applications. Respondents 1 and 2 stated normal values for u_o are approximately 1 m/s, while respondents 4 and 5 stated values for u_c often are in the range 0.2-0.5 m/s. This means the u_c/u_o-ratios found in practical environments is often in the range 0.2-0.5.
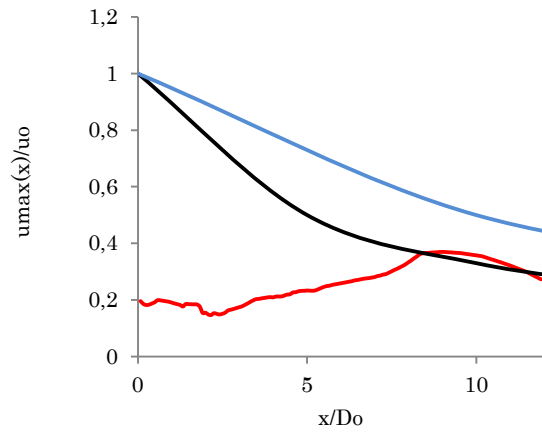
Figure 32: Dimensionless velocity profiles for the current design rules (black), the improvised design rules (blue) and the model results (red) for the situation with a double outlet with valve angle 90°. To extract the required bed protection length, $u_{max(x)}$ can be translated to u_c and x can be translated to L. Note that the model results show relevant information regarding the required bed protection length only at the right side of the crest

Besides showing the required length of the bed protection, the sensitivity analysis results show the effects of the presence of multiple outlets on the required bed protection width. The bed protection width behind multiple outlets is obviously wider than behind a single outlet. Looking at **Figure 23** and **Figure 26**, the width of the double jet seems to be approachable with the sum of the width of two single outlets.

Chapter 6

Discussion

The previous chapters discussed the interviews, the measurements and the model study carried out in this study. In this chapter the main assumptions and choices are discussed, along with their consequences for the study results. Additionally the practical use of the findings for the design of bed protection is discussed in section 6.4.

6.1 Expert study

When carrying out an expert study to map the thoughts of individual experts on a topic, it is important to keep the experts separated in order to gain insight in the actual independent thoughts of each individual. Although the interviews were carried face-to-face without the presence of other experts, the selected experts could still be influenced by opinions of other individuals. These influences could be nested in the initial motivation of this study and the fact that many respondents (5/6) are working for the same company. The findings of the expert study can be tested on relevance for engineers at other companies, by carrying out a similar expert study here.

The initial motivation of the study was an insufficiently robust bed protection at Houtkade. Here the bed protection was eroded, while it was designed with the design rules of the CUR. Observations at the pumping station showed the valve angle was smaller than the expected 90°. Also Houtkade is a pumping station with a double outlet. From this analysis the questions arose what the actual effect of the valve angle and the double outlet was on the downstream velocity field. As many of the respondents work for the same company, the experts work on the similar projects and are likely having frequently contact. This can also cause the presence of a selection of questions at all experts. These effects were minimized by interviewing the experts individually and encouraging them to think 'out of the box'. The selection of features can however still be considered especially interesting for engineers at Tauw.

This is the same for the selection criteria of the pumping stations. As only experts were asked from Tauw, the defined criteria resemble the dimensional characteristics of pumping stations where Tauw often is involved in designing or renovating. This is therefore the applicability area of the study.

6.2 ADCP measuring

The measurements are influenced by systematic errors, random errors and errors induced by the measurement setup (STOWA, 2009). Systematic errors are caused by the equipment's performance and are relatively small (0.4-1.0 cm/s). Random errors are caused by vegetation, fish movement and weather conditions. These conditions are likely

to affect the number of unreliable measurements, which are filtered when post processing the data. During the measurements the weather was good (little wind and dry conditions) and vegetation had no influence (besides in the side channel of Rapijnen). Corrupted data due to fish movement was extracted from the data sets where necessary. The influence of random errors is considered negligible.

The largest errors are nested in the measurement setup. Here the locations of the measurements, the measurement duration and the moment of the measurements are of importance. The **locations of the measurements** are important as the discharge occurs in a turbulent manner. In largely turbulent regions water bubbles are often found throughout the water column. These bubbles disturb the acoustic signal, resulting in erratic data. As the locations of the measurements were chosen to map the flow pattern directly downstream of the structures, the turbulence was large at these locations. Therefore the **measurement duration** and frequency are of increased importance. As presented in paragraph 3.1.2, the measurements at Rapijnen and Barwoutswaarder were carried out during 60 seconds, with a frequency of 5 ensembles per second. For Houtkade the measurements were also carried out during 60 seconds, but the ensemble interval was significantly larger. One ensemble was measured during 3 seconds. The **moment of the measurements** is also important, as the discharge needs time to develop a velocity field. When the pumping station is switched on, the discharge enters still water in the adjacent channel. It takes a couple of minutes for the flow field to develop and reach an equilibrium situation. At all locations the measurements were started after waiting 5-8 minutes.

6.3 CFD modeling

The model study is influenced by errors and uncertainties nested in the definition of the model and physical approximation of the software. In the **model definition**, geometrical and physical approximation of the solver are main causes of errors and uncertainties:

1. Geometrical approximation of the pumping station and the channel. For all structures the bed profiles and the pressure lines were modeled with very low resolution (i.e. only general contours were included). At Barwoutswaarder and Rapijnen the exact bed profiles were not included for reasons regarding computational effort and time. At Houtkade exact bed profiles were not available.
2. Near the bed, the processes were simulated using wall functions rather than a very fine mesh. The wall functions give an alternative method of describing the logarithmic profile near the bed while keeping the computation time relatively low. They give however a rough approximation of the near wall processes, while high resolution meshes are often more accurate.
3. A simplified stationary solution was used to define initial values for the time-dependent solver. For this stationary solution the viscosity was increased from 0.001 Pa·s to 1 Pa·s. The initial solution was therefore affected by less processes.
4. Probably the most important uncertainty is nested in the definition of the bed velocity. It is very hard to tell at which height the velocities still affect the erosion of the bed. During this study the lower 20 centimeters were used as an approximation.

The **physical approximation of the software** contains errors and uncertainties regarding the results of the models nested in assumptions made in the theoretical background of the model:

1. The surface roughness induced by bed material with large Nikuradse values could not be included in the model. The only way to take into account these effects in COMSOL is by adjusting the geometry of the bed. The roughness parameter defined in COMSOL is only applicable for describing small roughness elements in pipe flow. When turbulence of the model increases, the effect of this roughness parameter decreases. The effect of this restriction is that velocities decrease at a lower rate and higher velocities are found further downstream of the structure.
2. The water surface is defined as a wall with a slip function. This means water cannot penetrate the wall, but there are also no boundary layers developing near the wall. This means the water level does not fluctuate.
3. The circulation flow caused by the water entrainment and the channel boundaries is overestimated in all models. This affects the dispersion pattern of the jet and with it the decrease rate of the centerline velocity. When the circulation flow would be simulated correctly, the decrease rate of the velocity would likely be higher.
4. The model computes a time averaged velocity field downstream of the pumping stations. This means that high turbulent regions with varying velocity directions but large velocity magnitudes cannot easily be identified in the models. For instance the region at the opposing bank at Houtkade where the jets collide seems very calm (see **Figure 22**). The measurements however show that velocity magnitudes can be quite high here.

6.4 Practical use

The results of the model study describing the velocity field and the development of the jet are case specific. As respondent 6 already mentioned in chapter 2, pumping stations vary largely in geometrical details. Therefore it is not realistic to sketch a single velocity field that is applicable at all pumping stations. For instance the influence of the geometrical dimensions of the outlet structure can clearly be observed when comparing the results at Houtkade with the results of the 'adjusted' Houtkade in the sensitivity analysis. Here the discharge leaving the wider outlet structure disperses significantly larger than at the small outlet structure at the sensitivity analysis. Also the location of the outlet in the water column is likely to affect the velocities near the bed. Therefore, to make exact estimations of these characteristics for all individual pumping stations, engineers will need to carry out an optimization study for each case. The quantitative results of this sensitivity study can therefore not be applied 1-on-1 for each situation or structure.

This being the case does not mean that the results of this study cannot be useful in designing bed protection. The sensitivity analysis showed the required bed protection length is not necessarily larger for smaller valve angles or additional outlets. This while the improvised rules discussed in chapter 2 definitely lead to an increased bed protection length. This means that the necessity of the improvised rules is proven to be smaller than anticipated prior to the study. Also the sensitivity analysis shows the maximum near-bed velocity magnitudes are under 'normal' conditions (i.e. single outlet, 90°) significantly smaller than the depth and width averaged outlet velocity (a factor 0.43). For smaller valve angles the maximum near-bed velocity can exceed the outlet velocity. This means at smaller angles of the valve, the bed protection material should be heavier than for larger angles of the valve. This cannot be translated to exact values, but this behavior can be considered during the motivation of a material choice.

Chapter 7

Conclusions and recommendations

This chapter focuses on the conclusions drawn from the study (section 7.1) and the corresponding recommendations on how the finding of this study can be used in designing bed protection, but more importantly, how they can be sharpened in further research (section 7.2).

7.1 Conclusions

The conclusions of this study are presented by answering the research questions as they were formulated in chapter 1.

1. *To what extend do the contents of the current design rules for bed protection match with the engineers' need?*

Interviews amongst engineers with experience in the design of bed protection, show the individual effects of respectively the angle of the valve, the interaction of multiple parallel outlets and the outlet orientation with respect to the channel on the velocity field downstream of pumping stations should be investigated further. During the design of bed protection, the current design rules do not provide sufficient guidance on how to take these aspects into account. During this study mainly the effects of the valve angle and the interaction of multiple outlets are investigated.

2. *What is the effect of the subjects of the appointed knowledge gaps on the velocity field downstream of pumping stations?*

The **valve angle** affects mainly the maximum near-bed velocity magnitude downstream of the structure, the location where this maximum velocity magnitude occurs and the deceleration of the discharge when moving away from the structure. A smaller valve angle causes a deflection of the jet towards the bed and an increase of turbulence inside the outlet structure. The deflection of the jet causes larger velocity magnitudes to occur near the bed (an increase with a factor of 2.6 was found during this study between an angle of 90° and an angle of 30°). For smaller valve angles this happens closer to the structure. Due to the angle at which the jet collides with the bed, the dispersion of energy is larger here. This, in combination with the energy losses in the outlet structure, causes the deceleration of the jet to increase. Therefore, even though maximum near-bed velocity magnitudes are higher and therefore occur further downstream of the structure,

the distance downstream of the structure where the smaller velocities are no longer exceeded, is likely to be smaller when the valve angle is smaller.

The interaction of **multiple outlets** affects mainly the maximum near-bed velocity magnitude and the development of the velocity magnitudes downstream of the structure. This effect depends largely on the valve angles of the outlets. At larger valve angles the maximum near-bed velocity magnitude behind a double outlet is smaller than at a single outlet and smaller velocity magnitudes are reached at a smaller distance downstream of the structure. However, for smaller valve angles the smaller velocity magnitudes are reached further downstream of the structure. The increase of velocity magnitude at a certain distance downstream of the structure is however very small (maximal 7%).

3. How can these effects be translated into rules for the design of bed protection?

Translation of the effects into rules for bed protection design is very hard. The results however provide engineers with insight in the order magnitude with which the investigated features affect the required bed protection dimensions. For the **valve angle**, improvised rules are necessary, as higher critical velocities are more likely to be exceeded at smaller valve angles. The results show also that the bed protection length should not necessarily be larger for smaller valve angles and can sometimes even be designed smaller. Although improvised rules are needed, the improvised rules which are currently used overestimate the required bed length significantly. At smaller critical velocities, the effect of the valve angle on the bed protection length is smaller and the current design rules design a relatively good bed protection. The required sorting of the bed protection is also affected by the valve angle. At smaller angles the expected maximum near-bed velocity magnitudes are close to the outlet velocity. At smaller angles this magnitude is approximately halved and lighter material can be used.

For the **interaction of multiple outlets**, the improvised design rules are proved to be unnecessarily conservative. Where the improvised design rules design a bed protection with twice the length of the bed protection behind a single outlet, the results of the sensitivity analysis translate into a required additional length of 11% with respect to the corresponding single outlet situation. The results show that the lengthening of the bed protection is not always necessary. While the effect of the extra outlet on the required sorting of the bed protection material is negligible, the width of the bed protection should be larger than at a single outlet. The width can be approximated by the sum of the widths calculated downstream of two single discharges.

7.2 Recommendations

The results of this study are mainly based on the expert study, which was carried out to investigate how the contents of the bed protection design rules matches the engineers' needs, and the model study/sensitivity analysis carried out to investigate the effect of the valve angle and the interaction of multiple outlets on the required bed protection. The results of the interviews can be assessed and sharpened by carrying out more interviews amongst engineers working for different companies. Validation of the model study indicated that some turbulent flow field characteristics, like the dispersion and the circulation flow, were not properly resembled by the model. Better turbulence modeling and the ability to include surface roughness with large Nikuradse values into the model, can help to compute the velocity field behind pumping stations more accurate, increasing its relevance in the practical context.

The sensitivity analysis was performed on an adjusted geometrical model representing Houtkade. This means important geometrical features such as the width of the outlet structure, the tailwater depth, the height of the outlet in the water column and the channel geometry were not adjusted during the analysis. The results therefore still show very case specific flow characteristics. Further analysis regarding the effect of these geometrical aspects, or the research of the effects of the valve angle and the interaction of multiple discharges under different geometrical conditions should be carried out in order to place the presented results in the proper context.

During this study the effects of the valve angle and the interaction of multiple discharges on the near-bed velocity field was investigated. The results show the features affect the velocity field significantly. However an essential part of information misses. It is very important to map the dimensionless velocity profiles further downstream of the structures to see how they relate for even smaller critical velocities. Especially as u_c/u_o-ratios are often in the range 0.2-0.5. With this information, **Figure 29**, representing the required bed protection length per valve angle for different u_c/u_o-ratios, and **Figure 31**, representing the relative effect of a double outlet on the required bed protection length, can be complemented with essential information regarding the required bed protection length for smaller u_c/u_o-ratios.

Until further information is available on the effect of the study subjects, the optimization of bed protection dimensions stays a case specific affair. The velocity field downstream of pumping stations depends on to many geometrical and hydraulic features, to use the found quantitative relations in a practical context. The results however do show the currently used improvised design rules are very conservative. This, in combination with the suggested undersizing of the required bed protection by the CUR design rules in this study, should trigger additional studies regarding the actual accuracy of the design rules and the effects of the valve angle and the presence of multiple outlets in different environments.

Bibliography

Albertson, M. L., Dai, Y. B., Jensen, R. A., Hunter, R. (1950). Diffusion of submerged jets. American Society Civil Engineers Trans, 115, 639-697.

Bakker, J. J. (2000). *Breuksteen in de praktijk: Dl. 2.* (Breuksteen in de praktijk.) Gouda: CUR, Civieltechnisch Centrum Uitvoering Research en Regelgeving.

Biesboer, F. (2013, august 30). Erosie ondermijnt Oosterscheldekering. De Ingenieur. Obtained on 25th of september 2013 via http://www.deingenieur.nl/nl/nieuws/21087/ erosie-ondermijnt-oosterscheldekering.html

CIRIA, CUR, CETMEF (2007). *The Rock Manual: The use of rock in hydraulic engineering, second edition.* C683, London: CIRIA.

Hartong, J., & Termes, P. (2009). *Handboek debietmetingen in open waterlopen.* Utrecht: STOWA.

Johnston, A. J., Halliwell, A. R. (1986). Jet behavior in shallow receiving water. *Proc. Institution of Civil Engineers 81*(2), 549–568.

Johnston, A. J., Volker, R. E. (1993). Round buoyant jet entering shallow water. Journal of Hydraulic Research, 31:1, 121-138.

Kortlever, W. C. D. (2006). Trial and Scour: Scour and Bed Protection in the Discharge Sluices in the Afsluitdijk, The Netherlands. In CURNET, Proceedings Third International Conference on Scour and Erosion (pp 368-376). Gouda: CURNET

Muste, M., Yu, K., Pratt, T., Abraham, D. (2003). Practical aspects of ADCP data use for quantification of mean river flow characteristics; Part II: fixed-vessel measurements. Elsevier, 15 (2004), 17-28.

Rajaratnam, N. (1976). *Turbulent jets.* Amsterdam: Elsevier Scientific Pub. Co.

Schiereck, G. J. (2001). *Introduction to bed, bank and shore protection.* Delft: Delft University Press.

Schlichting, H. (1968). *Boundary-layer theory.* New York: McGraw-Hill.

Tu, J., Liu, C., & Yeoh, G. H. (2013). *Computational fluid dynamics: A practical approach, second edition.* Waltham, Mass: Butterworth-Heinemann.

White, F. M. (1974). *Viscous fluid flow.* New York: McGraw-Hill

Wilcox, D. C. (1993). *Turbulence modeling for CFD.* La Cãnada, CA: DCW Industries, Inc.

Appendices

Appendix A

Definitions

Bed protection

A bed protection is applied at locations where the bed is subjected to large currents that could induce erosion. Its main function is preventing erosion and, in doing so, ensuring the stability of nearby structures.

Centerline

The centerline is an imaginary line that is used to define the center of a geometrical entity, which in this case corresponds to a jet. At the centerline the velocity is at its maximum.

CFD modeling

Computational Fluid Dynamics (CFD) modeling is a branch of computer modeling in which fluid dynamics/flows can be simulated with the use of various numerical approaches.

CRESS

CRESS is a website, initiated by the Netherlands Ministry of Infrastructure and Environment, Delft University and UNESCO-IHE. It provides highly standardized routines important in coastal and river engineering.

Critical velocity

The critical velocity of a material is the velocity at which particles of that material start to move. When the velocity exceeds the critical velocity, erosion will most likely take place.

Dimensionless velocity profile

The dimensionless velocity profile of a jet concerns a distribution of the velocity over the width of a jet. Here the velocity is presented as a fraction of the centerline velocity and the location with respect to the centerline is presented as a fraction of the distance from the jet's orifice.

Dispersion

Dissipation of the jets energy to surrounding water. The dispersion describes the growth rate of the jet's width.

Ensemble

An ensemble is a collection of pings. It contains the data provided by the ADCP.

Entrainment

Entrainment is a process where nearby water starts to move along with a jet. This causes the widening of the jet, its dispersion.

Free environment

A free environment is defined as an environment without boundaries. For a jet this means there is an infinite amount of water above, beneath, next to and in front of the jet. There are no physical boundaries affecting the jets behavior.

Gaussian distribution

A Gaussian distribution, also called a normal distribution, describes a bell-shaped curve which is symmetrical about the mean.

Jet

A jet is a high-velocity fluid stream forced under pressure out of a relatively small-diameter opening.

Orifice

An orifice is an opening as of a tube or pipe. The source of a jet.

Ping

A ping is a sound wave transmitted by the ADCP equipment at a certain frequency. The ping is reflected towards the equipment by particles in the water column. The reflected pulse carries information regarding flow velocities.

Pressure line

A pressure line is a pipe inside a pumping station adjacent to the pump. Here the flow velocity is largest.

Structure

A structure is a hydraulic work like for instance a pumping station, a weir, a sluice, a dam, a sill, a culvert or a lock.

Tailwater depth

The tailwater depth is the water depth at the outlet of a structure.

Valve

A valve is a construction situated inside of or at the end of a pressure line of a pumping station. Its main function is to prevent water from flowing back into the pressure line when a pumping station is turned off.

Appendix B

List of symbols

B	Width of bed protection	Eq 2, 3
B_c	Roughness parameter COMSOL	F 2, 3
C	Constant of integration	F 1
D_o	Diameter of the outlet	Eq 1, 2, 3
L	Length of bed protection	Eq 2, 3
MD	Mean deviation	Eq 5
n	Number of simulations/measurements	Eq 4, 5
RD	Relative deviation	Eq 5
S_R	Dimensionless surface roughness function	F 4, 5
u_c	Critical bed velocity	Eq 2
u_i	Computed velocity	Eq 4
$\hat{u}_i$	Measured velocity	Eq 4
u_m	Centerline velocity	Eq 1
u_o	Velocity at the outlet	Eq 1, 2
u_y	Velocity at some distance of the wall	F 1, 2
u_{*0}	Velocity at the wall	F 1, 2
x	Distance from orifice	Eq 1
y_w	Distance from wall	F 1, 2
κ	Constant parameter with value 0.4	F 1, 2, 3
κ_{R^+}	Parameter taking into account the grain diameter	F 3, 4, 5

Appendix C

Interview questions

Three different interview formats were made with relation to the area of expertise of the experts. Here the interview questions are presented. These questions were used as a guideline throughout the interview.

Interview questions for respondents 1 & 2:
1. *What kind of structures do you deal with at Tauw?*
2. *What is your area of expertise with respect to designing and assessing these structures?*
3. *How are pumping stations often situated with respect to the adjacent channel or lake (what is the discharge orientation)?*
4. *What are the important aspects that determine the design of a pumping station and its dimensions?*
5. *What are common amounts of discharges that flow through these pumping stations?*
6. *At what range of velocities does the discharge often flow through the press line?*
7. *How is a valve dimensioned and at what angle is it positioned at maximum discharge?*
8. *What effect does the presence of multiple outlets have on the design of a pumping station?*
9. *At what height in the water column is the outlet of a pumping station often located?*

Interview questions for respondents 3, 4 and 5:
1. *In which situations is bed protection necessary and how often is Tauw involved in its design or assessment?*
2. *How is bed protection designed under normal circumstances and are there other available design methods?*
3. *Are additional, maybe computational, methods used to map the flow field when designing bed protection?*
4. *Do you think the design rules provided by the CUR are capable of designing bed protection in accurate manner?*
5. *If not, what would you like to see changed/investigated in the current design method?*
6. *Are there aspects in designing bed protection, which effect should be discussed (more) in the design rules?*
7. *Do you use additional, perhaps improvised, rules to take into account the effect the valve position or the presence of multiple outlets have on the flow field?*
8. *Do you think the dispersion pattern described by the CUR is realistic?*
9. *What are common critical velocities of bed material?*

10. *What do you do when there is not enough room (length or width) to decrease the velocity to acceptable margins?*

Interview questions for respondent 6:
1. *What is the application area of the design rules formulated in CUR 197?*
2. *How were these rules developed and formulated?*
3. *Do you think the design rules provided by the CUR should be adjusted to optimize bed protection design?*
4. *If yes, what aspects should be investigated first to realize a first optimization step?*
5. *Concerning the dispersion pattern described in CUR 197, where do the ratios 1:10 and 1:6 come from? Literature speaks about a dispersion of 1:5?*
6. *Are aspects like the position of a valve, the presence of multiple outlets, the bed roughness and the water depth all taken into account when defining this dispersion angle?*
7. *Do the rules take into account only horizontal dispersion or also vertical dispersion?*

Appendix D

ADCP equipment

The measurements were performed with the use of advanced ADCP (Acoustic Doppler Current Profiler) equipment (**Figure 33**). This equipment can be used to analyze the flow structure (current velocity profiles), the echo intensity profile (for sediment transport characteristics), the velocity over bottom (both for the water column as for the equipment) and altitude above the bottom. These measurements were performed simultaneously using water pulses (WP) and bottom tracking (BT) pulses. These pulses are transmitted from four transmission 'heads' with a constant frequency. In the water column the pulses collide with suspended sediment particles. These collisions cause the pulses to be echoed. Subsequently the echoes are again received by the ADCP. When the sediment particle is moving, the time between two consecutive echoes differs from the time between the original transmissions of the two pulses. The variation of phase between the several reflected pulses is measured to obtain information about flow characteristics and bathymetry. This is schematized in **Figure 34**. The water velocity is measured with respect to the ADCP. This means the velocity of the ADCP is not taken into account. Therefore the transmitted pulses consist of bottom tracking pulses and water pulses. The water pulses determine the flow characteristics with respect to the ADCP. The bottom tracking pulses determine the distance of the ADCP to the bottom and the velocity of the ADCP with respect to the bottom.

Figure 33: (a) the Workhorse rio grande ADCP (b) the riverboat to move the ADCP
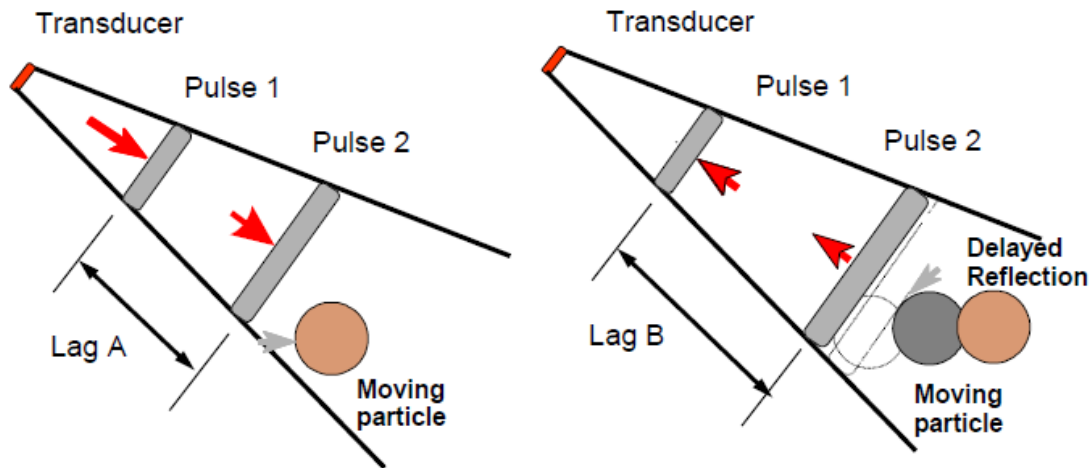
Figure 34: The phase change of a pulse

To obtain a vertical velocity profile, the transmitted pulse is partly reflected towards the ADCP, while the other part continues its trajectory. The depth at which the particle flows is determined knowing the time of return of the wave and the speed of sound. The vertical profile is build by dividing the flow area into bins (depth cells). The number of bins can be regulated/defined by the user of the equipment and is together with the quantity of measurements determinative for the accuracy of the measurement. This process is shown in **Figure 35**. Some limitations exist however to the vertical velocity profile. At the surface, the depth of immersion of the ADCP is circa 25 cm. Directly below the transmitter a blind zone is situated, called the blank. Also, the ADCP cannot measure the velocities near the bed. This is because of acoustic reflection from the bottom, caused by interference of side lobes (pulses generated besides the main beam). This polluted layer extents to 6% of the distance transmitter-bottom above the stream bed. In the upper and bottom layers the flow values are extrapolated. The limitations of the ADCP measuring range are shown in **Figure 36**.
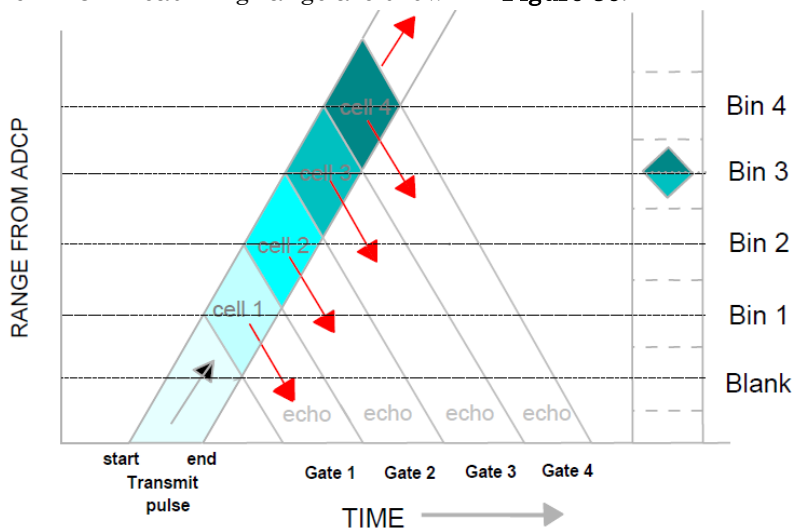
Figure 35: The vertical profiling of the adcp equipment
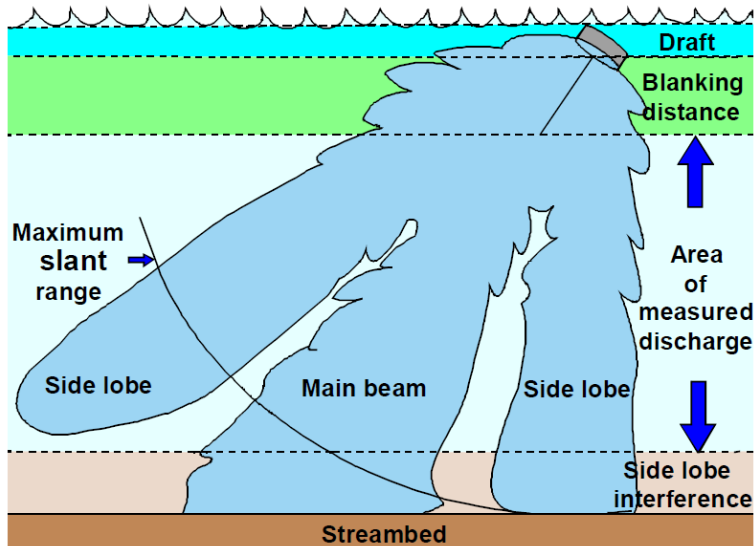
Figure 36: The ADCP measuring range

An advantage of four transmission heads, compared to three transmission heads, is the possibility to identify vertical velocities and to some extent the turbulence as well. Beams 1 and 3 (**Figure 37**) determine the horizontal component and the vertical component of the velocity. Beams 2 and 4 determine the other horizontal component and the same vertical component. The turbulence of the medium is described by the error velocity. This parameter is derived from comparison of the vertical components measured by the different beams. Other advantages exist for equipment with four transmission heads. The variance in the measurements is smaller and measurements in adverse conditions are more reliable than with three less transmission heads.
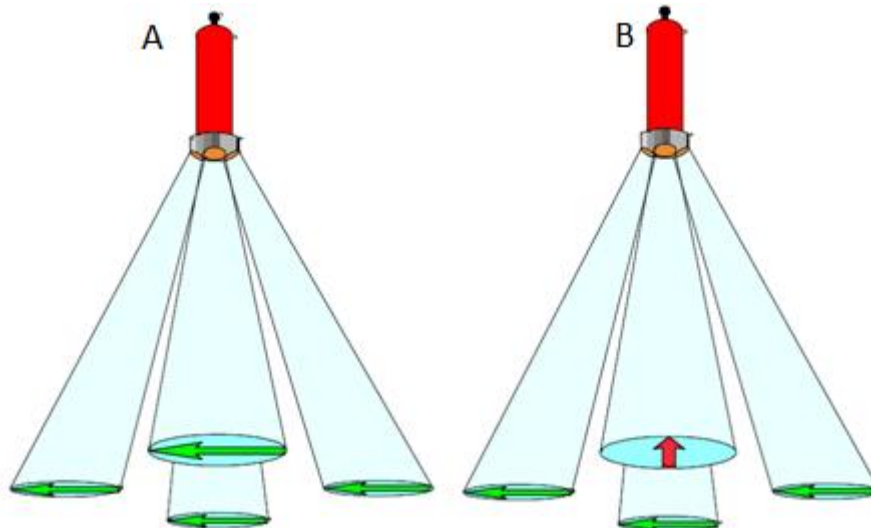
Figure 37: The beams determining the flow characteristics (A) homogenous medium (B) turbulent medium

To determine the location of the boat and the measurements, the ADCP is equipped with a GPS receiver which also holds a SIM-card. This way the location of the boat can be derived very accurate on each moment. In the horizontal direction the deviation of the real position is maximal 3 cm and in the vertical direction this is 5 cm.

Appendix E

Measurement and model results

Velocity tables

In this appendix the measured and simulated velocity data over the entire column for all measurement locations are presented in tables. This data was used during the validation of the models. The first column represents the measurement location and the first row represents the depth for which the velocity is presented.

Table 10: Measured velocity magnitudes at every location through the entire water column at Houtkade

	0,42	0,52	0,62	0,72	0,82	0,92	1,02	1,12	1,22	1,32	1,42	1,52	1,62	1,72	1,82	1,92	2,02
1	0,31	0,28	0,27	0,27	0,29	0,18	0,16	0,14	0,08	0,12	0,10	0,11	0,16	0,21	0,19	0,19	
6	0,40	0,35	0,33	0,35	0,35	0,44	0,56	0,65	0,72	0,78	0,98	1,02	1,17	1,27	1,32	1,33	
7	0,48	0,48	0,47	0,46	0,40	0,32	0,32	0,33	0,44	0,61	0,79	0,95	1,02	1,01	0,96	0,91	0,78
12	0,03	0,04	0,05	0,05	0,07	0,04	0,15	0,23	0,37	0,35	0,52	0,66	0,76	0,87	1,00	1,09	
13	0,26	0,20	0,23	0,20	0,12	0,11	0,08	0,14	0,12	0,13	0,06	0,14	0,32	0,50			
18	0,24	0,27	0,30	0,28	0,24	0,30	0,27	0,21	0,14	0,18	0,16	0,22	0,35				
2	0,33	0,28	0,34	0,25	0,27	0,25	0,26	0,23	0,30	0,27	0,24	0,23	0,29	0,26	0,31	0,31	0,36
5	0,12	0,15	0,16	0,25	0,21	0,35	0,48	0,50	0,59	0,66	0,75	0,91	0,98	1,06	1,10	1,16	1,10
8	0,41	0,43	0,42	0,47	0,38	0,42	0,43	0,44	0,53	0,63	0,79	0,88	0,96	1,06	1,06	1,01	
11	0,38	0,41	0,38	0,38	0,31	0,35	0,28	0,34	0,40	0,43	0,49	0,60	0,61	0,63	0,73	0,76	0,53
14	0,06	0,03	0,06	0,10	0,12	0,09	0,14	0,18	0,22	0,23	0,34	0,46	0,48	0,55	0,71		
17	0,19	0,12	0,18	0,21	0,17	0,16	0,12	0,14	0,24	0,34	0,41	0,52	0,56	0,53			
3	0,21	0,23	0,28	0,19	0,25	0,27	0,21	0,24	0,27	0,32	0,29	0,28	0,26	0,26	0,30	0,32	0,35
4	0,28	0,25	0,22	0,30	0,30	0,28	0,33	0,36	0,40	0,51	0,53	0,52	0,56	0,62	0,67	0,76	0,71
9	0,42	0,43	0,51	0,50	0,49	0,58	0,60	0,57	0,64	0,67	0,72	0,85	0,83	0,90	0,96	0,92	
10	0,38	0,41	0,38	0,38	0,31	0,35	0,28	0,34	0,40	0,43	0,49	0,60	0,61	0,63	0,73	0,76	0,53
15	0,08	0,06	0,02	0,04	0,02	0,06	0,09	0,19	0,36	0,34	0,38	0,51	0,60	0,65	0,53	0,25	
16	0,17	0,11	0,06	0,05	0,06	0,05	0,09	0,25	0,20	0,24	0,38	0,34	0,30	0,33	0,18	0,10	

Table 11: Measured velocity magnitudes at every location through the entire water column at Barwoutswaarder

	0,37	0,47	0,57	0,67	0,77	0,87	0,97	1,07	1,17	1,27	1,37	1,47
1	0,1	0,11	0,1	0,07	0,09	0,11	0,09	0,14				
2	0,21	0,11	0,08	0,1	0,14	0,21	0,18	0,24	0,22	0,21	0,19	
3	0,57	0,46	0,35	0,23	0,15	0,04	0,04	0,08	0,13	0,14	0,14	0,1
4	0,23	0,16	0,11	0,05	0,02	0,05	0,09	0,06	0,15			
5	0,42	0,32	0,33	0,3	0,19	0,16	0,12	0,13	0,11			
6	0,41	0,34	0,29	0,22	0,19	0,2	0,14	0,14	0,16	0,09		
7	0,14	0,07	0,05	0,1	0,1	0,09	0,07	0,1	0,17	0,16		
8	0,13	0,09	0,09	0,06	0,07	0,07	0,14					
9	0,24	0,2	0,17	0,2	0,17	0,22	0,18	0,21				
10	0,37	0,35	0,3	0,34	0,28	0,22	0,17					
11	0,34	0,32	0,3	0,3	0,34							
12	0,25	0,24	0,21	0,19	0,2							
13	0,08	0,03	0,04	0,04	0,02	0,07	0,16					
14	0,1	0,1	0,06	0,07	0,03							
15	0,22	0,26	0,2	0,24	0,18							
16	0,35	0,34	0,26	0,15	0,2							

Table 12: Measured velocity magnitudes at every location through the entire water column at Rapijnen

	0,37	0,47	0,57	0,67	0,77	0,87	0,97	1,07	1,17	1,27	1,37	1,47	1,57	1,67	1,77
1	0,61	0,63	0,65	0,59	0,45										
2	0,18	0,19	0,19	0,21	0,21	0,15	0,17	0,15	0,14	0,17	0,15	0,15			
3	0,2	0,18	0,18	0,15	0,15	0,16	0,15	0,1	0,06	0,04	0,03	0,04	0,06		
4	0,19	0,14	0,19	0,18	0,14	0,13	0,09	0,03	0,02	0,03	0,04	0,08	0,08		
5	0,1	0,11	0,09	0,04	0,1	0,09	0,11	0,11	0,12	0,07	0,09	0,12	0,13		
6	0,07	0,09	0,09	0,05	0,05	0,07	0,09	0,06	0,08						
7	0,1	0,1	0,1	0,05	0,03	0,02	0,09	0,07	0,02	0,07	0,09	0,1	0,11		
8	0,16	0,15	0,18	0,14	0,13	0,08	0,03	0,06	0,05	0,04	0,02	0,04	0		
9	0,43	0,43	0,4	0,38	0,4	0,3	0,31	0,24	0,2	0,17	0,15	0,14	0,13		
10	0,17	0,2	0,14	0,08	0,14	0,27									
11	0,11	0,12	0,09	0,09	0,13	0,11	0,1	0,12	0,13	0,12	0,09	0,07	0,07	0,1	0,09
12	0,31	0,33	0,35	0,33	0,35	0,28	0,26	0,2	0,26	0,23	0,18	0,16	0,14	0,07	0,07
13	0,28	0,28	0,27	0,25	0,18	0,21	0,16	0,15	0,12	0,05	0,09	0,07	0,05	0,05	
14	0,09	0,08	0,08	0,08	0,02	0,04	0,02	0,06							
15	0,25	0,28	0,22	0,19	0,23	0,23	0,26	0,24	0,21	0,21	0,13	0,26			
16	0,16	0,17	0,24	0,22	0,23	0,21	0,2	0,22	0,18	0,16	0,16	0,19	0,2	0,15	0,15
17	0,17	0,11	0,09	0,09	0,11	0,12	0,13	0,07	0,13	0,1	0,07	0,04	0,06	0,07	0,07
18	0,06	0,03	0,07	0,03	0,04	0,04	0,01	0,07	0,04	0,11					

Table 13: Simulated velocity magnitudes at every location through the entire water column at Houtkade

	0,42	0,52	0,62	0,72	0,82	0,92	1,02	1,12	1,22	1,32	1,42	1,52	1,62	1,72	1,82	1,92	2,02
1	0,24	0,23	0,23	0,22	0,22	0,21	0,21	0,19	0,18	0,17	0,15	0,11	0,11	0,15	0,21	0,26	
6	0,25	0,24	0,24	0,21	0,17	0,16	0,17	0,21	0,25	0,40	0,55	0,71	0,85	0,95	0,96	0,85	
7	0,17	0,16	0,13	0,10	0,06	0,04	0,05	0,18	0,34	0,48	0,66	0,83	1,00	1,17	1,15	0,96	0,71
12	0,08	0,06	0,03	0,05	0,09	0,13	0,17	0,23	0,29	0,35	0,41	0,49	0,56	0,60	0,62	0,53	
13	0,14	0,12	0,11	0,10	0,11	0,13	0,22	0,34	0,47	0,62	0,77	0,89	1,01	1,13			
18	0,14	0,13	0,12	0,10	0,09	0,08	0,08	0,08	0,09	0,11	0,09	0,08	0,15				
2	0,19	0,19	0,18	0,18	0,17	0,17	0,17	0,16	0,15	0,15	0,15	0,17	0,22	0,28	0,36	0,41	0,39
5	0,19	0,19	0,18	0,15	0,14	0,13	0,13	0,19	0,28	0,38	0,48	0,63	0,78	0,94	1,03	0,98	0,80
8	0,11	0,11	0,10	0,07	0,05	0,08	0,14	0,20	0,26	0,36	0,52	0,67	0,87	1,04	1,09	0,99	
11	0,05	0,04	0,02	0,04	0,07	0,11	0,16	0,22	0,30	0,37	0,45	0,54	0,64	0,68	0,69	0,62	0,51
14	0,10	0,10	0,10	0,11	0,15	0,20	0,28	0,35	0,42	0,54	0,66	0,79	0,91	1,02	1,06		
17	0,13	0,13	0,12	0,11	0,10	0,10	0,09	0,08	0,08	0,07	0,07	0,11	0,15	0,19			
3	0,15	0,15	0,15	0,15	0,15	0,15	0,14	0,14	0,16	0,18	0,21	0,30	0,35	0,41	0,53	0,59	0,54
4	0,13	0,13	0,13	0,13	0,13	0,13	0,16	0,20	0,25	0,35	0,45	0,58	0,73	0,92	1,02	1,01	0,86
9	0,06	0,06	0,06	0,05	0,06	0,08	0,11	0,15	0,22	0,33	0,45	0,58	0,77	0,91	0,97	0,92	
10	0,05	0,05	0,05	0,06	0,09	0,13	0,19	0,25	0,31	0,38	0,47	0,57	0,66	0,73	0,73	0,68	0,58
15	0,15	0,15	0,16	0,19	0,23	0,28	0,34	0,39	0,48	0,58	0,67	0,76	0,84	0,93	0,97	0,94	
16	0,13	0,13	0,13	0,12	0,12	0,12	0,11	0,11	0,10	0,10	0,10	0,12	0,13	0,17	0,25	0,32	

Table 14: Simulated velocity magnitudes at every location through the entire water column at Barwoutswaarder

	0,37	0,47	0,57	0,67	0,77	0,87	0,97	1,07	1,17	1,27	1,37	1,47
1	0,16	0,16	0,15	0,15	0,15	0,14	0,13	0,13	0,09			
2	0,13	0,13	0,12	0,12	0,12	0,13	0,13	0,13	0,15	0,14	0,14	0,15
3	0,67	0,67	0,66	0,64	0,60	0,54	0,47	0,39	0,48	0,25	0,21	0,19
4	0,15	0,14	0,14	0,14	0,13	0,13	0,12	0,11	0,15	0,09		
5	0,06	0,05	0,04	0,03	0,02	0,01	0,01	0,02	0,07	0,04		
6	0,65	0,64	0,61	0,56	0,51	0,44	0,37	0,30	0,44	0,19	0,15	0,11
7	0,09	0,10	0,11	0,11	0,13	0,14	0,15	0,17	0,09	0,19	0,19	0,18
8	0,16	0,16	0,17	0,17	0,16	0,16	0,15					
9	0,54	0,50	0,46	0,41	0,36	0,32	0,27	0,24	0,37			
10	0,04	0,04	0,03	0,03	0,02	0,02	0,02	0,02	0,10			
11	0,05	0,05	0,05	0,05	0,05	0,05	0,04	0,04				
12	0,42	0,40	0,37	0,34	0,31	0,28	0,26	0,23				
13	0,15	0,15	0,14	0,14	0,13	0,12						
14	0,21	0,20	0,20	0,19	0,19	0,18						
15	0,39	0,38	0,36	0,34	0,32	0,30	0,27					
16	0,05	0,05	0,05	0,05	0,05	0,05	0,04					

Table 15: Simulated velocity magnitudes at every location through the entire water column at Rapijnen

	0,37	0,47	0,57	0,67	0,77	0,87	0,97	1,07	1,17	1,27	1,37	1,47	1,57	1,67	1,77
1	0,64	0,64	0,64	0,63	0,63										
2	0,27	0,26	0,26	0,25	0,24	0,22	0,21	0,20	0,18	0,16	0,15	0,13			
3	0,04	0,04	0,04	0,04	0,04	0,04	0,04	0,04	0,04	0,04	0,04	0,04	0,04		
4	0,04	0,04	0,04	0,04	0,04	0,04	0,04	0,04	0,04	0,04	0,04	0,04	0,04		
5	0,07	0,07	0,07	0,07	0,07	0,07	0,07	0,07	0,07	0,07	0,07	0,07	0,07		
6	0,14	0,13	0,13	0,13	0,13	0,13	0,13	0,13							
7	0,03	0,03	0,03	0,03	0,03	0,03	0,03	0,03	0,03	0,04	0,04	0,04	0,04		
8	0,14	0,14	0,14	0,13	0,13	0,12	0,12	0,11	0,11	0,10	0,10	0,09	0,09		
9	0,45	0,44	0,43	0,41	0,39	0,37	0,35	0,33	0,30	0,27	0,24	0,22	0,19		
10	0,30	0,26	0,21	0,16	0,12	0,10	0,09								
11	0,09	0,09	0,09	0,09	0,08	0,08	0,08	0,08	0,08	0,08	0,08	0,08	0,08	0,08	0,09
12	0,39	0,39	0,38	0,37	0,36	0,35	0,34	0,33	0,31	0,30	0,28	0,27	0,25	0,23	0,22
13	0,22	0,22	0,21	0,21	0,21	0,20	0,20	0,19	0,19	0,18	0,18	0,17	0,16	0,16	
14	0,04	0,04	0,04	0,04	0,04	0,04	0,04	0,04							
15	0,28	0,28	0,28	0,27	0,27	0,27	0,26	0,26	0,25	0,25	0,24	0,24			
16	0,26	0,26	0,26	0,26	0,26	0,26	0,26	0,25	0,25	0,25	0,25	0,25	0,25	0,24	0,24
17	0,05	0,05	0,05	0,05	0,05	0,05	0,05	0,05	0,05	0,06	0,06	0,06	0,06	0,05	0,06
18	0,14	0,14	0,13	0,13	0,12	0,11	0,11	0,10	0,08						

Vertical profiles of measured and computed velocity magnitudes
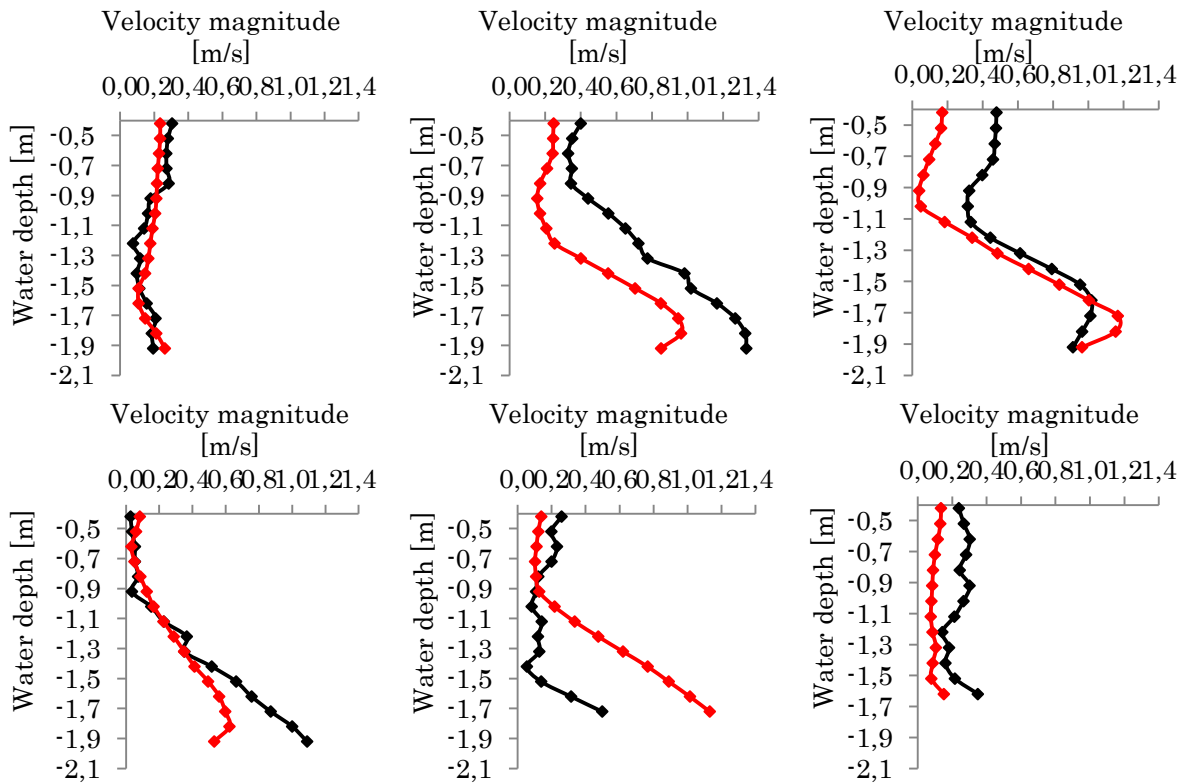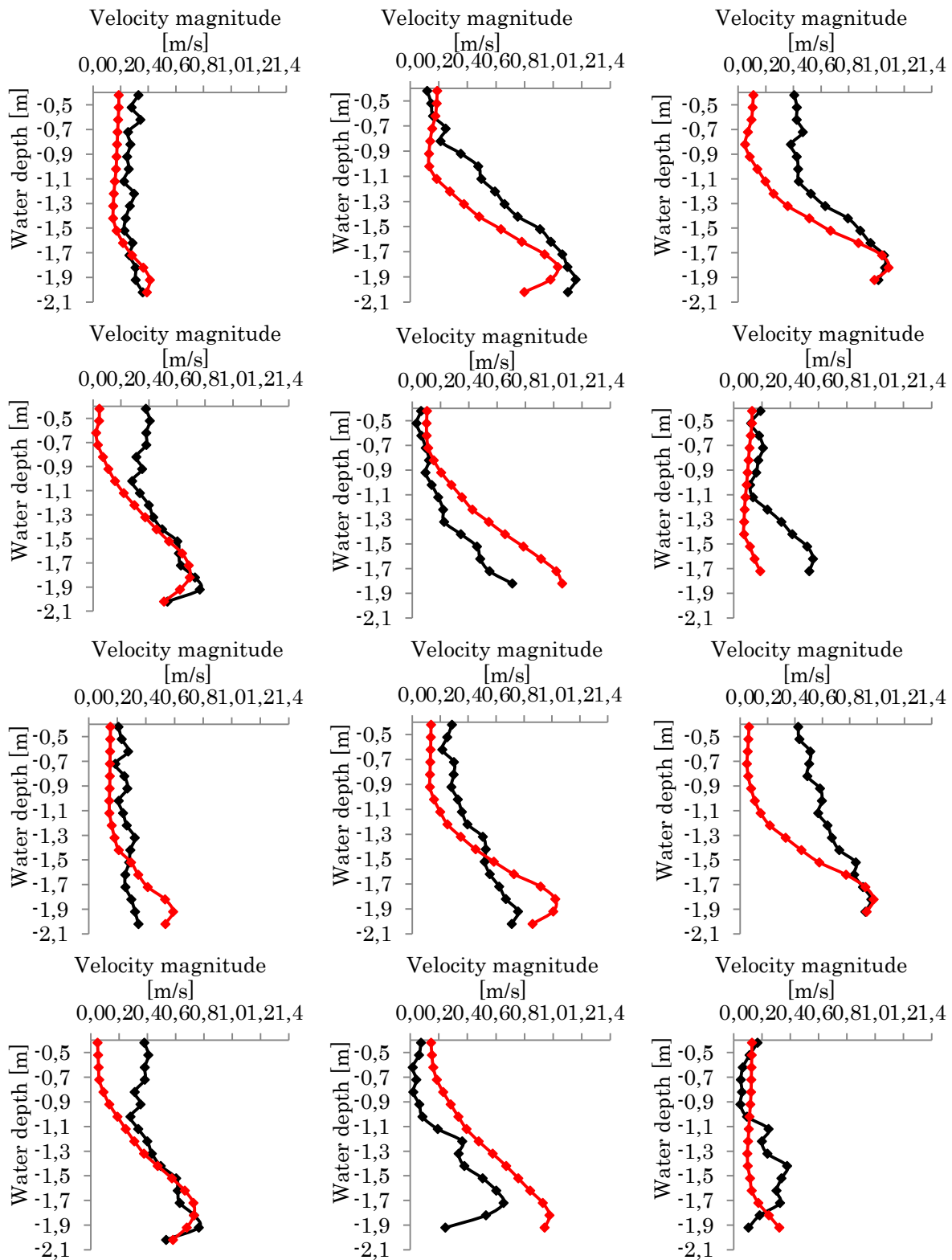
Figure 38: Vertical profiles of measured velocity magnitudes (black) and simulated velocity magnitudes (red) at all 18 locations behind Houtkade. The figures are sorted per cross line. The first six plots are for respectively locations 1, 6, 7, 12, 13 and 18 (cross line at 4 meters). The following six plots are for respectively locations 2, 5, 8, 11, 14 and 17 and the last six plots represent locations 3, 4, 9, 10, 15 and 16.
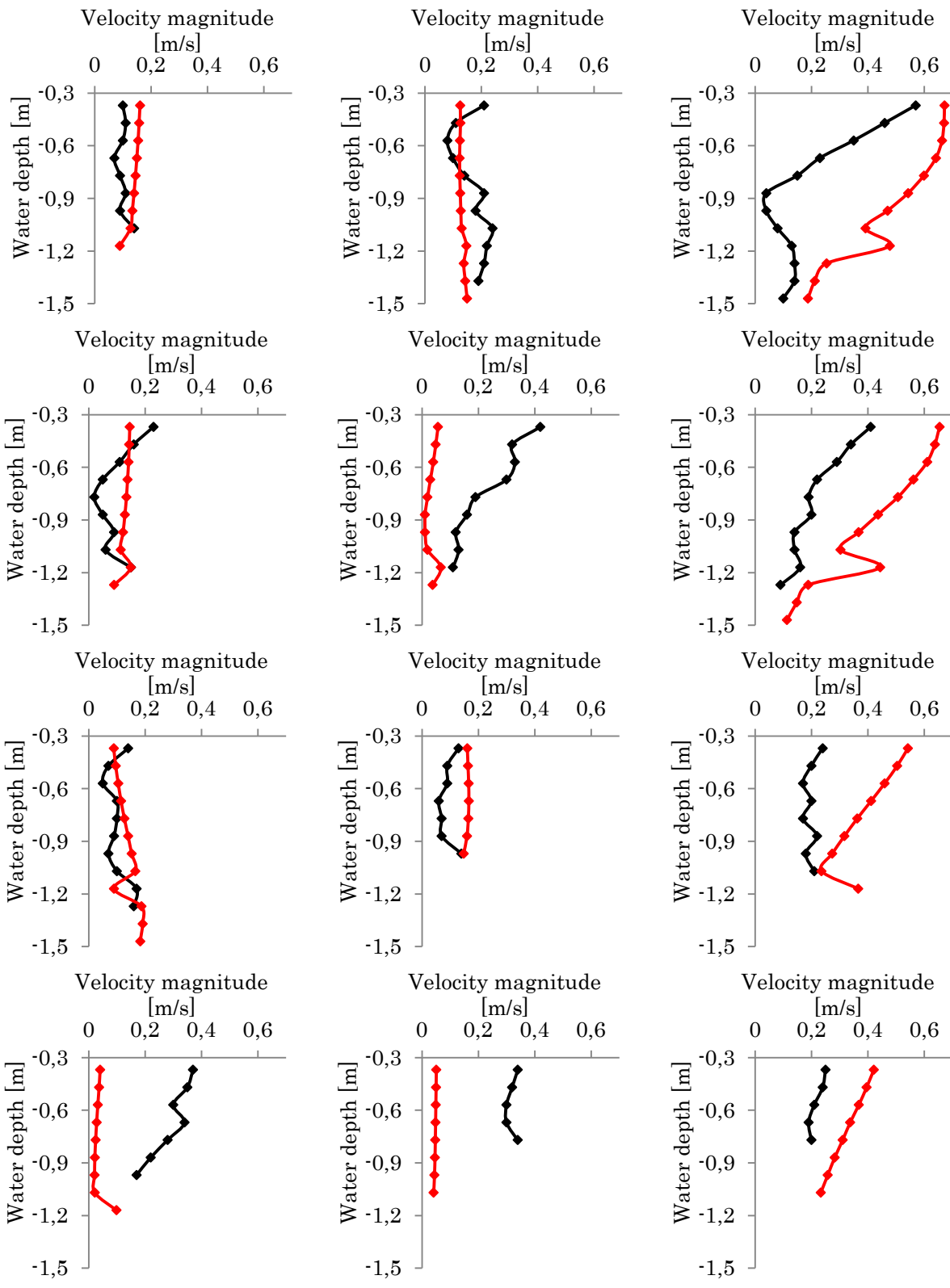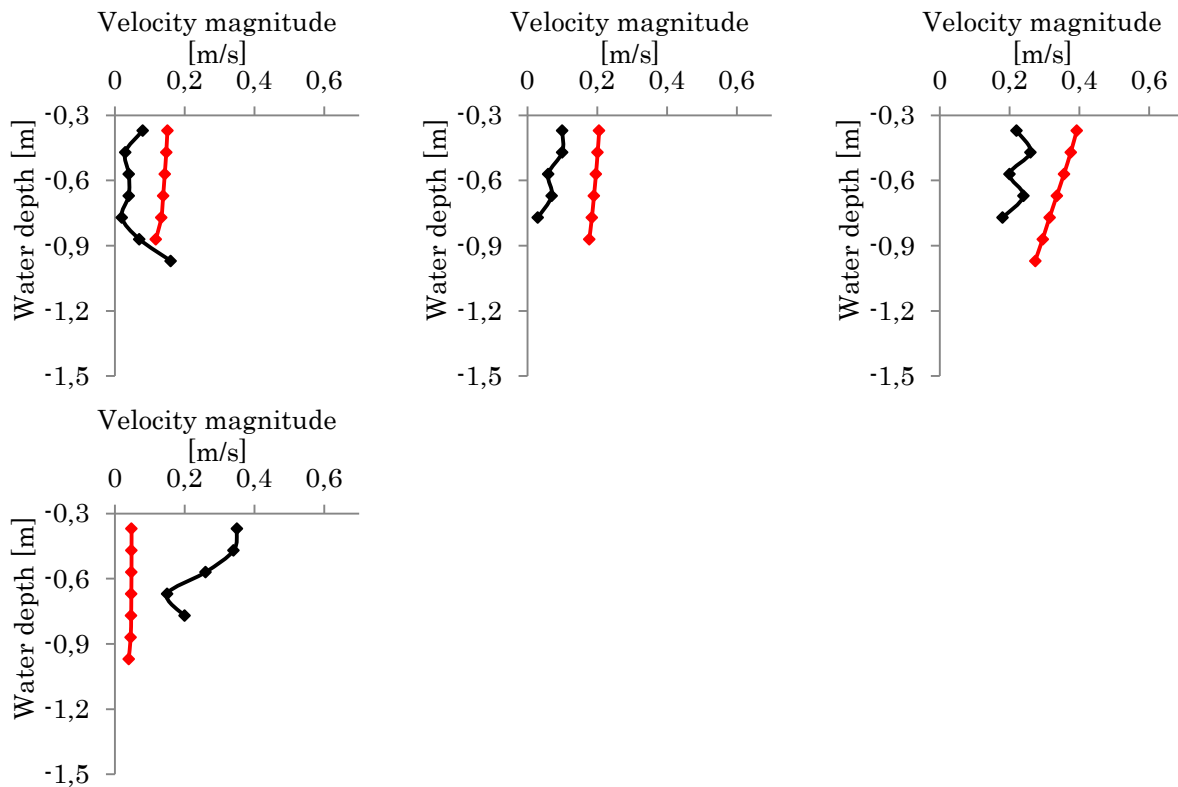
Figure 39: Vertical profiles of measured velocity magnitudes (black) and simulated velocity magnitudes (red) at all 16 locations behind Barwoutswaarder. The figures are sorted chronological from 1 to 16.
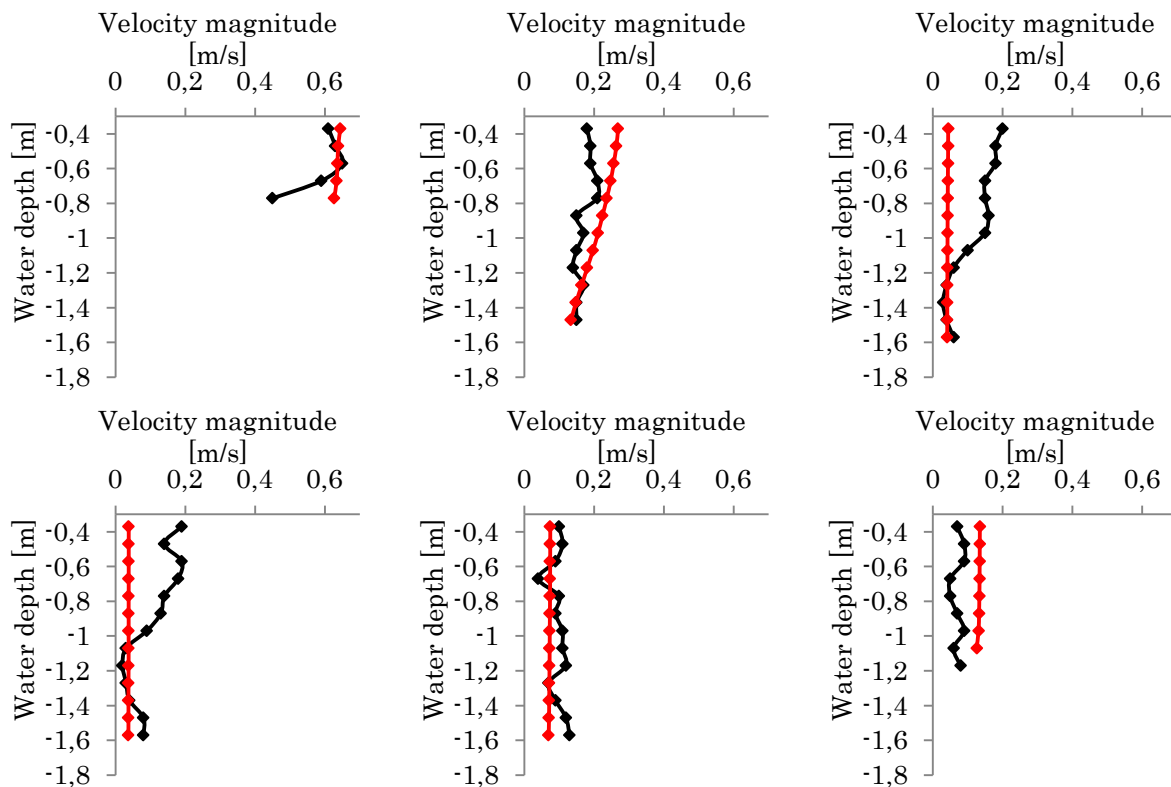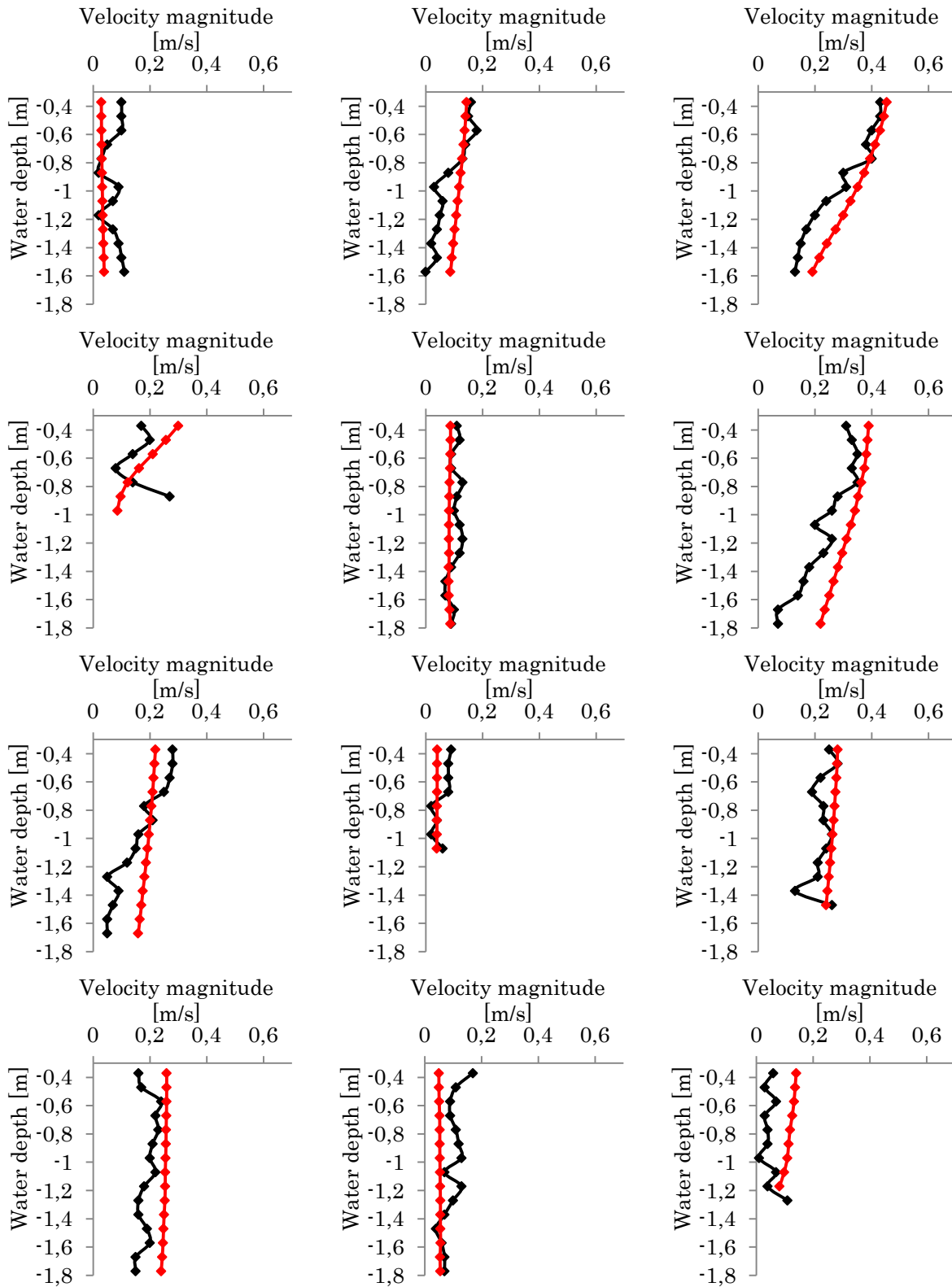
Figure 40: Vertical profiles of measured velocity magnitudes (black) and simulated velocity magnitudes (red) at all 18 locations behind Rapijnen. The figures are sorted chronological from 1 to 18.

Vertical profiles of measured and computed current directions
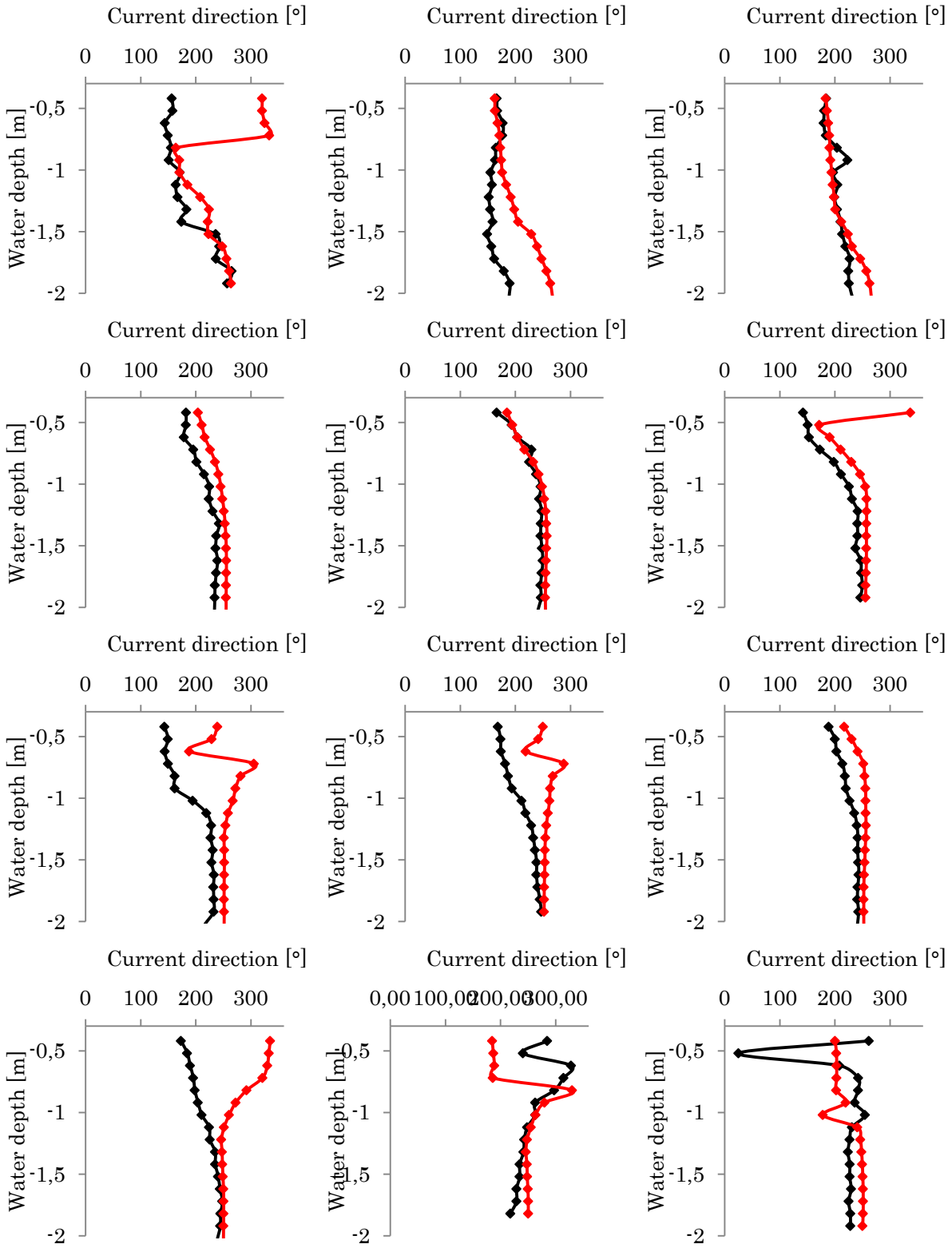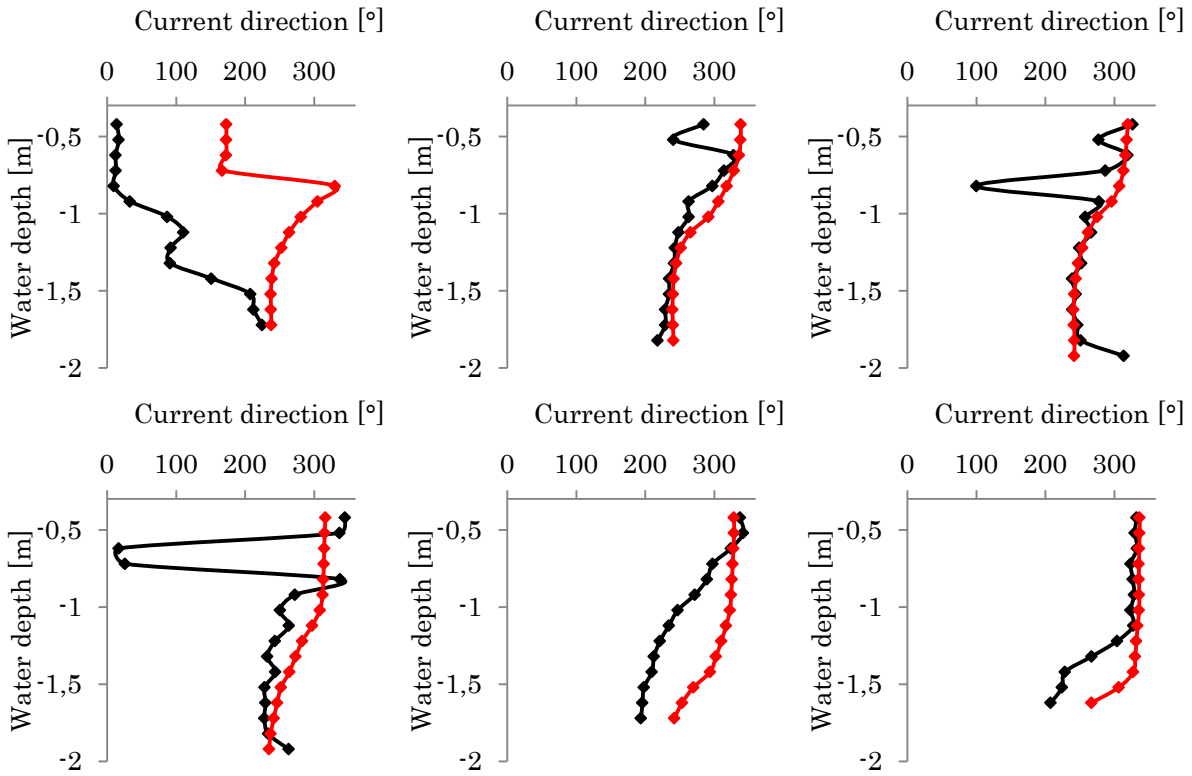
Figure 41: Vertical profiles of measured current directions (black) and simulated current directions (red) at all 18 locations behind Houtkade. The figures are sorted per cross line. The first six plots are for respectively locations 1, 6, 7, 12, 13 and 18 (cross line at 4 meters). The following six plots are for respectively locations 2, 5, 8, 11, 14 and 17 and the last six plots represent locations 3, 4, 9, 10, 15 and 16.
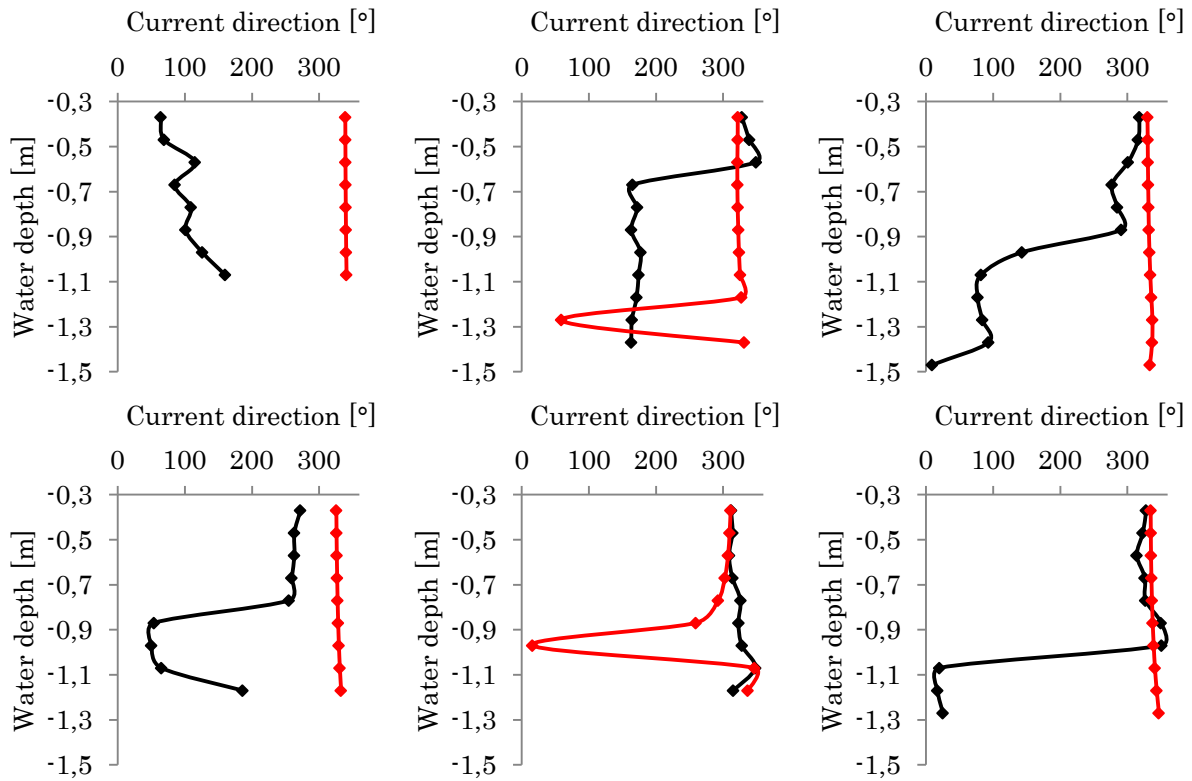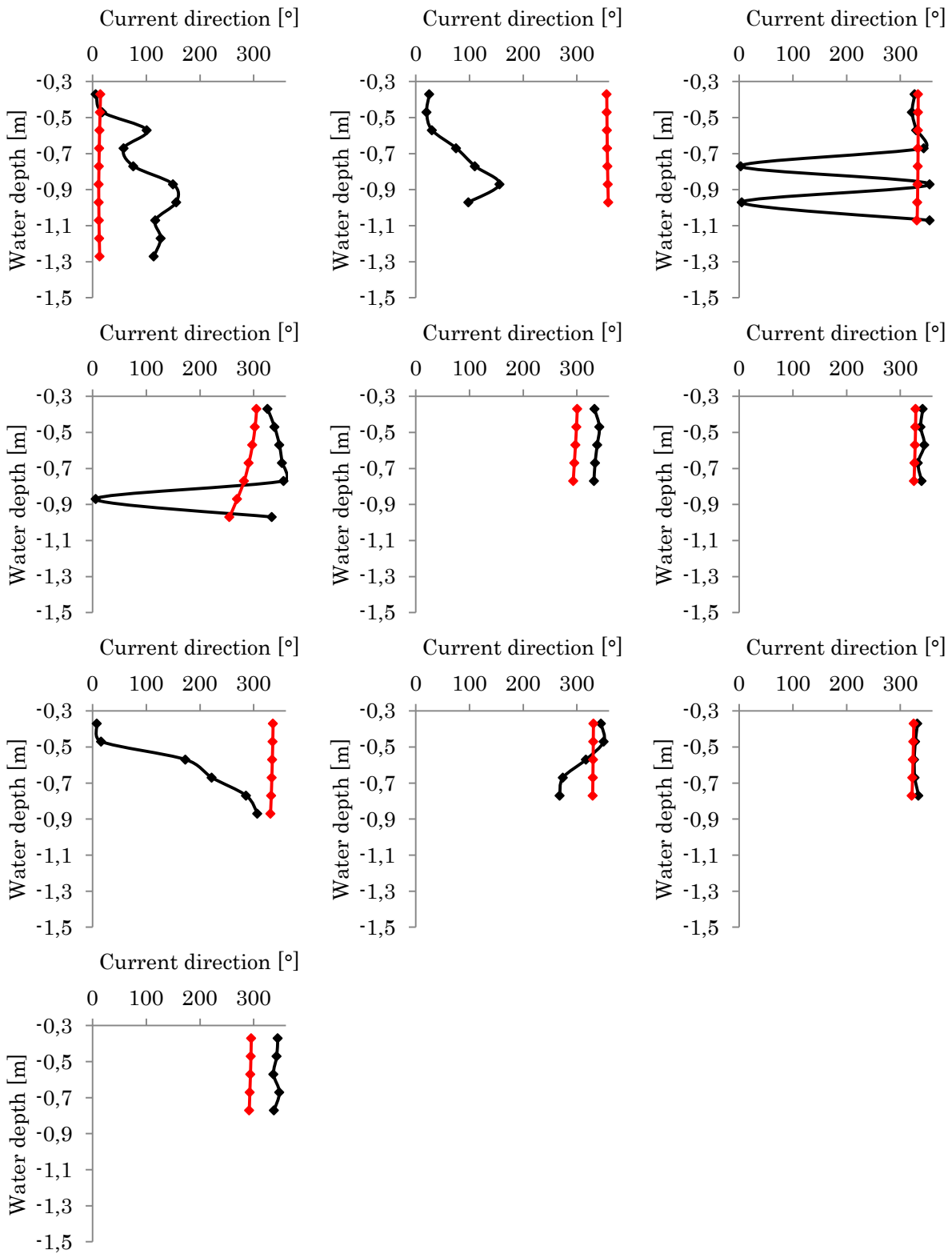
Figure 42: Vertical profiles of measured current directions (black) and simulated current directions (red) at all 16 locations behind Barwoutswaarder. The figures are sorted chronological from 1 to 16.
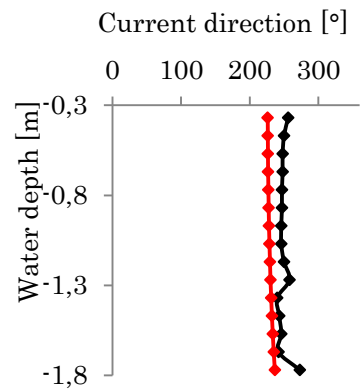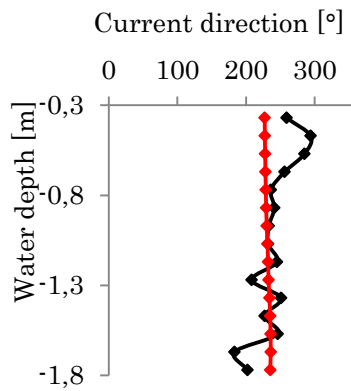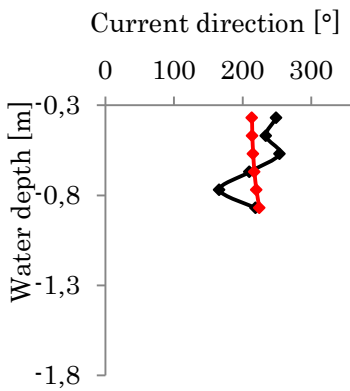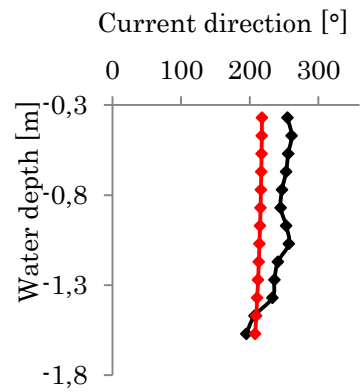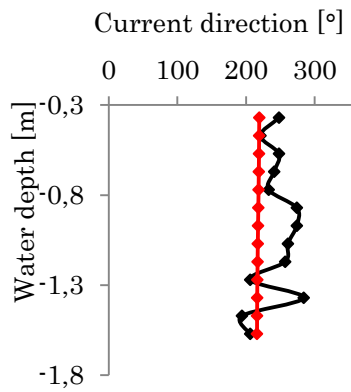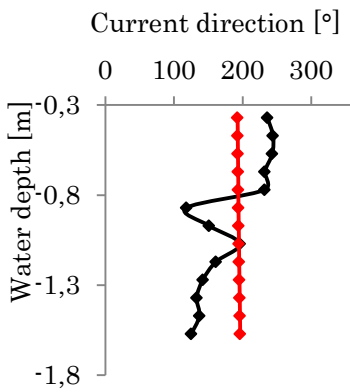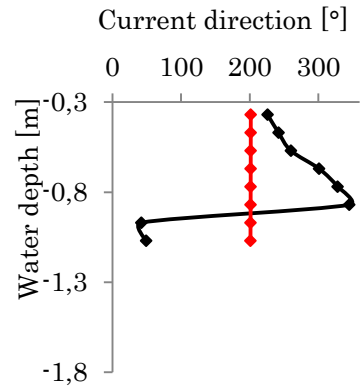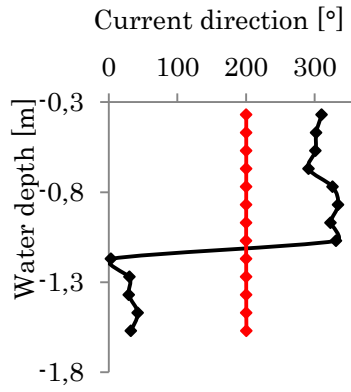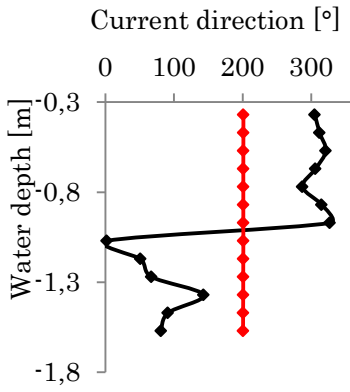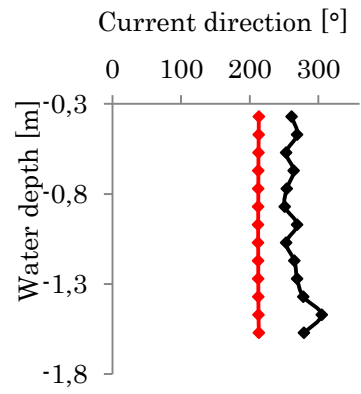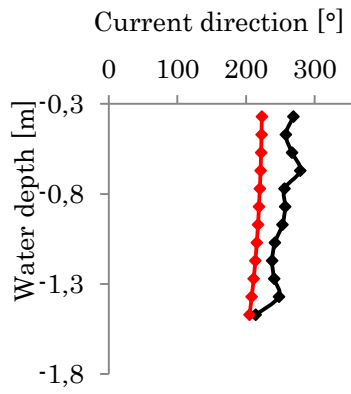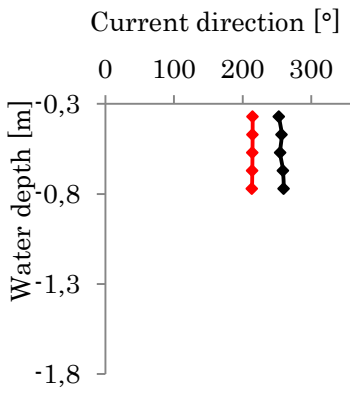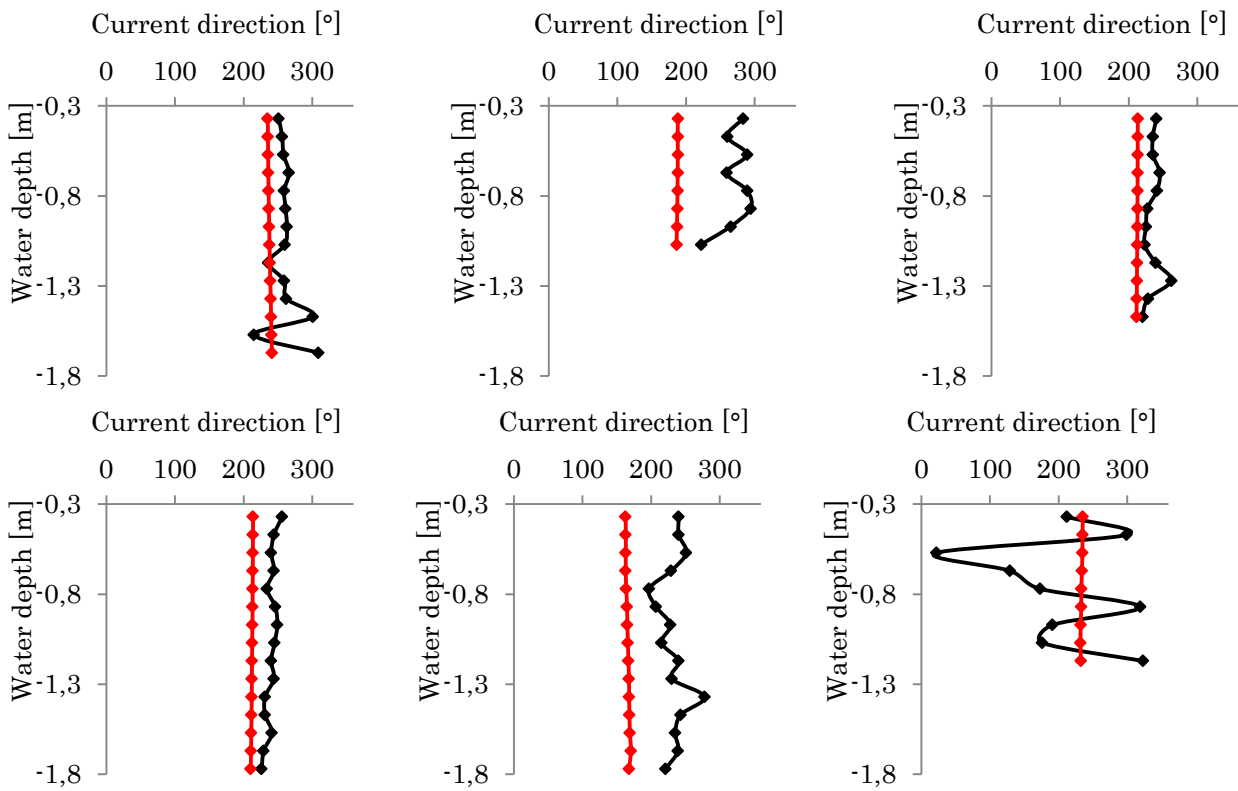
Figure 43: Vertical profiles of measured current directions (black) and simulated current directions (red) at all 18 locations behind Rapijnen. The figures are sorted chronological from 1 to 18.

Appendix F

Roughness parameter COMSOL

To consider surface roughness in the model, a relation formulated by Prandtl (Schlichting, 1968) is used. He found the velocity at some distance from the wall can be described with the formula:

$$u_y = \frac{u_{*0}}{\kappa} \ln y_w + C \qquad\qquad F.1$$

David C. Wilcox (1993) transposed this theoretical formula into a formula also used in COMSOL:

$$\frac{u_y}{u_{*0}} = \frac{1}{\kappa} \ln y_w + B_c \qquad\qquad F.2$$

The parameter B_c can be used to include surface roughness into the model. At default the parameter's value is 5.2. Physically this means that the surface does not induce tension and friction to the flow. For flow over rough surfaces, this approach is not likely to produce reliable results. Therefore Wilcox (1993) derived a formula for the parameter B_c for very rough surfaces:

$$B_c = 8.5 + \frac{1}{\kappa} \ln(1/k_R^+) \qquad\qquad F.3$$

In general the value for B_c can be estimated by a relationship between B_c and the dimensionless surface roughness function S_R. The dimensional surface roughness can be calculated with the following formulas:

$$S_R = (50/k_R^+)^2, k_R^+ < 25 \qquad\qquad F.4$$

$$S_R = 100/k_R^+, k_R^+ \geq 25 \qquad\qquad F.5$$

Using the value gained from either one of these functions and the curve in **Figure 44**, the value for B_c can be found.
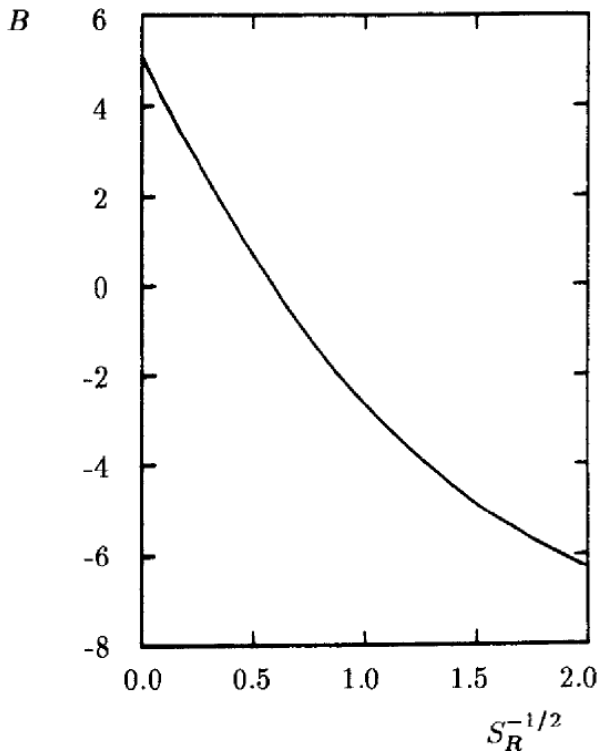
Figure 44: Curve for values of B (Wilcox, 1993)

The effect of varying the value of B in COMSOL was analyzed prior to the investigation. The effect of the parameter depended on the turbulence of the model. Highly turbulent models, such as the models built during this study, were found to be insensitive for the parameter. Therefore the value of this parameter was considered not important, and kept at default (i.e. 5.2).

      Another method that was tested during the model development, was to include more surface complexion by adding small cubes and pyramids at the boundaries. Due to this adjustment the computational effort needed to solve the models increased drastically, resulting in large calculation times and several software crashes. Therefore this method was not used during the study.